Winter 2013

# Engineering microenvironments to modulate calcium information processing in neuronal cells

Kinsey Cotton Kelly

# ENGINEERING MICROENVIRONMENTS TO MODULATE CALCIUM INFORMATION PROCESSING IN NEURONAL CELLS

by

Kinsey Cotton Kelly, B.S.

A Dissertation Presented in Partial Fulfillment
Of the Requirements for the Degree
Doctor of Philosophy

COLLEGE OF ENGINEERING AND SCIENCE
LOUISIANA TECH UNIVERSITY

March 2013

LOUISIANA TECH UNIVERSITY

**THE GRADUATE SCHOOL**

December 14, 2012
Date

We hereby recommend that the dissertation prepared under our supervision by KINSEY COTTON KELLY

entitled

ENGINEERING MICROENVIRONMENTS TO MODULATE CALCIUM INFORMATION PROCESSING IN NEURONAL CELLS

be accepted in partial fulfillment of the requirements for the Degree of DOCTOR OF PHILOSOPHY IN BIOMEDICAL ENGINEERING

Supervisor of Dissertation Research

Head of Department

BIOMEDICAL ENGINEERING
Department

Recommendation concurred in:

Advisory Committee

**Approved:**

Director of Graduate Studies

**Approved:**

Dean of the Graduate School

Dean of the College

GS Form 13a
(6/07)

# ABSTRACT

Tissue engineered microenvironments were constructed to test the effects glial cells have on calcium information processing, and to mimic conditions *in vivo* for tumor invasion and residual cancer after resection of tumor. Submaximal, nM, glutamate (GLU) stimuli were applied to the engineered environments, and the resulting calcium dynamic behavior of neuronal cells was measured to help predict and interpret chaotic systems in the experimental realm. Calcium is a key signaling ion which signals through the N-methyl-D-aspartate (NMDA) glutamate receptor on the neuronal membrane. GLU binding to the NMDA receptor (NMDAR) causes a large and dynamic increase in neuronal intracellular calcium. Perturbations in calcium homeostasis by means of the NMDAR have been linked to several neurodegenerative diseases, such as Alzheimer's, Parkinson's and Huntington's disease. Primary rat cortical cells were used in both co-culture (neurons and glia) and in cultures treated with Cytosine Arabinoside (AraC) to deplete glia. Rat glioma cells were added to the cultured cells to mimic residual cancer cells. In addition, the glioma cells were formed into novel spheroids that modeled tumor invasion. The calcium response was monitored after exogenous glutamate was added in three concentrations (250, 500 and 750 nM), in all (3!) sequences. Calcium was imaged with Fluo 3/AM, 8 to 9 days after plating. The co-culture system responded to increasing submaximal additions of glutamate with calcium spikes, as previously demonstrated in this system. Neuronal cultures depleted of glia responded to increasing nM additions of

GLU with large synchronized broad transient responses which returned to baseline more slowly, leading to a greater area under the fluorescence intensity-time curve (AUC) that we believe is an indicator of excitotoxicity, as well as, normal calcium signaling. Cancer environments did not have excitotoxic calcium area under the curve AUC to glutamate stimulus; however, the residual environment did display excitotoxic conditions due to rapid glutamate induced calcium oscillatory behavior from glioma expressing system Xc-. Determining how neurons will respond and behave in altered systems, such as, in the presence of brain tumor glia may help our understanding of cell loss in the brain, and may provide better protective strategies.

## APPROVAL FOR SCHOLARLY DISSEMINATION

The author grants to the Prescott Memorial Library of Louisiana Tech University the right to reproduce, by appropriate methods, upon request, any or all portions of this Dissertation. It is understood that "proper request" consists of the agreement, on the part of the requesting party, that said reproduction is for his personal use and that subsequent reproduction will not occur without written approval of the author of this Dissertation. Further, any portions of the Dissertation used in books, papers, and other works must be appropriately referenced to this Dissertation.

Finally, the author of this Dissertation reserves the right to publish freely, in the literature, at any time, any or all portions of this Dissertation.

Author _____

Date February 5, 2013

GS Form 14
(5/03)

# DEDICATION

To my wonderful daughter Aedyn James, and my loving, supportive husband Robert, I say thank you and dedicate this dissertation to you both, for without each of you I would find little joy in this success. Thank you for your support, praise and tolerance of my mood swings while in graduate school and for helping me to keep my sanity.

I would also like to dedicate this dissertation to my mother Donna, and my father Jackie. Thank you both for your support, love and encouragement for me to pursue my interests. My journey has been a long road well-traveled and I thank you both for teaching me the information I needed to prepare for life, helping to guide me down the correct paths, and holding my hand along the way when I underwent adversity. I have finally reached the culmination of my formal education and greatly appreciate everything you have done and sacrificed for me in arriving to this point.

I also dedicate this dissertation to my Nanny. Thank you for always being there for me when I needed help; you have given yourself wholeheartedly to help me further my education and that is something I do not take lightly and will cherish forever. I would like to also dedicate this dissertation to the following people who were all essential in my pursuit of furthering my education: Colin, Erin, Pappy, Memawl, Honey and Granny Opal. For everyone who has passed and is present, I will never forget all the love, help and support you provided to me while undergoing the endeavors to achieve my doctorate. With all my love and gratitude, Kinz.

# TABLE OF CONTENTS

# LIST OF TABLES

# LIST OF FIGURES

# ACKNOWLEDGEMENTS

I would like to say thank you to my mentor and advisor, Dr. Mark DeCoster. I will be leaving Louisiana Tech University a competent and skilled scientist due to his advice, support, and training in politics, cell culture and high-end microscopy. Most importantly, thank you for your support in all the decisions I made throughout my graduate career; I will forever be grateful. I would also like to acknowledge my advisory committee, Drs. Katie Evans, Paul Hale, Jr., Steve Jones, David Mills, and James Spaulding, for their advice and support of my research.

I would like to extend a special thanks to Dr. Jamie J. Newman for her guidance, advice and persistence to have everything finished within a certain time frame. I am glad to have worked with her in my last year of graduate school, and will always be grateful for her contribution in my development as a scientist and her friendship.

I would also like to acknowledge all of my lab members, past and present. Thank you all for your help, support and friendship. I hope to have contributed to your science and lives as much as you all have contributed to mine.

Lastly, I would like to thank my family and friends for their love, support, and encouragement for all the years I have been in school. Yes, I am finally finished!

# CHAPTER 1

# INTRODUCTION

## 1.1 Neuronal Calcium

### 1.1.1 Calcium Channels

Calcium in its ionic form is very dynamic, especially in excitable cells such as muscle and brain cells, moving from the high concentration exterior of the cell to the much lower concentrations inside the cell where calcium is used as a second messenger. In brain cells and neurons especially, calcium is a key signaling ion which is involved in numerous biological processes within neuronal cells with some activities including gene expression, synaptic plasticity, neurotransmitter release, neurite outgrowth during development, [1, 2] learning and memory and apoptosis; however, disrupting normal calcium signaling can cause multiple forms of neurodegenerative diseases. Numerous receptors are located on the neuronal membrane which can allow calcium influx into the cell. The type of signal which is initiated depends on the receptor in which calcium influx was activated. Three main types of calcium channels on the neuronal membrane are voltage gated ion channels, ligand gated channels and glutamate receptors, Figure 1.1 [3].

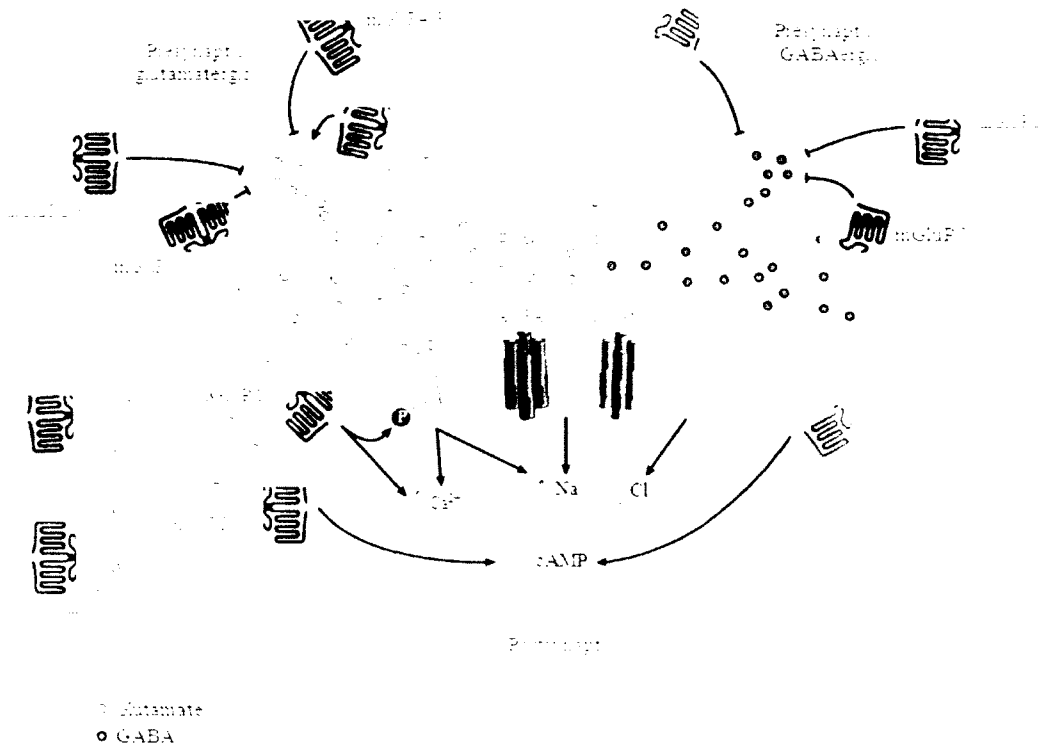


Figure 1.1 Calcium receptors located on the membrane of neurons and glia. Tubular colors: purple (NMDA,) blue (AMPA,) green (KA,) pink (GABAA) Transmembrane line color: Pink-purple (GABAB,) green (mGluR1/5,) blue (mGluR 2/3,) and burgundy (mGluR4/7/8) [3].

Voltage Gated Ion Channels. Voltage gated ion channels are typically a calcium ($Ca^{2+}$) and sodium ($Na^{+}$) channel. However, the channel has a 1000 fold greater affinity for calcium over $Na^{+}$. The voltage gated ion channel converts the electrical activity from the action potential once calcium enters into the cell cytosol, initiating second messengers responsible for synaptic transmission. The type of $Ca^{2+}$ current initiated depends on the cell type. Table 1.1 lists the six different calcium currents and the neurodegenerative diseases associated with each current [4, 5].

Table 1.1 Calcium channel function and related disease [4].

| $Ca^{2+}$ current type | α1 Subunits | Specific blocker | Principal physiological functions | Inherited diseases |
|---|---|---|---|---|
| L | $Ca_v1.1$ | DHPs | Excitation-contraction coupling in skeletal muscle, regulation of transcription | Hypokalemic periodic paralysis |
| | $Ca_v1.2$ | DHPs | Excitation-contraction coupling in cardiac and smooth muscle, endocrine secretion, neuronal $Ca^{2+}$ transients in cell bodies and dendrites, regulation of enzyme activity, regulation of transcription | Timothy syndrome: cardiac arrhythmia with developmental abnormalites and autism spectrum disorders |
| | $Ca_v1.3$ | DHPs | Endocrine secretion, cardiac pacemaking, neuronal $Ca^{2+}$ transients in cell bodies and dendrites, auditory transduction | |
| | $Ca_v1.4$ | DHPs | Visual transduction | Stationary night blindness |
| N | $Ca_v2.1$ | ω-CTx-GVIA | Neurotransmitter release, Dendritic $Ca^{2+}$ transients | |
| P/Q | $Ca_v2.2$ | ω-Agatoxin | Neurotransmitter release, Dendritic $Ca^{2+}$ transients | Familial hemiplegic migraine, cerebellar ataxia |
| R | $Ca_v2.3$ | SNX-482 | Neurotransmitter release, Dendritic $Ca^{2+}$ transients | |
| T | $Ca_v3.1$ | None | Pacemaking and repetitive firing | |
| | $Ca_v3.2$ | | Pacemaking and repetitive firing | Absence seizures |
| | $Ca_v3.3$ | | | |

Abbreviations: DHP, dihydropyridine; ω-CTx-GVIA, ω-conotoxin GVIA from the cone snail *Conus geographus*; SNX-482, a synthetic version of a peptide toxin from the tarantula *Hysterocrates gigas*.

Ligand Gated Channel. The GABA receptor is both a ligand gated and a G protein-coupled receptor based on whether it is a $GABA_A$ or $GABA_B$ receptor. $GABA_A$ is responsible for depolarizing the membrane potential releasing chloride ions into the extracellular space and activating voltage gated ion channels allowing $Ca^{2+}$ to enter the cytosol. Calcium entry through the $GABA_A$ receptor is very important in developing neurons to lead to neurite outgrowth. $GABA_B$ receptors are found on both presynaptic and postsynaptic neurons and are known to decrease $Ca^{2+}$ conductance and play a critical role in development in regulating cytosolic $Ca^{2+}$ in developing neurons.

1.1.2 Glutamate Receptors

Multiple types of glutamate receptors are found on neurons: α-amino-3-hydroxy-5-methyl-4-isoxazolepropionic acid (AMPA), metabotropic glutamate receptors (mGluR), Kainate receptor (KA) and N-methyl-D-aspartate (NMDA) receptors. AMPA receptors on the postsynaptic membrane are responsible for plasticity and synaptic transmission and act as both glutamate receptors and cation channels. Long-term potentiation (LTP) has been the most studied form of plasticity and is only activated when glutamate binds to both the AMPA and NMDA receptors [6-8].

The KA receptor responds to glutamate and is found on the presynaptic and postsynaptic terminals. KA functions as a modulator of the inhibitory neurotransmitter GABA through the presynaptic terminal. KA acts in excitatory neurotransmission when located on the postsynaptic terminal.

A type of metabotropic receptor belonging to group C of the G-protein-coupled receptors is the mGluR. This glutamate receptor has eight different subunits $mGluR_1$-$mGluR_8$ and the subunits are separated into three groups, I, II and III [9]. Group I is the only group located on the presynaptic terminal and function to increase NMDA receptor activity [10]. Group II and III are both found on postsynaptic terminals of neurons and function to decrease NMDA receptor activity and decrease excitotoxicity.

Calcium is also a key signaling ion involved in memory and learning with NMDA receptor on the neuronal membrane [11]. NMDARs are ionotropic receptors responsible for binding glutamate, the most abundant excitatory neurotransmitter (excitatory stimulus) in the human brain. Activation of NMDARs opens the ion channel at the plasma membrane to allow calcium influx into the cell cytosol [11, 12], Figure 1.2 [13].

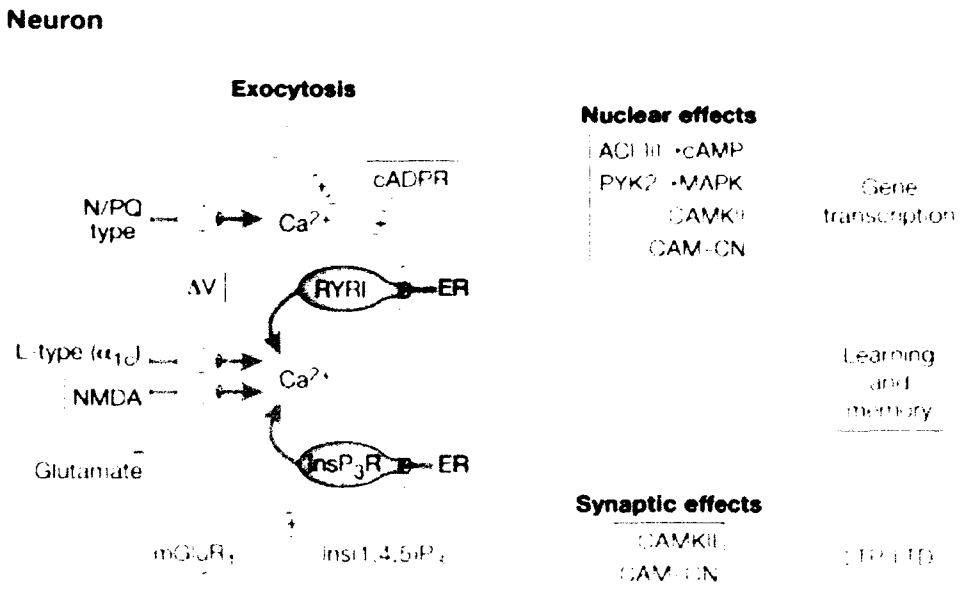


Figure 1.2 Different pathways for Ca2+ to enter the neuron and the effects Ca2+ has on processes once entered into the cytosol [13].

Glutamate is an excitatory neurotransmitter that turns neurons "on" [14]. It excites the neurons in part by causing large and dynamic changes in intracellular calcium concentration ($[Ca^{2+}]_i$) increases. While these $[Ca^{2+}]_i$ dynamics are essential for normal signaling in the brain, excessive and sustained elevations in neuronal $[Ca^{2+}]_i$ are related to neuronal injury [1] including long-term neurodegenerative processes [2]. Glial cells, known as astrocytes, help to regulate these dynamics in the brain [15]. Astrocytes express glutamate transporters [3], which bind glutamate diminishing the time neurons are exposed to glutamate, and thus shaping the $[Ca^{2+}]_i$ dynamics in neurons [16, 17].

## 1.2 Calcium Mediated Cell Death

Different forms of cell death occur, such as, necrosis, necroptosis and apoptosis. Apoptosis is usually referred to as "cell suicide," and it occurs during development and is

used as a mechanism to control cell populations by means of programmed self-destruction. Calcium plays an important role in cell homeostasis and is considered to regulate apoptotic events [18, 19].

NMDARs can be excessively stimulated by glutamate, which can lead to an abundance of calcium influx into the cytosol which will cause neuronal damage and can lead to excitotoxicity [20], triggering a form of cell death termed oncosis, shown in Figure 1.3 [21]. Glial cells are responsible for removing excess glutamate from the surrounding environment, but are limited to the amount of glutamate they can uptake. Many neurodegenerative diseases are caused by defects in the aforementioned cellular pathway, such as, Alzheimer's, Parkinson's and Huntington's disease [12, 22, 23].

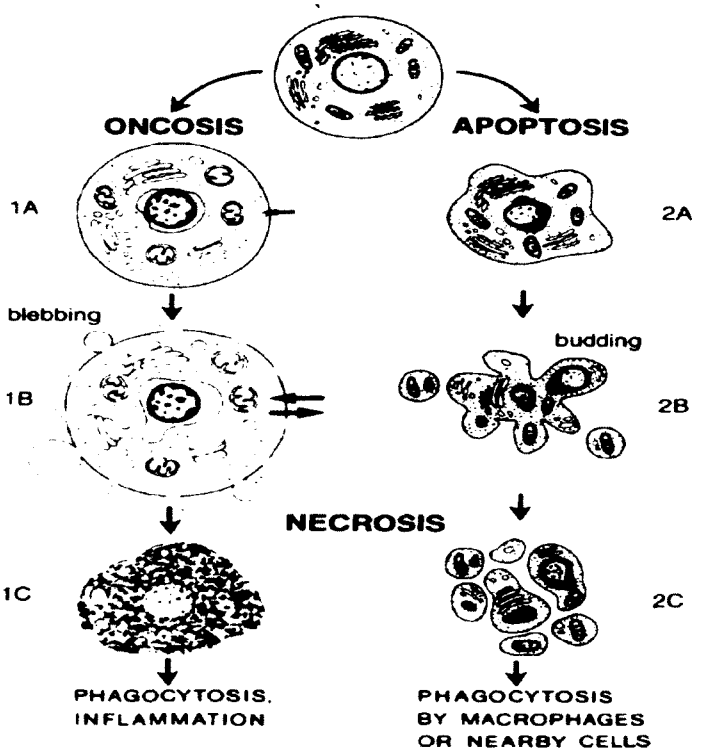


Figure 1.3 The pathways of cell death leading to necrosis. 1A) depicts oncosis which is triggered by excitotoxicity [21].

## 1.3 Calcium Fluorescence

Glutamate homeostasis is maintained by neuronal release, neurotransmission, and glial uptake [24]. However, the chance of any neuron to release vesicular glutamate is stochastic. When exogenous glutamate is introduced to cells *in vitro* we expect calcium to enter the neurons, because glutamate is an excitatory neurotransmitter [25]. Furthermore, the more one stimulates neurons with glutamate the higher possibility neurotransmission is likely to occur. In the experimental realm, calcium influx into the cells is expressed as an increase in fluorescence, due to the fluorescence probe for calcium in which we are using, Fluo 3/AM. The AM ester has very low water solubility; therefore, a detergent (Pluronic F-127) is used to ease cell permeability. Fluo 3/AM does not fluoresce when conjugated to the ester. Once Fluo 3/AM is in the cytosol, the endogenous esterases cleave the ester and the fluorescent probe binds to calcium, causing fluorescence to occur when excited by the appropriate excitation wavelength; Figure 1.4 shows fluorescence probe binding to calcium. However, this bond is not covalent; Fluo 3/AM can disassociate from calcium allowing us to observe the dynamics of calcium changes in neurons [26].


Figure 1.4 Representative image of calcium imaging in primary astrocytes when loaded with Fluo 8AM in response to 50 mM potassium chloride with a 40X oil objective. *Scale bar= 20 μm.*

## 1.4 Calcium Information Processing

Calcium information processing is initiated when calcium enters the cytosol by means of a plasma membrane receptor. Cytosolic calcium concentration, at resting potential, is approximately 200 nM; however, when the cell is stimulated via calcium receptors, calcium concentrations can rise into the micromolar range. The amplitude and duration of the calcium signal determines which processes will be utilized. Calcium entry by the NMDA receptor can actually initiate mitochondrial and endoplasmic reticulum calcium stores to be released. When calcium enters the cytosol and activates the intracellular endoplasmic calcium stores, it is responsible for membrane excitability, secretion, proliferation, learning, memory, vesicle trafficking and crosstalk with other signaling pathways. However, mitochondrial intracellular calcium release is responsible

for ATP and steroid synthesis, as well as, apoptosis. These pathways are elucidated in Figure 1.5.

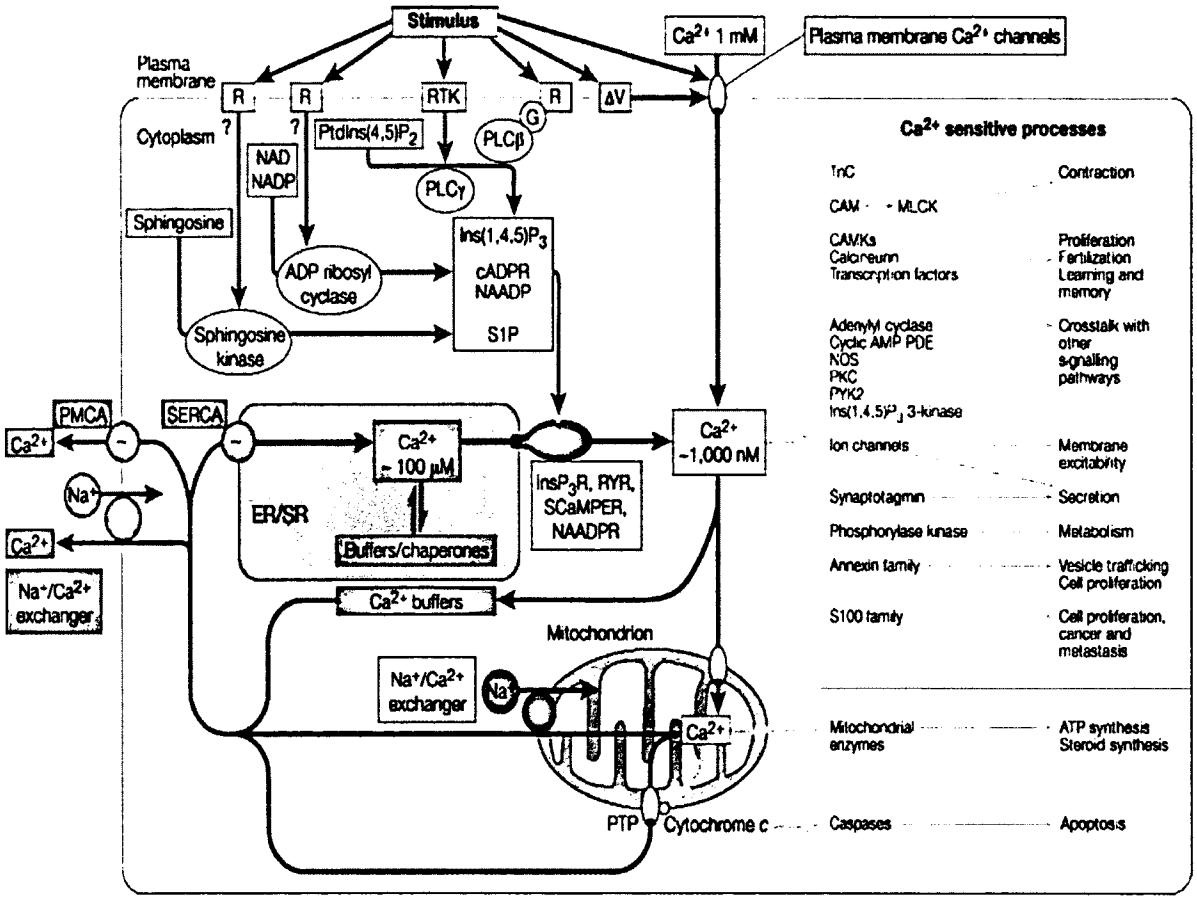


Figure 1. 5 Calcium pathways and the processes they facilitate within the cell [13].

## 1.5 Excitotoxicity and Disease States from Perturbations in Calcium Information Processing

The location of the NMDA receptor on the neuron will determine the processes which calcium will activate. When an overabundance of glutamate is present in the system, an overload of glutamate on the presynaptic NMDA receptor will occur causing a spillover to the NMDA receptors on the dendritic spine which are responsible for excitotoxic stimulation. Excitotoxicity is a process which can lead to stroke and

numerous diseases like autism and Alzheimer's disease [12, 22, 24]. Brain injury or disease occurs when an NMDA receptor binds excess glutamate, allowing an influx of calcium in the extracellular fluid ($[Ca^{2+}]_{EF}$) [21, 27, 28]. Figure 1.6 is a cartoon of neurodegenerative diseases caused by perturbations in cell calcium homeostasis [29-32].

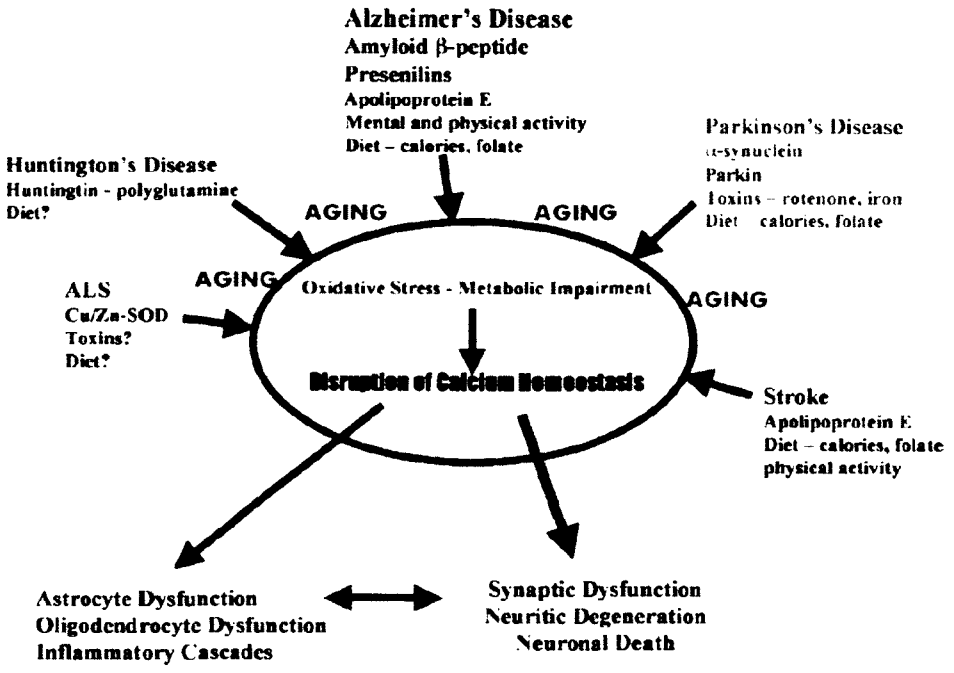


Figure 1.6 Age-related neurodegenerative diseases caused by perturbations in calcium homeostasis [29].

### 1.5.1 Alzheimer's Disease

Alzheimer's disease (AD) is one of the few neuronal disorders which is age related and affects both men and women without discrimination of ethnicity or race. It is thought to be a treatable disease; however, a successful treatment has yet to be unveiled. One of the first symptoms of AD is the inability to remember newly learned information. This coincides with studies finding amyloid-β (Aβ) plaques and tangles in the center of the brain responsible for learning and memory [29, 34]. As the disease progresses to

alterations in mood, behavior or disorientation and speech impairments, the Aβ plaques and tangles have been found in other parts of the brain, Figure 1.7 [35, 36].

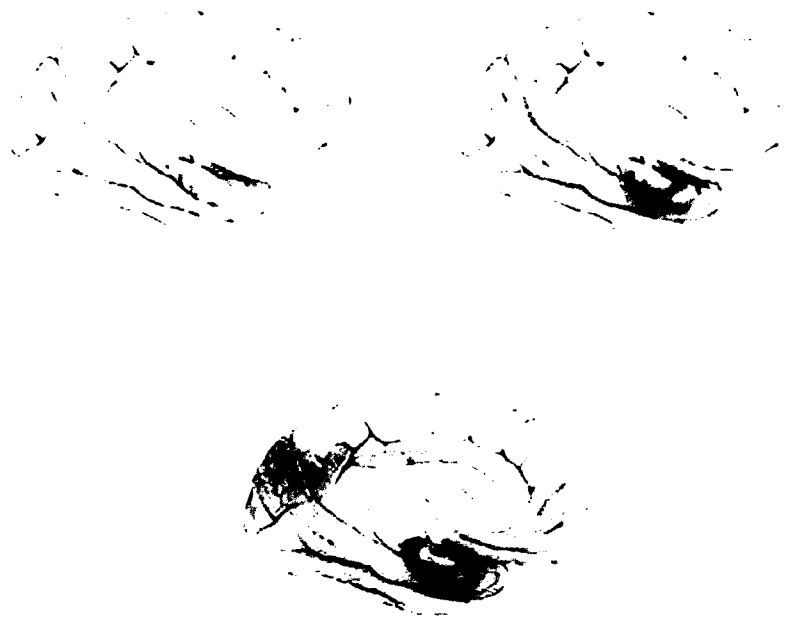

Figure 1.7 AB plaques and tangles in progression of Alzheimer's disease. Top left) first stages of disease, learning and memory affected. Top right) progression of disease and spread of plaques and tangles to other locations of the brain. Bottom) Late stage AD [37].

There have been studies that suggest Aβ increases excitotoxic conditions of neurons via the NMDA receptor and increase NMDA agonists and glutamate in AD [33, 38]. This excitotoxicity leads to irreversible damage initiating apoptosis in neurons and glia. In another report, glial cell death due to AD is thought to disrupt glutamate transport and calcium regulation [39], Figure 1.8 [33].

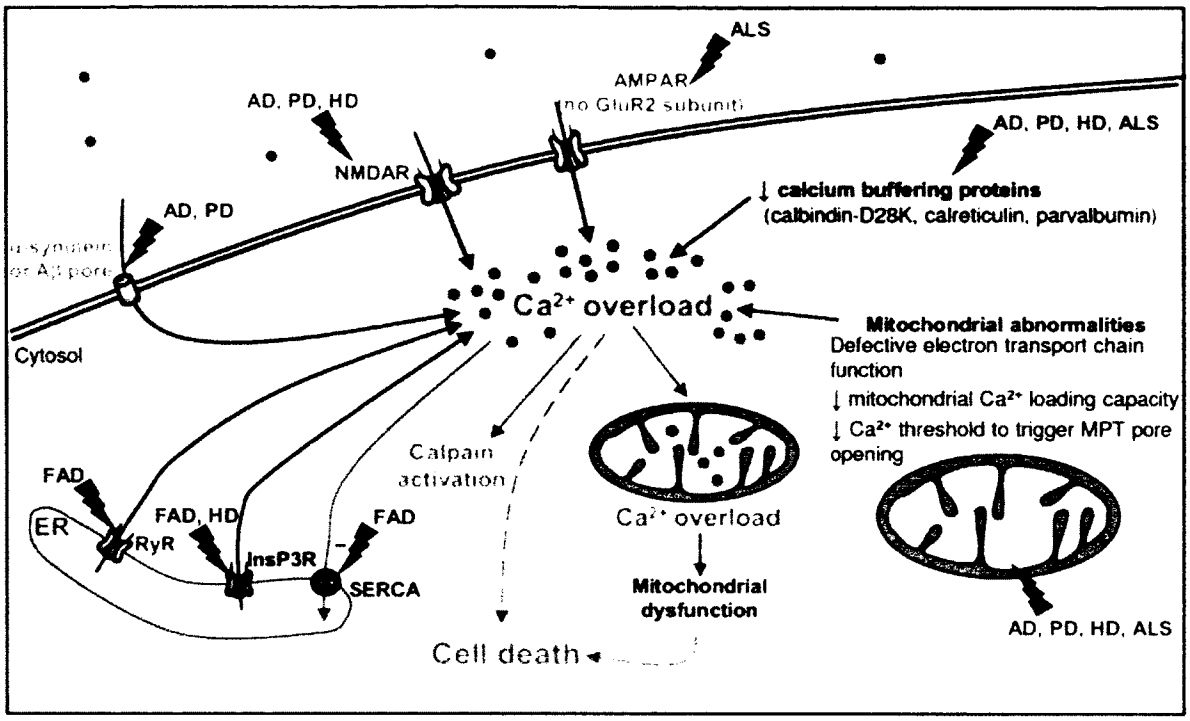


Figure 1.8 Perturbations in calcium signaling leading to neurodegenerative diseases. Alzheimer's Disease (AD,) Parkinson's Disease (PD,) Huntington's Disease (HD,) Amyotrophic Lateral Sclerosis (ALS) [33].

1.5.2 Parkinson's Disease

Parkinson's disease (PD) is a disease that is non-curable and causes tremors, rigidity, bradykinesia, as well as other symptoms. PD is attributed to the death of dopaminergic neurons located in the substantia nigra pars compacta in the midbrain, not the cortex. Investigations are still in progress as to the cause of PD, but several studies indicate a disturbance in calcium signal processing to be a cause. Studies have determined mitochondria and the endoplasmic reticulum both play a role in the death of dopaminergic neurons, as well as, L-type $Ca^{2+}$ channels. However, $Ca^{2+}$ ion channels have been reported to be engaged allowing $Ca^{2+}$ to enter the cytosol increasing calcium concentrations within the cell [40], this coupled with the L-type channel being activated

longer than necessary, allowing calcium to influx into the cytosol, can cause deleterious effects on the cell.

### 1.5.3 Huntington's Disease

The whole brain is affected by Huntington's disease (HD) which is caused by a genetic defect on chromosome 4. HD is a hereditary disease which is incurable, and causes cognitive decline, as well as, abnormalities in muscle coordination. Studies are starting to look at NMDA receptors as the cause for excitotoxicity in HD cells in the striatum [33]. Also, one study inserted NMDA receptor agonists into the rodent and non-human primate striatum mimicking damage caused by excitotoxicity in HD [41].

### 1.5.4 Stroke

The National Stroke Association reports there will be approximately 800,000 strokes this year in which 87% will be facilitated by ischemia. During a stroke, 200 million brain cells per minute may die and one in four people do not survive the episode [42]. Cerebral ischemia is caused by a reduced glucose-oxygen supply to a particular area of the brain, which causes mitochondrial ATP deregulation. This deregulation causes NMDA, AMPA, and KA receptors to permeate calcium, sodium and zinc into the cytosol. If permeation of calcium reaches a certain threshold, excitotoxicity occurs, leading to neuronal cell death, Figure 1.9 [43, 44].

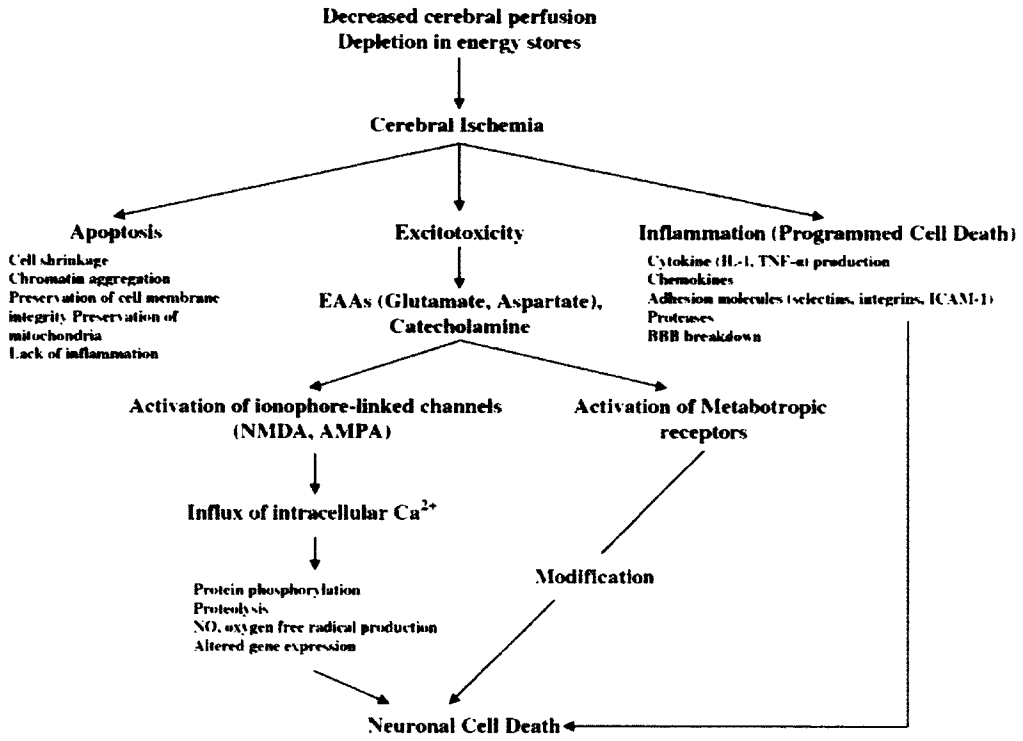


Figure 1.9 Pathway of induced calcium excitotoxicity in ischemia [45].

## 1.6 System Xc-

### 1.6.1 System Xc- Background

System Xc-, also known as the cystine-glutamate antiporter, functions in astrocytes to exchange one extracellular cystine with an equivalent amount of intracellular glutamate. *In vivo*, the reuptake by glutamatergic receptors of extracellular glutamate released via this antiporter system is known to shape synaptic plasticity [46]. Figure 1.10 is a diagram describing system Xc-, where a cystine linked glycine molecule is cleaved, and the astrocyte takes in the cystine. Reduction of the cystine molecule to cysteine occurs in the astrocyte. Cysteine can then facilitate glutathione (GSH) production; GSH is a known antioxidant [47]. GSH is then released into the extracellular

space where it is degraded by peptides into cysteine and transported into the neuron to facilitate GSH production.

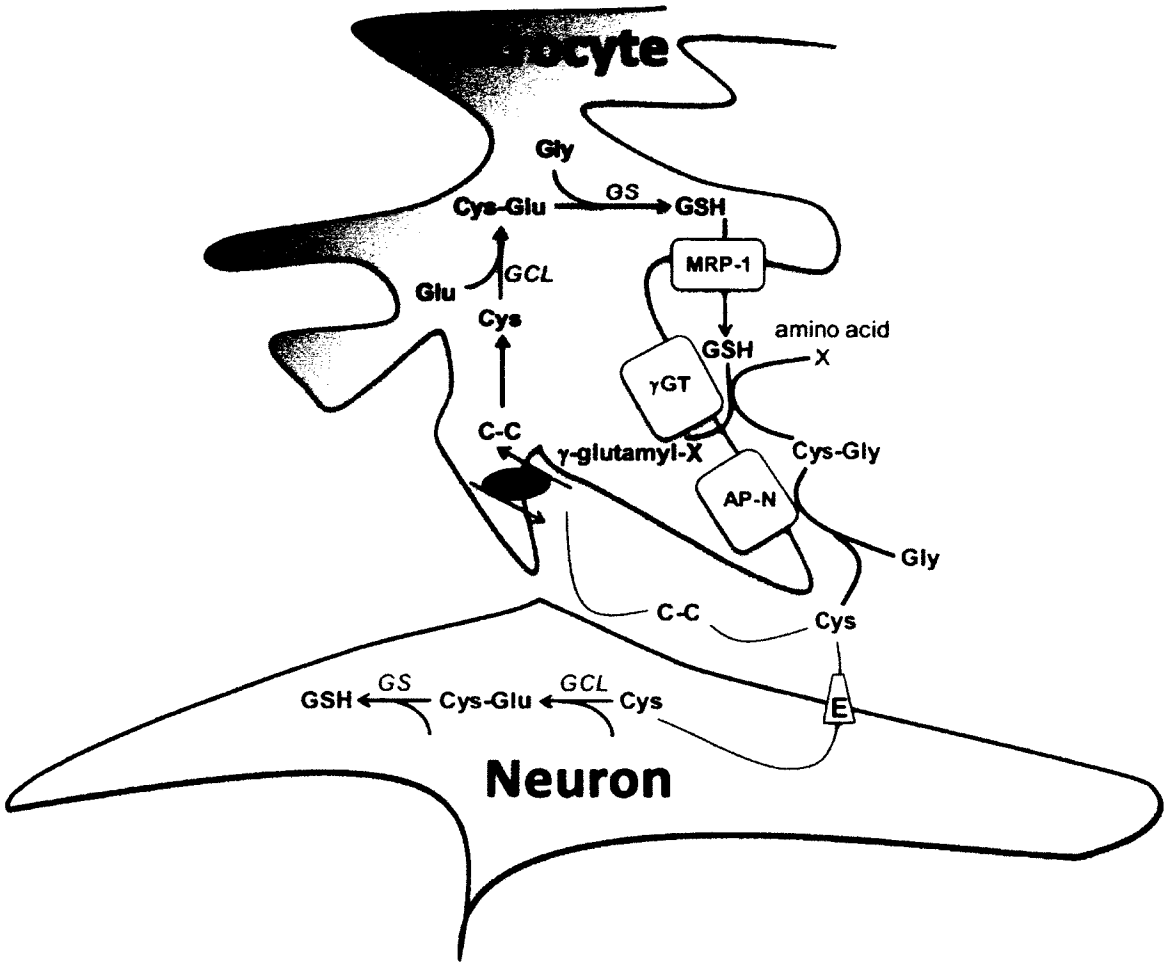


Figure 1.10 System Xc- and the cysteine (Cys):glutamate (Glu) exchange. Cystine (C-C) glycine (Gly,) and glutothione (GSH) [46].

1.6.2 System Xc- in Disease

1.6.2.1 Glioma. Gliomas are malignant glial cells, and use system Xc- in a most advantageous way to promote glioma proliferation. Glioma use excitotoxic levels of glutamate to kill surrounding tissue; the high levels of glutamate is used as an autocrine signaling factor to increase invasion. Gliomas utilize the autocrine system, as a self-

signaling mechanism- the more glutamate in the system glioma reduces production of glutamate and invades tissue, Figure 1.11 [46, 48-50].

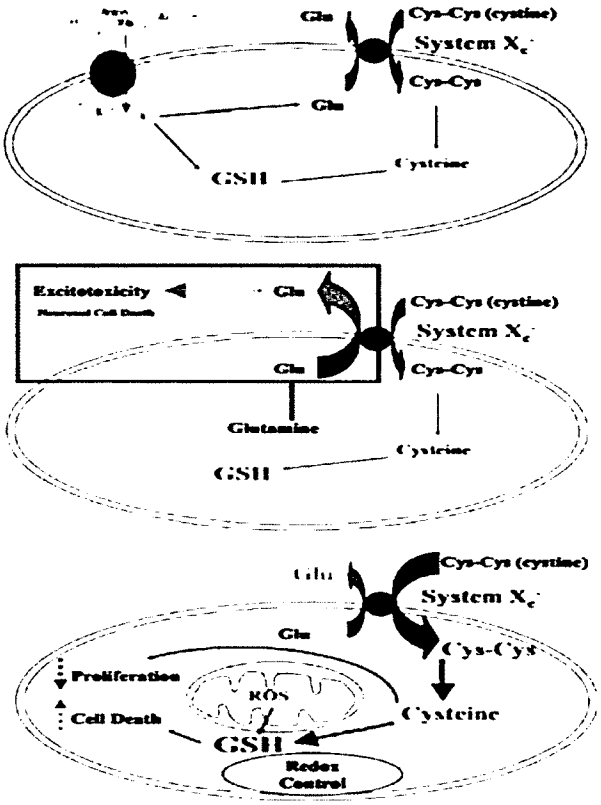


Figure 1.11 Top) Normal astrocyte system Xc- production with Na+ reuptake. Middle) Glioma system Xc- with lack of the Na+ reuptake system, resulting in cell survival and excitotoxicity of surrounding tissue. Bottom) Normal system Xc- in neurons and astrocytes for the production of glutathione [50].

1.6.2.2 Alzheimer's Disease. NMDA activation from glutamate released by the system Xc- may result in increased amyloid-β production [46]. A study directly linking a perturbation in system Xc- and Alzheimer's disease has yet to be examined [38, 46, 51].

## 1.7 Engineering Microenvironments to Modulate Calcium Signaling

Calcium processing in the brain has long been thought of as a neuronal process, but an emerging viewpoint is glial cells contribute to this process [52]. To investigate this viewpoint further, environments must be engineered to control glial activity to glutamatergic receptor stimulation. This can be achieved by controlling glial proliferation within primary cortical cultures with an antimitotic. Also, system Xc- is the main contributor to excitotoxicity in normal tissue when exposed to glioma. Tissue engineering was applied to develop systems that mimic *in vivo* scenarios: 1) non-vascularized tumor invasion or metastasis and 2) residual cancer cells- cancer cells left in brain tissue after resection of tumor. Engineering these environments allows researchers to understand how these different cancerous environments perturb calcium processing in normal primary cortical cultures. The engineered cancer environments can then be compared to normal cortical cell calcium processing to submaximal increasing glutamate concentrations.

## 1.8 Motivation and Hypotheses

An *in vitro* engineered cell culture system is composed of rat brain cortical neurons with different densities of astrocytes which has been used to statistically analyze the $[Ca^{2+}]_i$ dynamics in individual neurons with subthreshold concentrations of glutamate by excitation of the NMDA receptor. Subthreshold concentrations of GLU describe GLU additions which physiologically would not elicit a toxic calcium response, in these experiments nM concentrations of GLU are used in random (3!) sequences, and the response (spike) would return to baseline. This work follows our long-standing interest in

brain cell $[Ca^{2+}]_i$ dynamics [4], but with proposed engineered environments coupled to applied statistical and mathematical tools to elucidate the following questions in calcium processing dynamics in neurons: 1) whether the order of repeated glutamate stimulation alters neuronal $[Ca^{2+}]_i$ dynamics, 2) how the presence of different densities of astrocytes modulates neuronal $[Ca^{2+}]_i$ dynamics and 3) how engineered cancerous environments perturb neuronal calcium processing. It is anticipated, this combined experimental/analytical approach will also have utility in understanding additional brain diseases such as glioma and neurodegeneration linked to deregulated homeostatic calcium [49].

1.8.1 Hypothesis 1:

The randomization order in which glutamate stimulus is administered to the cells will affect neuronal calcium processing in which larger concentrations of glutamate stimulus prior to addition of lower glutamate stimulus will desensitize NMDA receptors to the lower concentration of glutamate, thus altering the calcium dynamics.

1.8.2 Hypothesis 2:

Glial cells will affect neuronal calcium dynamics by decreasing the amount of glutamate to which neurons will be exposed, thus altering the influx of calcium into the cytosol.

1.8.3 Hypothesis 3:

The engineered cancerous environments, tumor invasion and residual, will elicit excitotoxic responses to normal ordering of glutamate additions compared to normal engineered environments high in glia.

# CHAPTER 2

## CELL CULTURE, ENGINEERING MICROENVIRONMENTS, CALCIUM IMAGING AND ANALYSIS METHODS

### 2.1 Cell Culture

#### 2.1.1 Primary Cell Culture

Cortical cells were obtained by performing cervical disarticulation of outbred Sprague-Dawley newborn rats (age $\leq$ 48 hrs) in adherence to protocols approved by Louisiana Tech University's Institutional Animal Care and Use Committee (IACUC). Rats were decapitated and the brain tissue was quickly removed and placed into dissecting solution, Basal Media Eagle (BME, Sigma) consisting of 0.5% Penicillin Streptomycin (PS, Sigma.) The cerebellum and meninges were removed, and the cortical lobes were then stored in an ice-cold dissecting solution. (An average of n= 7 newborn rats were used for each culture set.) After dissection was completed, the brain tissue was then aspirated with a 25 mL pipette and placed into a 15 mL conical tube with a complementing volume of Trypsin EDTA (volume determined by value of **n**, Sigma) and inverted 5 times. Trypsin was then neutralized with Neuronal Culture Medium (NCM, Appendix A) comprised of BME, Ham's F-12 K (ATCC), 10% Horse Serum, 10% Fetal Bovine Serum (FBS), and glucose, glutamine and PS. The cells were then mechanically disassociated by trituration and allowed a duration of ten minutes to form a neuronal cell supernatant. The supernatant was then aspirated and stored in a 15 mL ice-cold conical

tube. NCM was then re-introduced to the brain tissue and the process repeated thrice in total. The neuronal cell supernatant was centrifuged at 160 rcf in $8^0$ C for 7 mins to form a pellet. Once the cells were resuspended in fresh NCM, a cell count was obtained with a hemacytometer; the cells were then plated in a poly-l-lysine (PLL, Sigma) coated, 24 multi-well plate (cell culture treated, Cellstar) at an optimal density of 200,000 cells per well. The cell cultures were maintained in $37^0$C, 5% $CO_2$, and 100% humidity incubation, Appendix A.

2.1.2 Glioblastoma Cell Culture

A rat glioblastoma cell line (CRL-2303) from ATCC was maintained based on vendor specifications with Delbucco's Modified Eagles Medium (DMEM, Sigma), 10% FBS, 1% Amino Acid Solution (Sigma), and 0.5% PS. The glioblastoma cell line was incubated at $37^0$C, $CO_2$, and 100% and retired by passage 20.

2.1.3 Preparation and Loading of Calcium Fluorescence Dye

The cortical cultures were imaged 8 to 9 *days in vitro* (DIV), by incubating cells in a loading solution, Pluronic acid (Sigma) at a 1000x dilution and Fluo 3/AM (Invitrogen) at 500x dilution in Locke's solution, for 45 mins. The cells were then washed and recovered in warmed Locke's solution and re-incubated for 30 mins. While the cells were recovering, fresh Glutamic acid ((GLU) 250, 500 and 750 nM, Sigma Aldrich) concentrations were prepared in Locke's solution.

Locke's Solution. Locke's solution is a solution used in fluorescence experiments because it lacks serum and phenol red, which is contained in media, therefore, eliminating auto-fluorescence or quenching of the calcium dye [53]. Locke's is

comprised of sodium chloride, potassium chloride, calcium chloride, calcium bicarbonate, glucose, Hepes buffer and sterile deionized water, Appendix A.

Glycine Bath. Glycine is a co-agonist of the NMDA receptor and can help prevent excitotoxicity of neuronal cells [54]. A glycine bath (10 μM, Sigma) was prepared with Locke's solution; this solution was warmed and introduced to experimental wells when cells were being recovered from the Loading Solution. The cells were recovered in the glycine bath for 30 mins and the experimental protocol was implemented as normal.

Glutamate. Three different glutamate (Sigma) concentrations were used throughout the main experiment: 250, 500, and 750 nM. Each concentration takes into account a 20x dilution factor when an addition to the experiment is performed. Glutamate is dissolved into Locke's solution and is made fresh for each experiment. Other concentrations of glutamate used for determining experimental concentrations are 1 μM and 4 mM.

Ionomycin. Ionomycin, (2 μM, Sigma Aldrich) a calcium ionophore, is used to perforate the cell membrane, allowing rapid calcium influx into the cell, maximizing the fluorescence calcium intensity. Ionomycin is frozen at -80 C° in aliquots of dimethyl sulfoxide (DMSO) at a stock concentration of 665 μM until it is ready to be used for experimentation, in which the stock concentration is then mixed with Locke's solution to obtain the working concentration.

Potassium Chloride. (KCL, Sigma) is known to produce a transient increase in calcium. KCL is dissolved into Locke's solution to reach a desired working concentration of 50 mM.

Bicuculline. Bicuculline is used to mimic epilepsy because it is an antagonist of the GABA receptor. Bicuculline is commonly used to isolate glutamate receptor function. Locke's solution was used to dissolve bicuculline to 50 μM working concentration.

Magnesium. (Mg) is a physiological block of the NMDA receptor, and it is used *in vitro* to inhibit calcium influx into the neuronal cells by way of ionotropic receptors.

## 2.2 Engineering Microenvironments

### 2.2.1 Engineering Primary Cortical Cell Microenvironment

After three days *in vitro* (DIV), the primary cell culture plates were divided in half, with one half of the culture treated with a 100x dilution of the anti-mitotic, Cytosine Arabinoside, (AraC, 1 mM, Sigma) to deplete glial cells from cultures, shown in Figure 2.1. AraC is effective because the anti-mitotic is loaded into the cell and causes damage in the S-phase of a proliferating cell; thus, depleting glial cells from neuronal cultures, leaving the viable non-proliferating cells, which are neurons. An example of primary cell cultures treated with and without AraC merged with each cultures respective calcium fluorescence imaging can be seen in Figure 2.2, the small round punctate cell bodies densely packed in the right image is representative of high glia cultures, as compared to the left image which is depleted of glia and lacking the high density of round cell bodies. The calcium fluorescence intensity is greater in the glial depleted culture due to the lack of glial cells and their ability to act as a negative feedback system for glutamate by removing excess GLU from the system.

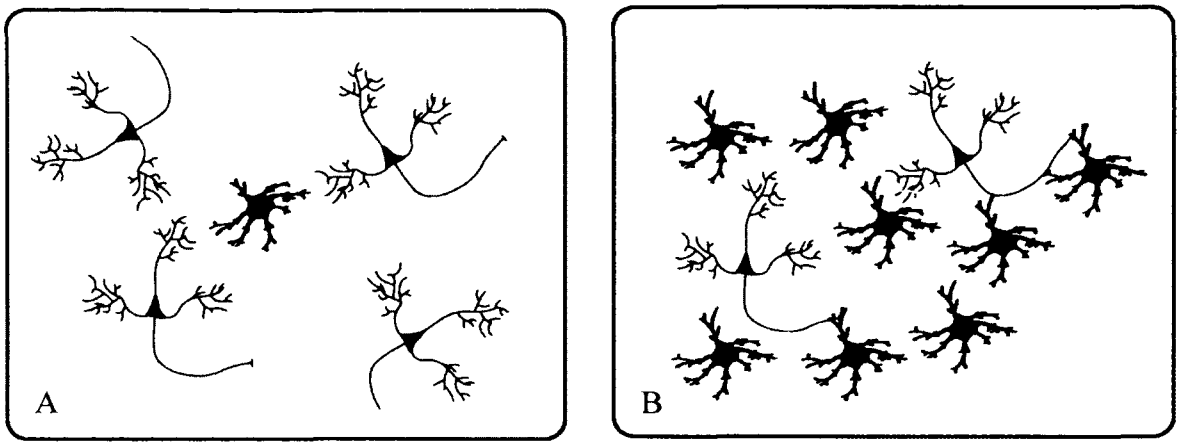


Figure 2.1 A) Primary cortical cultures after treatment with AraC to deplete cultures of glia. B) Primary cortical pictures high in glia. *Blue bodies-* neurons *Red bodies=* glia

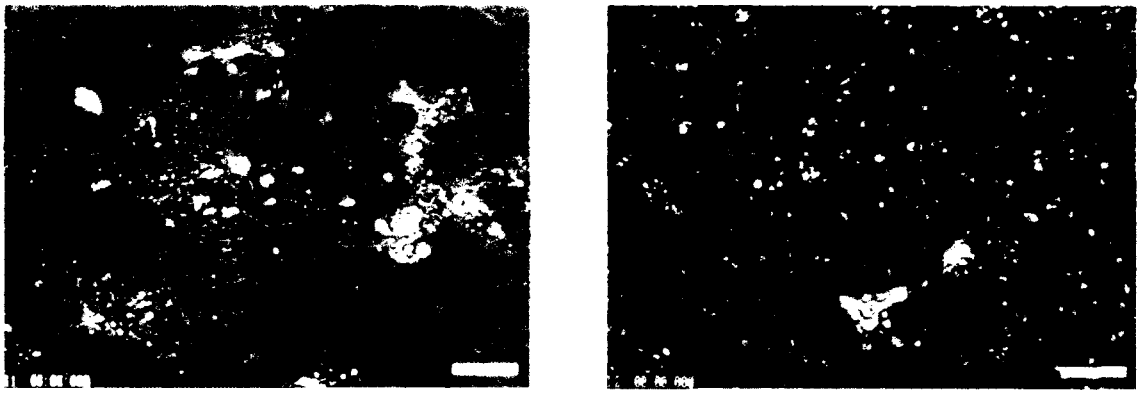

Figure 2.2 Left) Phase image merged with calcium fluorescence of primary cortical culture treated with AraC. Right) Phase image of primary cortical cultures high in glia with merged calcium fluorescence image. *Scale bar= 50 μm.*

The remaining wells were supplemented with warmed NCM and were used for co-culture experiments. Four multi-well plates from every culture set were treated with AraC; three culture sets were created in total (n= 21 rats and approximately 48 wells per culture type, co-culture and neurons).

### 2.2.2 Engineering Cellular Co-Culture Microenvironment with Primary Cortical Cells and Glioblastoma

Glioma co-cultures where engineered in two separate ways, emulating two very distinct and different cancerous microenvironments: metastatic and residual.

The metastatic microenvironment is engineered by using normal primary cortical cell cultures; however, on day 6 *in vitro*, a 3-dimensional glioma construct or spheroid (a novel proprietary procedure developed in DeCoster Lab) is added to the experimental culture well. The glioma spheroid then arbitrarily adheres to the primary cell layer, mimicking metastatic tumor invasion. The metastatic microenvironment is imaged after 2 days *in vitro* of tumor invasion/spheroid adhesion. Spheroids were developed based on a proprietary method and were transferred into experimental culture wells, based on a pipetting method developed in DeCoster Lab, 48 hrs after development. A cartoon of tumor invasion is in Figure 2.3.

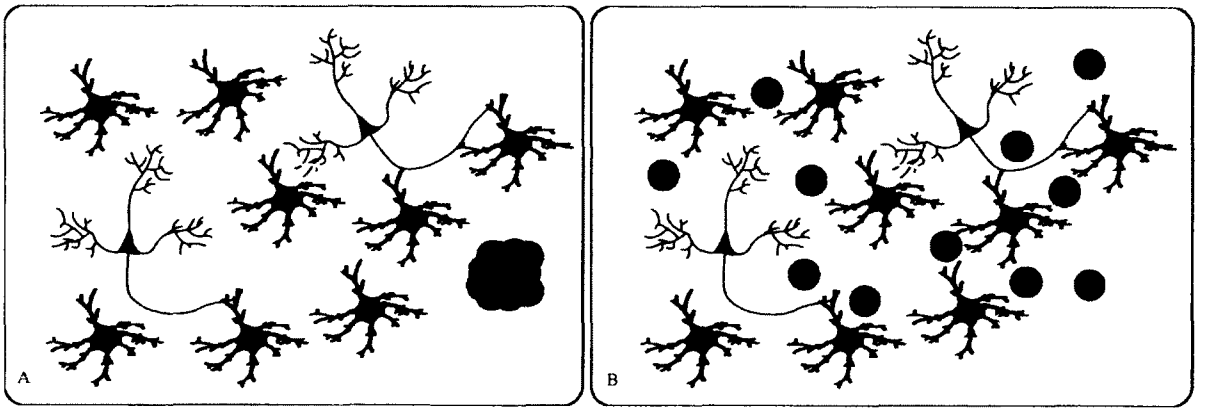


Figure 2.3 A) Tumor Invasion engineered environment with novel spheroid. B) Residual Cell engineered environment. *Red bodies*- glia *Blue bodies*- neurons *Green bodies*- glioma cells.

Resection of tumors is a common therapy option for diseased tissue; upon removal of the cancerous tumor, residual cancer cells are left in the surviving tissue. These residual cells are then treated with radiation; however, brain glioma has a high re-occurring tumor rate due to residual cancer cells [55]. To engineer this environment, 20,000 glioblastoma cells (CRL-2303) were added to normal 6 *days in vitro* primary cortical cell culture wells. The cultures were imaged after 2 *days in vitro* and remained in Neuronal Culture Media.

### 2.3 Calcium Fluorescence Imaging

Multiple experiments were implemented before a final experimental protocol was developed for the main research. Every protocol utilized weighed heavily on the substrate, cell type and reagents added while real-time imaging occurred. To determine the best methodologies in imaging calcium signaling, 50 mM KCL and 2 μM Ionomycin were used because the both provided known calcium influx, see Appendix A for image and DVD for video. All CRL-2303 cultures were loaded with Fluo 3/AM and imaged at 200X magnification. Astrocytes were imaged with the following objectives and substrates: chambered glass no.1 coverslips (Nunc) with 60X air and 40X oil objectives, glass bottom 35 mm dishes (Co) with a 40X oil objective, polystyrene 35 mm dishes (Falcon) with a 20X air objective and a 24 multi-well plate with a 20X air objective. The objective utilized for the experiment determined which fluorescence probe would be implemented. Fluo 3/AM was used with all plastic substrates; Fluo 4 and Fluo 8/AM were used on both 40X oil and 60X air objectives.

The main experiment employed primary cortical cells on a polystyrene surface with the Fluo 3/AM calcium indicator and a 20X objective. The cells were imaged with

an Olympus CKX31 inverted microscope with a 488 excitation wavelength filter over real time at 4 sec per frame with the InCyt Basic Im™ Imaging System (Intracellular Imaging, Inc., Cincinnati, OH.) A baseline (recording of spontaneous oscillations) was obtained for 60 sec, GLU concentrations were added to the experiment at predetermined intervals (60, 320, and 580 sec) without washing out the media between additions, Figure 2.4.

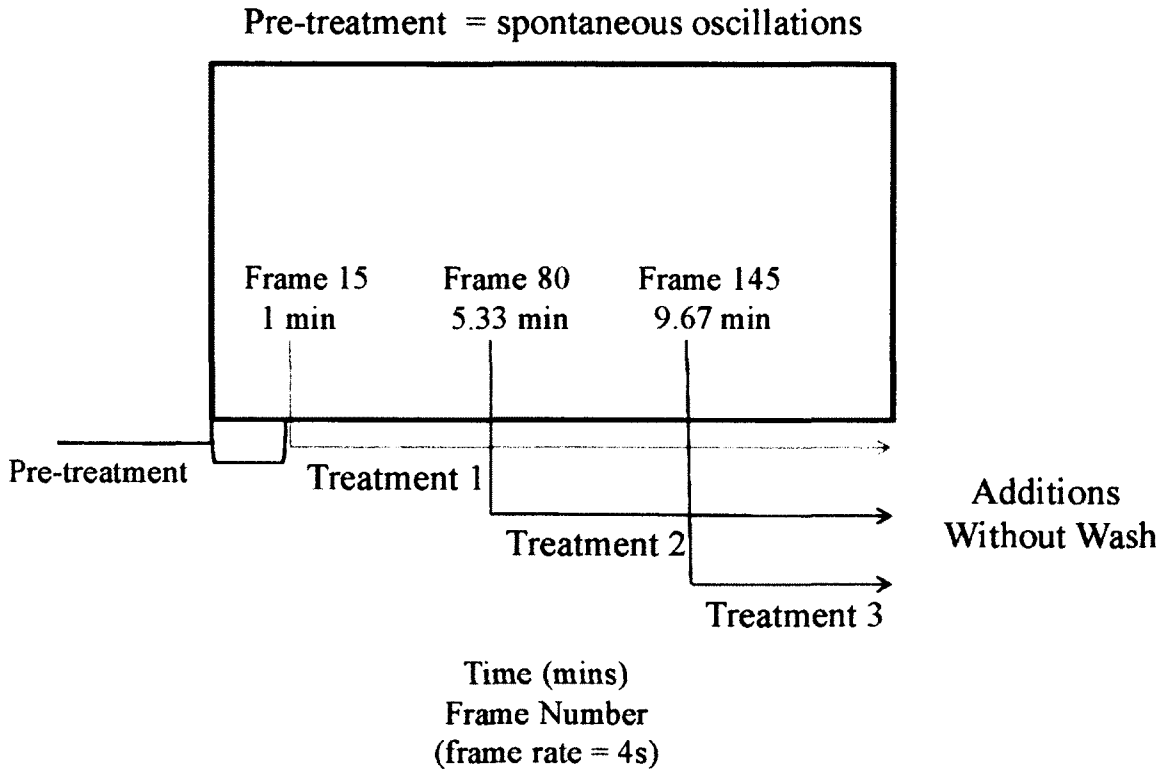


Figure 2.4 Stimulation protocol for experiments. Glutamate is added into the experiment at equally defined times and at three concentrations: 250 nM, 500 nM and 750 nM. Each concentration is added at a set treatment number without washing the glutamate addition from the experiment.

## 2.4 Measurement and Analysis of Fluorescence Intensity

InCyt Basic Im™ Imaging System software was utilized to create regions of interest (ROIs) around every neuron, which responded dynamically to glutamate with calcium influx, in the data set post experiment. The neurons are the main cell within these experiments that will respond to the subthreshold amounts of GLU. Glial fibrillary acidic protein stains have been performed (data not shown) to determine the amount of glia in cultures, also, the morphology and concentration of GLU are the main determinates that glia are not responding to the nM concentrations in which we are adding. Astrocytes require high concentrations (1 to 4 mM) of GLU to elicit fluorescence calcium responses, and the calcium response tends to slowly increase with time. The ROIs were then used to measure fluorescence intensity over time in the specified area. Every ROI was then normalized to 1; this was performed by dividing the ROI over-time by its starting value. Normalizing the data to 1 allows for correlation between the cells within an experiment and cross-experimentally. The data can then be represented with line tracings, and the average can then be calculated by averaging all ROIs for triplicate experiments.

Fluo 3/AM bonds non-covalently to calcium; therefore, it can easily disassociate from calcium. Free calcium concentration of a solution or the dissociation constant $K_d$ of a single-wavelength calcium indicator can be determined by the following equation [56]:

$$[Ca^{2+}]_{free} = K_d \left[\frac{F - Fmin}{Fmax - F}\right], \tag{2.1}$$

where F is the fluorescence of the indicator at experimental calcium levels, $F_{min}$ is the absence of fluorescence due to calcium chelation and $F_{max}$ is the fluorescence of the calcium-saturated probe.

Higher Statistics. Portions of the main experimental data were outsourced for higher order statistics and were compiled for the dissertation of Richard Idowu in Louisiana Tech University's Computational and Analysis program. Idowu developed multiple defining characteristics to determine key signaling dynamics within each experiment. Idowu developed analyses which can determine the Area Under the Curve (AUC, Figure 2.5) of a cells response to GLU and how many times the cell spikes per treatment of GLU (NumS, Figure 2.5) [57]. These two parameters are essential in determining calcium information processing and will be used throughout the discussion.

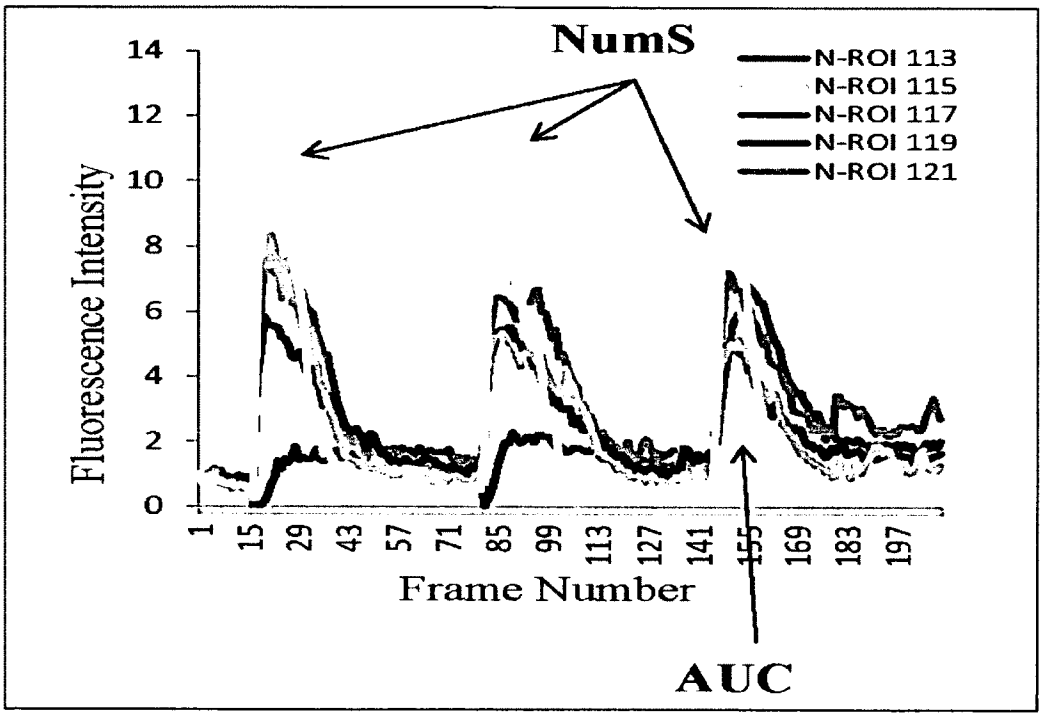


Figure 2.5 Representation of a line tracing depicting number of spikes (NumS) and area under the curve (AUC).

Area Under the Curve. The trapezoidal rule was applied to determine AUC for fluorescence-intensity time curve, f,

$$\int_a^b f(x)dx \approx (\mathrm{b} - \mathrm{a})\frac{f(a)+f(b)}{2}, \tag{2.2}$$

where time (s) is a and b, and their corresponding fluorescence intensities are f(a) and f(b) at the time interval's endpoints. A summation of evaluated areas is then compiled for every ROI [57].

Number of Spikes. A calcium fluorescence spike is defined as $X_{i+1}$ where $i$ = 1,……..,n and n is the range of the data, then the spike must reach 120% above the baseline (which baseline = 1) [57] if the inequality of $X_i < X_{i+1} > X_{i+2}$ is met.

# CHAPTER 3

## NORMAL MICROENVIRONMENT TO DETERMINE CALCIUM INFORMATION PROCESSING

### 3.1 The Normal Paradigm in Primary Cortical Cells

The resting concentration of cytosolic calcium in neurons is approximately 200 nM, and when stimulated the neuronal calcium can reach micromolar concentrations [33]; extracellular glutamate is also found in micromolar quantities around the synapse [46, 58], 50-160 mM in synaptic vesicles [59, 60], but intracellular vesicular glutamate concentration is approximately 10 mM. Sather and others have found L-glutamate at $\leq 1$ μM concentrations electro desensitized the NMDA receptor which was saturated with glycine; they also noted that ambient glutamate concentrations contributed significantly to synaptic plasticity [61].

This paradigm will test for calcium signaling of glutamate concentrations $4 \times 10^{-6}$ less than intracellular glutamate concentrations, 250 nM, and slightly less than one micromolar, which is present at the synapse to prevent any excitotoxic reactions. To determine which effect glia cells have on calcium signaling at submaximal stimulus concentrations, normal primary cortical cell microenvironments must be tested to obtain a control of overall calcium signaling. Primary cultures high in glia are able to regulate glutamate to keep homeostatic conditions. The regulation of glutamate in neurons is represented in a line tracing as sharp spikes. These spikes are only present in neurons in

these data sets, due to the high glutamate concentrations (millimolar) required to induce calcium spiking in glial cells.

The line tracings in Figure 3.1 displays glutamate receptor induced calcium fluorescence in response to increasing sequential, submaximal glutamate concentrations, 250, 500 and 750 nM. The colored lines represent individual neuron responses to the glutamate additions and were chosen randomly. The line tracings display whole spikes (rise in calcium and return to baseline) suggesting the data is not aliased; biochemical responses in calcium are slower than electrical stimulations and require multiple seconds to produce a calcium spike. The length of time in which it takes a calcium spike to occur is dèpendent on the negative feedback system provided by the glutamate reuptake system in glial cells. The black line represents the averaged individual responses to triplicate or greater experiments of the same experimental conditions. The individual ROIs in Figure 3.1 represent typical calcium signaling which should be observed in cultures high in glia. The average depicts how glia uptake the exogenous glutamate with very little neuronal excitation.

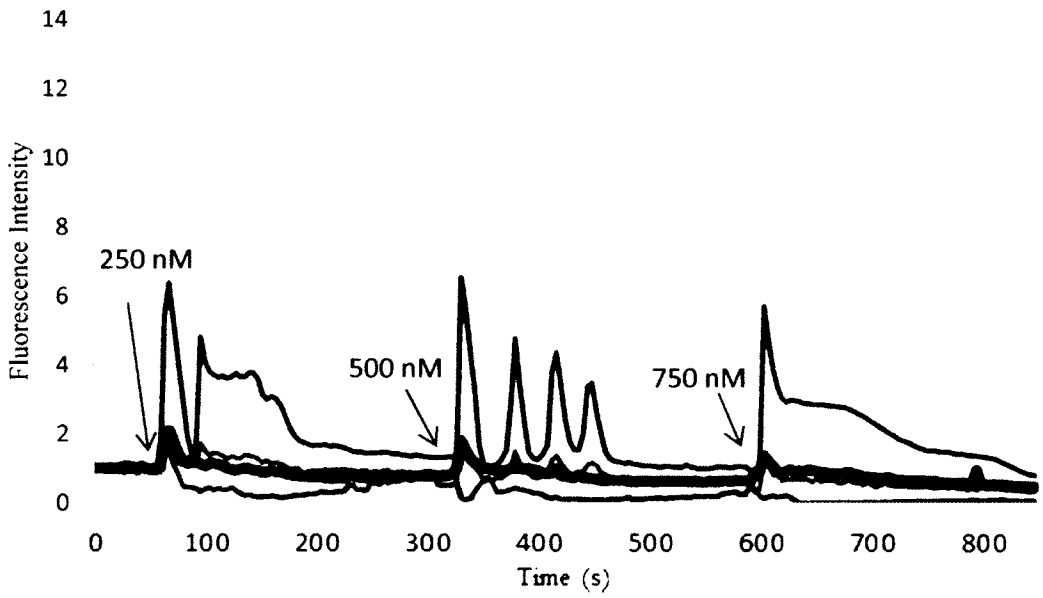


Figure 3.1 Line tracings of primary cortical cultures high in glia in response to additions of 250, 500 and 750 nM GLU concentrations. *Colored line*= individual ROI, *Black line*= average of n= 116.

To corroborate how glial cells affect calcium signaling in the normal paradigm, a microenvironment must be engineered to control glial cells in culture. This microenvironment is engineered with cytosine arabinoside (AraC) at 3 DIV. The AraC cultures are depleted of glia and when exposed to glutamate display very broad and high amplitude response to calcium influx, see Figure 3.2. These broad peaks are also indicators of excitotoxicity; line tracings of excitotoxic responses plateau, meaning the tracing does not return to baseline. The excitotoxic response in calcium signaling to glutamate could infer spillover of glutamate onto the dendritic NMDA receptors.

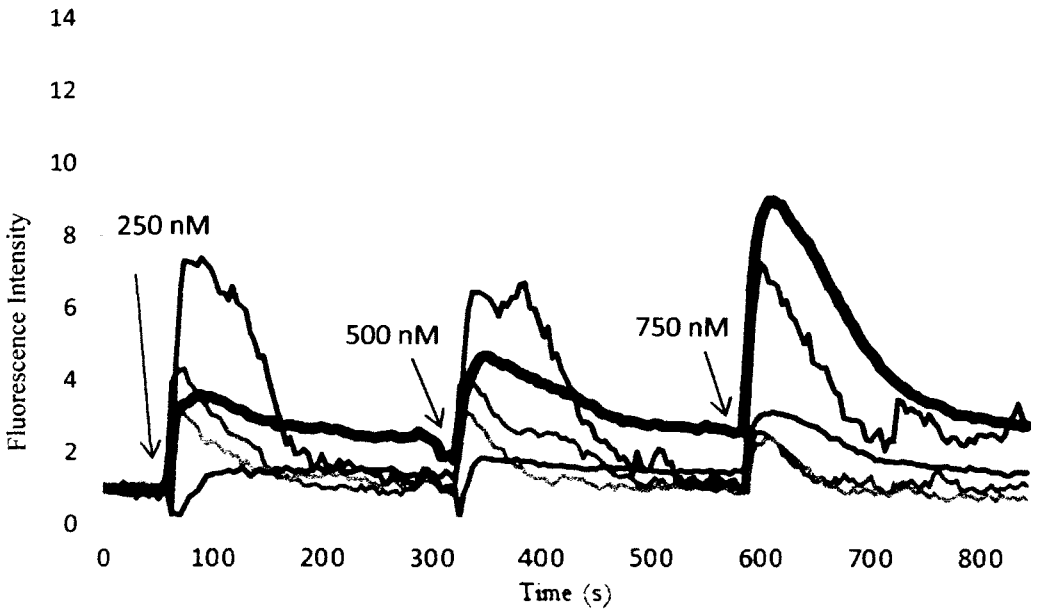


Figure 3.2 Primary cortical cells depleted of glia with the additions of 250, 500 and 750 nM glutamate concentrations. *Colored line*= individual ROI, *Black line*= average of n= 127.

To further elucidate the effects glial cells have on calcium signaling, area under the curve (AUC) and number of spikes (NumS) were analyzed per microenvironment. Figure 3.3 displays how glial cells reduce the NumS in cultures high in glia while, cultures depleted of glia have a high volume of spikes per treatment type. However, the NumS for every pre-treatment is low regardless of engineered microenvironment, which represents very few spontaneous calcium spikes.

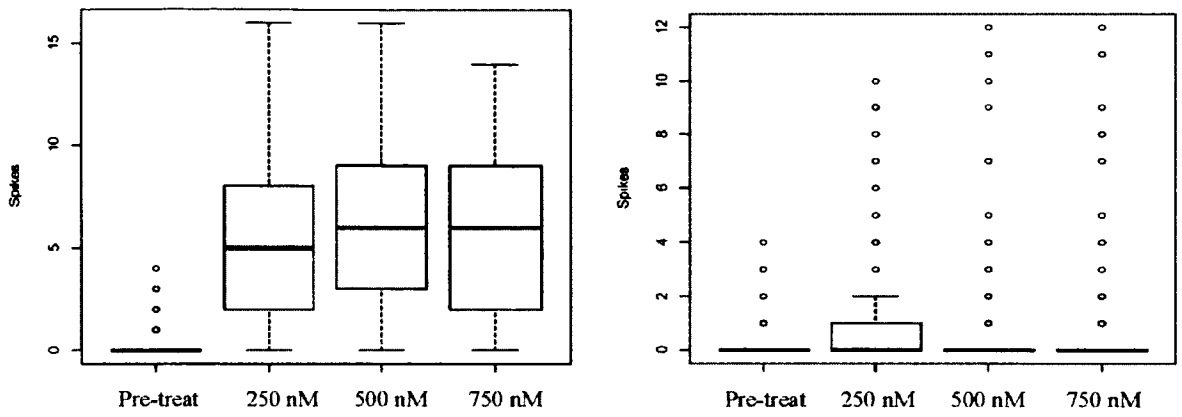


Figure 3.3 Number of spikes (NumS) in response to glutamate treatments. *left)* Cultures depleted of glia *right)* Cultures high in glia *Circles-* indicate outliers.

AUC better elucidates the effects glial cells have on calcium signaling when trying to determine the amount of calcium which has permeated into the cytosol. As expected, cultures depleted of glia increase in AUC as concentrations in GLU increase. In contrast, cultures high in glia have very low AUC per treatment and a slight decrease in AUC with increasing treatment additions, as seen in Figure 3.4.

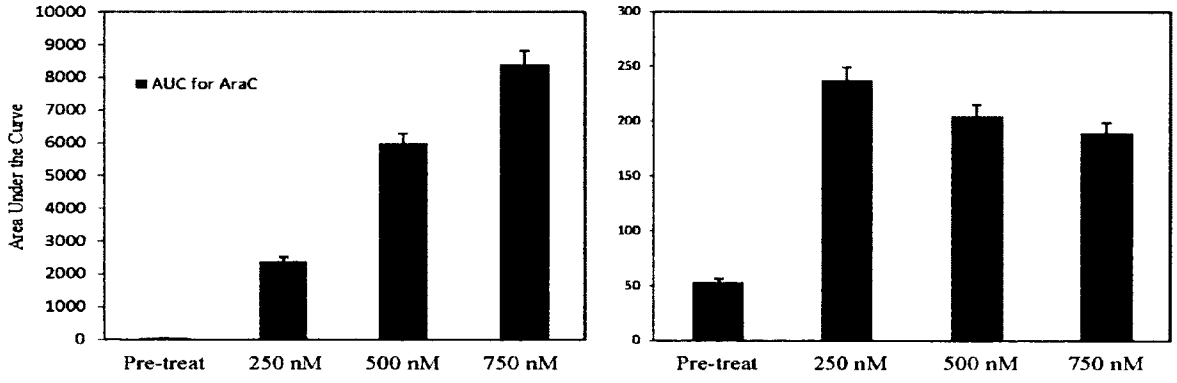


Figure 3.4 Area under the curve (AUC) in response to glutamate treatments. *left)* Cultures depleted of glia *right)* Cultures high in glia.

## 3.2 Glycine Bath with Normal Paradigm

To further test the experimental microenvironment, the engineered microenvironments were incubated for 30 minutes after dye loading in a glycine bath to allow cells to recover from loading; the experiment was also performed in the glycine bath. Glycine is a known co-agonist of the NMDA receptor and without simultaneous binding of glycine and glutamate the NMDA receptor will not fully open. The line tracings in Figure 3.5 show glycine treated cultures to exhibit the same calcium dynamic behavior as previously seen in the normal glutamate additions in cultures depleted of glia. This stepwise, increasing AUC and amplitude behavior can be attributed to glycine binding from media prior to recovery in glycine bath.

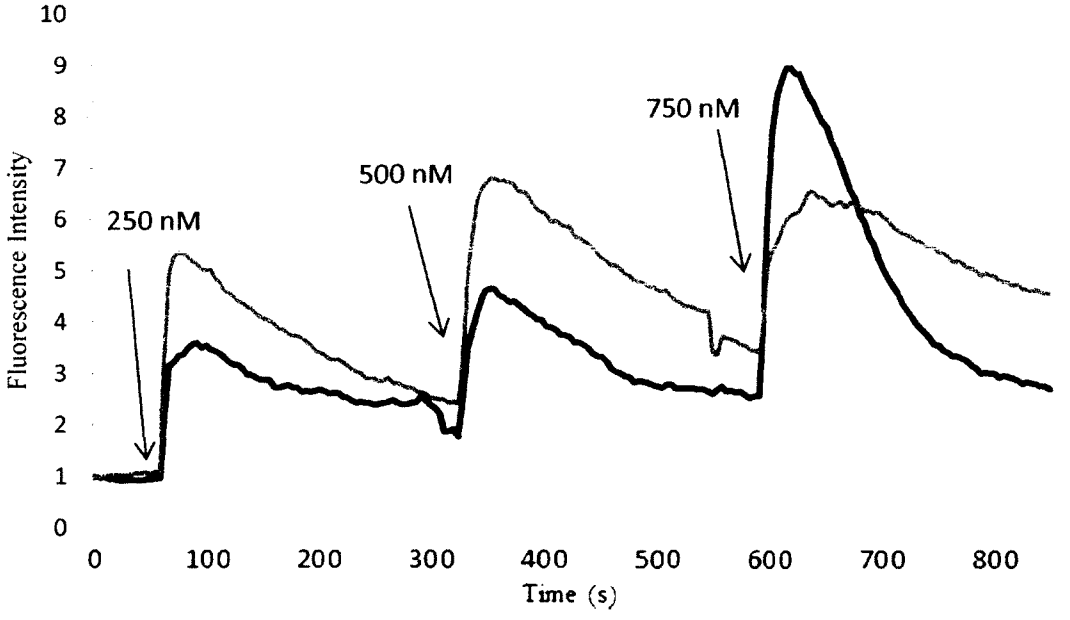


Figure 3.5 Line tracing of primary cortical cultures depleted of glia recovered in a 10 μM glycine bath with additions of 250, 500 and 750 nM Glu. *Black line*= average of individual ROIs in depleted glia cultures, *Red line*= average of individual ROIs in depleted glia cultures recovered in glycine bath.

The cultures high in glia were then analyzed to determine if glycine bath recovery had an effect on calcium signaling. The results can be seen in Figure 3.6, and there are not any visible differences between the two treatment types in amplitude of the spike and AUC.

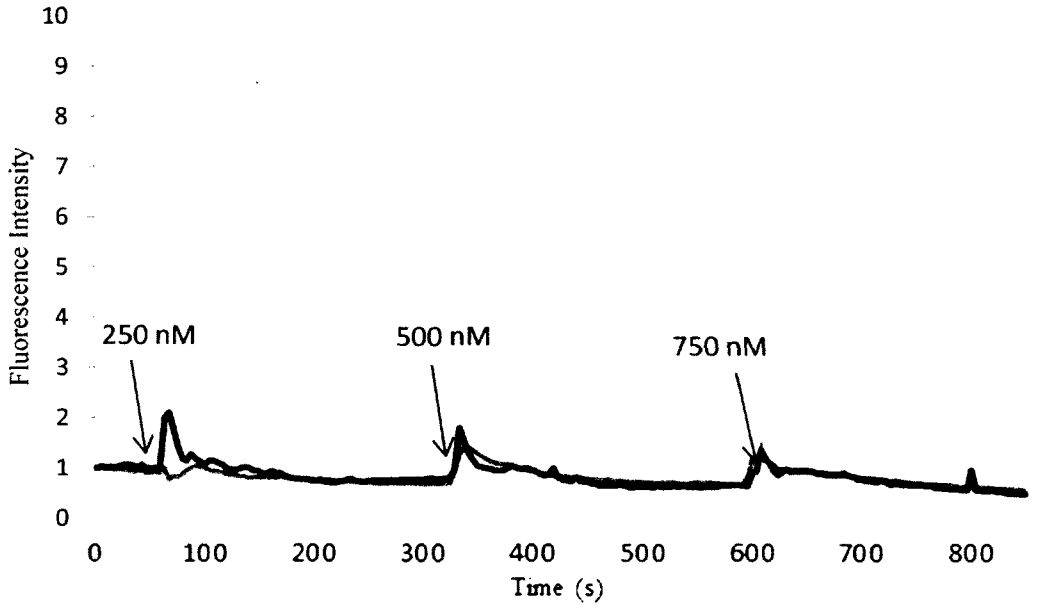


Figure 3.6 Line tracing of primary cortical cultures high in glia recovered in a 10 μM glycine bath with additions of 250, 500 and 750 nM Glu. *Black line*= average of individual ROIs in depleted glia cultures, *Red line*= average of individual ROIs in depleted glia cultures recovered in glycine bath.

### 3.3 NMDA Receptor Inhibitors and Blockers

Recent studies [62] in the lab have reported the effects of $Ca^{2+}$ channel blockers and antagonists of the NMDA and GABA receptors. Bicuculline is an inhibitor of the GABA receptor, which inhibits inhibition causing calcium signaling seen in epilepsy. However, when bicuculline is used at a concentration of 50 μM, it can have inhibitory effects on the NMDA receptor [63]. Dizocilpine (MK-801) is a non-competitive blocker

of the NMDA receptor and has been used in studies for ischemia. Figure 3.7 displays primary cortical neurons in response to bicuculline which exhibits epileptic calcium responses, these broad calcium responses are then blocked by the non-competitive MK801. The NMDA receptor remains blocked until a high concentration of glutamate is added exogenously to the system. The line tracing allows elucidation of the NMDA receptor responsible for calcium influx into the cytosol by means of exogenous glutamate stimulation.

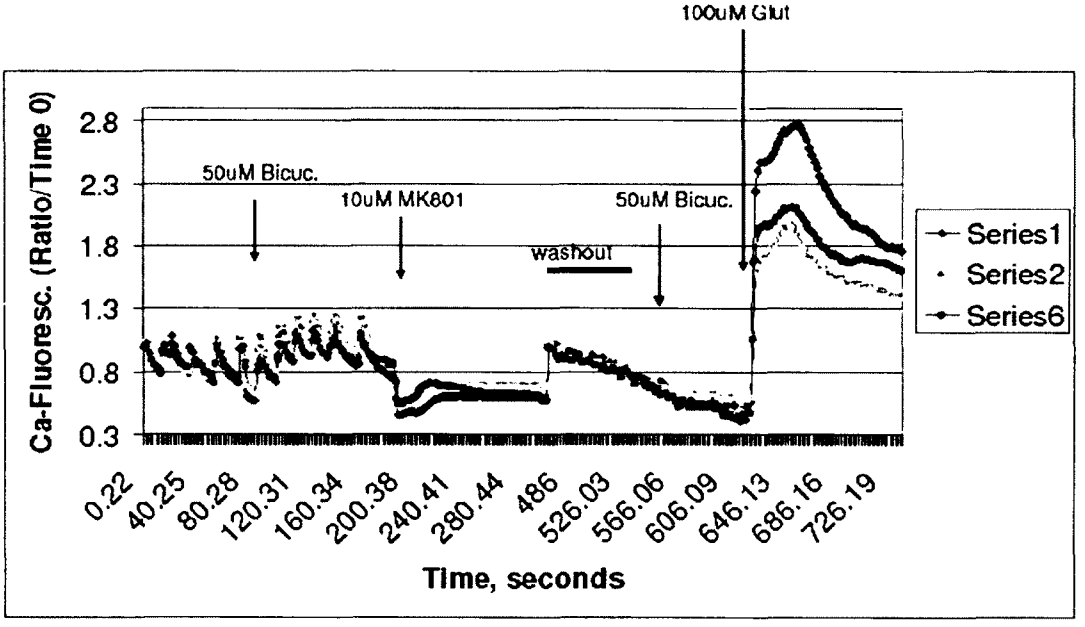


Figure 3.7 Line tracings of neurons in response to inhibition and blocking of the NMDA receptor [62].

One of the overall motivations of this project was to engineer an environment to determine how calcium signaling is affected by residual or metastatic microenvironments and how these environments differ to one another in calcium signaling dynamics. Glioblastoma cell lines are provided by ATCC with their own respective media; however,

the following experiments would need to be performed to see if engineering an environment which places CRL-2303 cells in neuronal culture medium would have deleterious effects on calcium signaling to glutamate. Figure 3.8 represents the glioblastoma cell line, CRL-2303, in its respective media, with the additions of the normal paradigm of increasing submaximal glutamate concentrations after 3 DIV.

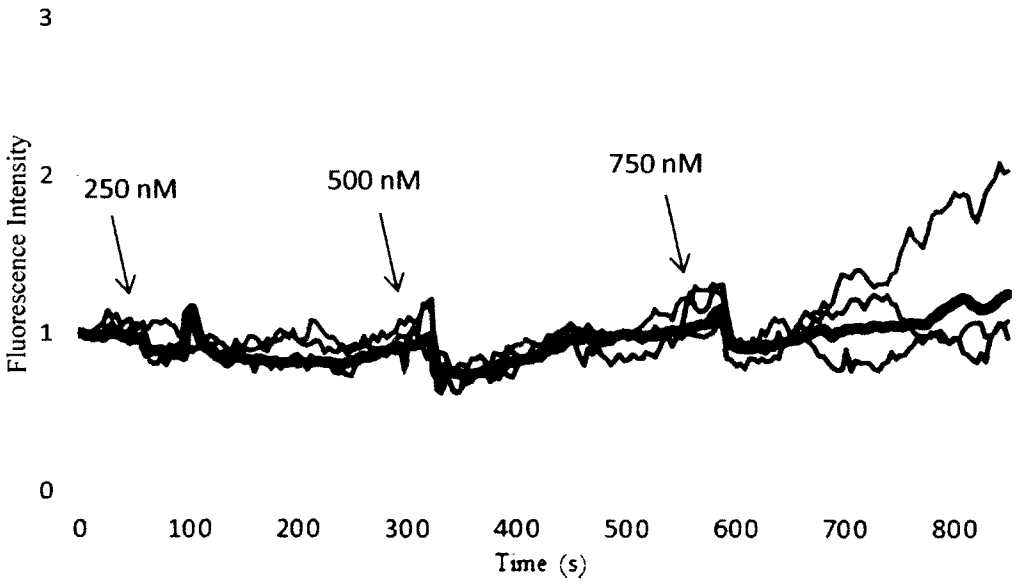


Figure 3.8 Line representations of glioblastoma cells in respective media with additions of 250, 500 and 750 nM glutamate concentrations. *Colored lines*= individual ROIs, *Black line*= averaged ROIs n= 42.

Glutamate does not appear to have a significant impact on calcium signaling, based on AUC or NumS except maybe at 750 nM GLU concentration. Next, CRL-2303 cells were cultured in NCM media for 3 DIV and then imaged for glutamate calcium responses. As seen in Figure 3.9, the average calcium response to glutamate is negligible when cells are cultured in neuronal culture medium. These effects are expected since

glioblastoma cells are a derivate of a normal glial cell. Figure 3.10 displays both glioblastoma graphs in the different medias to better compare the data.

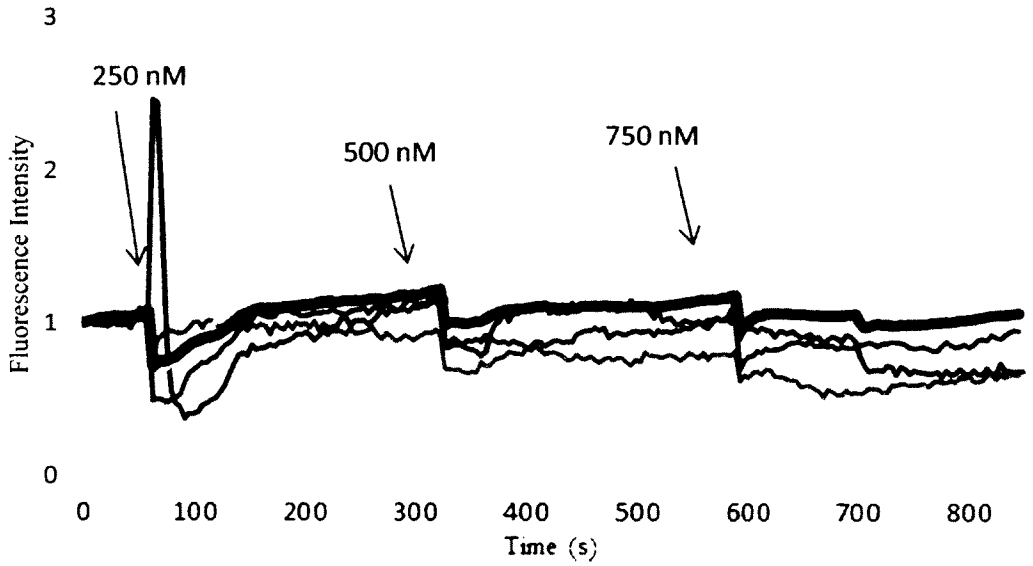


Figure 3.9 Line tracings of glioblastoma cultured in Neuronal Culture Media with the additions of 250, 500 and 750 nM glutamate concentrations. *Colored line* = individual ROIs, *Black line* = average of individual ROIs n= 73.

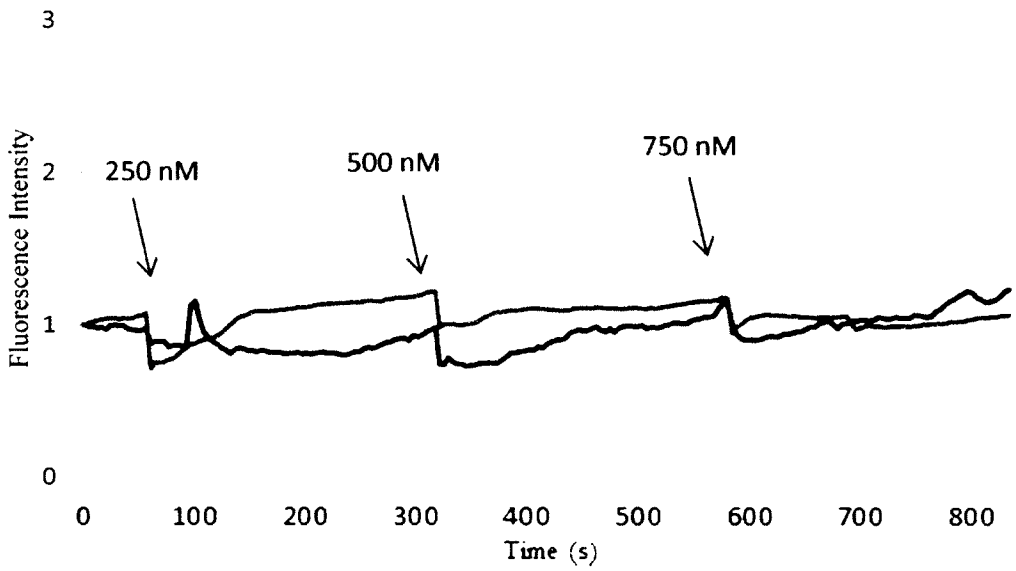


Figure 3.10 Line tracings of glioblastoma cultured in NCM versus CRL-2303 media with the additions of 250, 500 and 750 nM glutamate concentrations. *Red line*= average ROIs in NCM, *Blue line*= average ROIs in 2303 media.

# CHAPTER 4

## ENGINEERING THE MICROENVIRONMENT AND RANDOMIZATION OF STIMULUS TO MODULATE INFORMATION PROCESSING

### 4.1 Calcium Processing in Cultures

#### 4.1.1 Calcium Processing in Cultures Depleted of Glia

Once the microenvironments have been established, high in glia and depleted of glia, randomization of submaximal glutamate stimulus is employed to determine the effects glial cells have on calcium information processing. In addition to the normal paradigm five other paradigms will be employed to test the effects glia cells have on calcium processing. It has been established that the normal paradigm is increasing submaximal glutamate stimulus. The other five paradigms are randomizations of the aforementioned sequence, (3!). Only one randomization paradigm which was selected for higher level statistics based on the sequence of glutamate additions and will be presented for discussion in both engineered microenvironments.

As discussed in Chapter 3, the depleted glial cultures in the normal paradigm had large AUC and NumS per treatment of glutamate; this paradigm is represented once again in Figure 4.1 to easily compare the AUC and NumS in the following graphs.

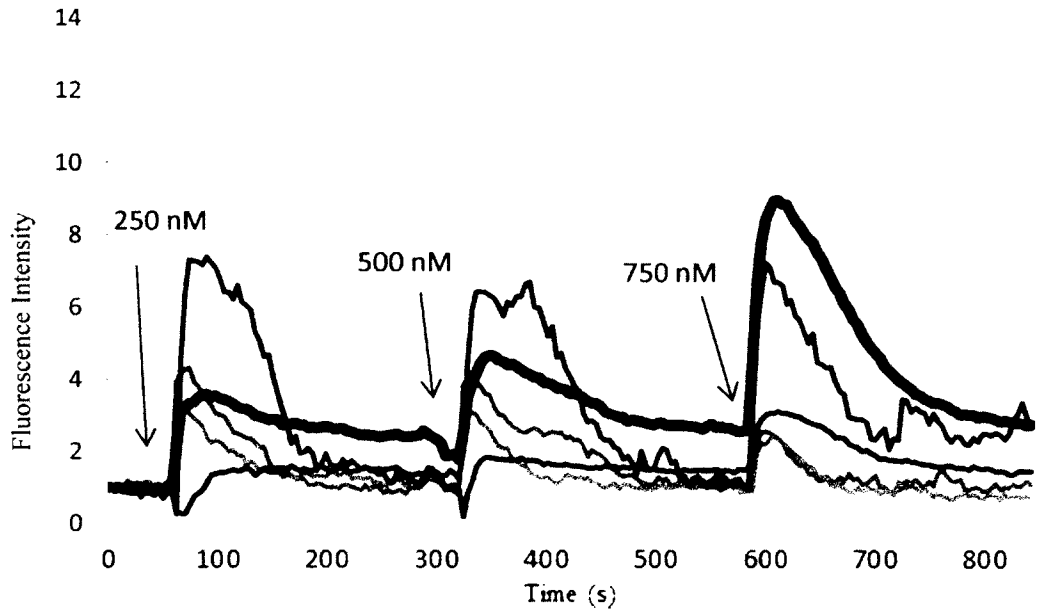


Figure 4.1 Line tracings of primary cortical cells depleted of glia with the additions of 250, 500 and 750 nM glutamate concentrations. *Colored line*= individual ROI, *Black line*= average of n= 127.

Randomization of the Stimulus. Randomization of the sequence of glutamate stimulus will help elucidate how neurons process stimuli, as well as, how glial cells affect the processing of each stimuli. The first randomized sequence which will be discussed is 250, 750 and 500 nM GLU; the scale in which the cells are fluorescing is low, however, the regions of interest in the line tracing have plateaued oscillations representing excitotoxic conditions, Figure 4.2. These plateaued oscillations would project high area under the curves when compared to oscillations in the environment with high glia, shown later in the chapter.

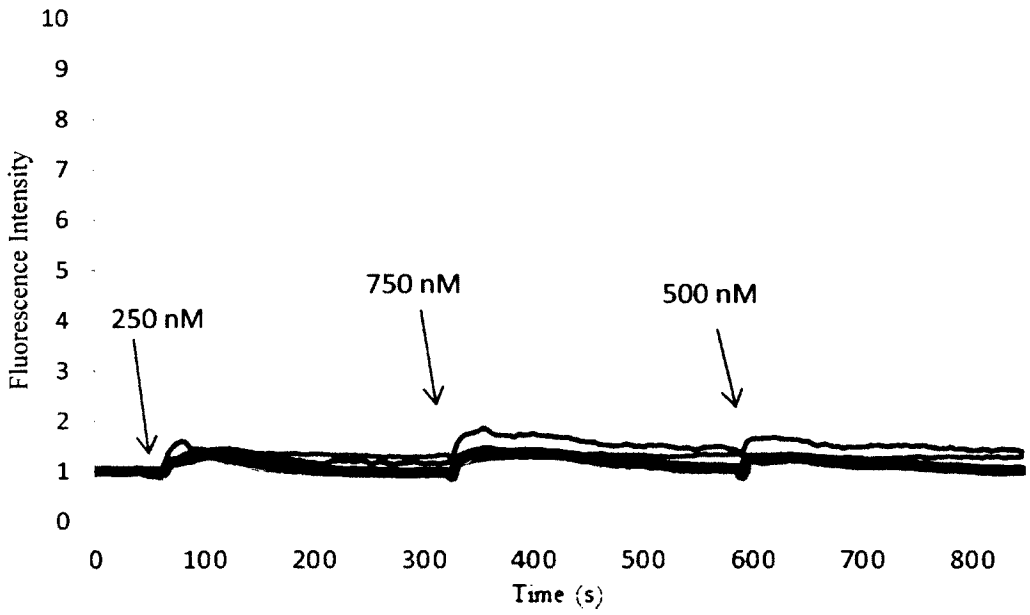


Figure 4.2 Line tracing of primary cortical cells depleted of glia with the additions of 250, 750 and 500 nM glutamate concentrations. *Colored line*= individual ROI, *Black line*= average of n= 67.

The next randomization sequence is 500, 250 and 750 nM GLU and the line tracings are represented in Figure 4.3. The line tracings per glutamate treatment display different calcium processing than in the previous two paradigms. The first treatment of GLU, 500 nM, caused the neurons to respond to calcium transiently; if the treatment were allotted more time, it most likely would have completely returned to baseline. Due to the transient response to the first treatment, the lower concentration of the second stimulus was recognized by the neurons with another transient response. The third stimulation was the highest concentration of glutamate and has the lowest amplitude of calcium fluorescence, however, the response plateaus representing excitotoxicity. Excitotoxicity is represented in a line tracing as a non-transient influx of calcium or the spike does not

return to baseline, resulting in a plateaued appearance, depending on the amplitude of fluorescence, excitotoxicity can have less AUC than a normal response spike.

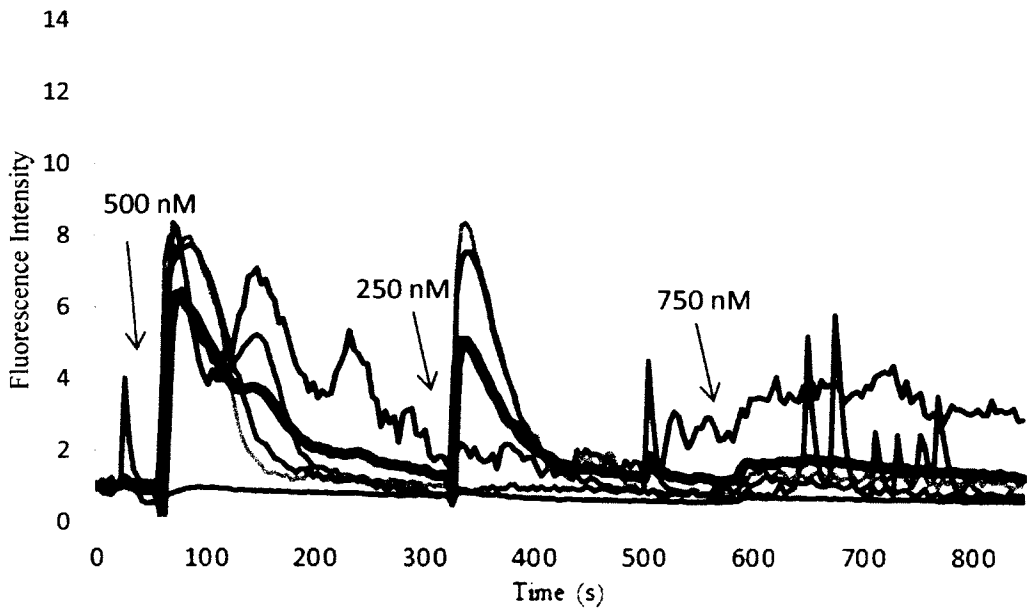


Figure 4.3 Line tracings of primary cortical cells depleted of glia with the additions of 500, 250 and 750 nM glutamate concentrations. *Colored line*= individual ROI, *Black line*= average of n= 82.

This paradigm was outsourced for higher statistical analysis and if the outsourced data is not shown with the line tracings it could be misinterpreted. The NumS per treatment type displayed in Figure 4.4 shows the median NumS per cell actually decreases with the lower glutamate stimulus; this decrease in number of spikes to glutamate is the known reaction of how neurons would typically respond to a decreased glutamate stimuli. When looking at the outsourced data for AUC, a decreasing trend in the data is observed. This data was very intriguing until paired with the line tracings. Correlating AUC and the line tracings for the 750 nM treatment elucidates why the least

area under the curve represented is paired with the highest concentration of glutamate- it is excitotoxic.

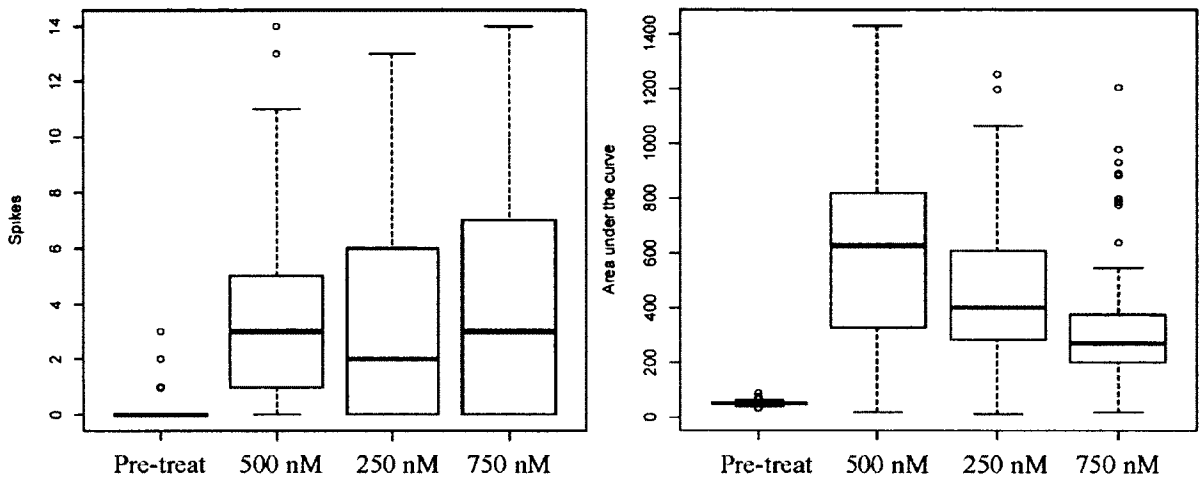


Figure 4.4 Higher statistics performed for *left)* Number of Spikes and *right)* Area Under the Curve in cultures depleted of glia with the additions of 500, 250 and 750 nM glutamate concentrations. *Circles*- represent outliers.

The next paradigm is the 500, 750 and 250 nM GLU concentration sequence. The first treatment does not completely return to baseline, however, when the second stimulus is higher than the first the neuron is forced to respond to the increased glutamate signal. The second treatment line tracing average, Figure 4.5, displays a transient spike. This transient response does not return to the experimental baseline, but instead to the starting baseline of the second treatment. The neurons then recognize the lower glutamate stimulus in the third treatment type, even though the area under the curves is substantially increasing.

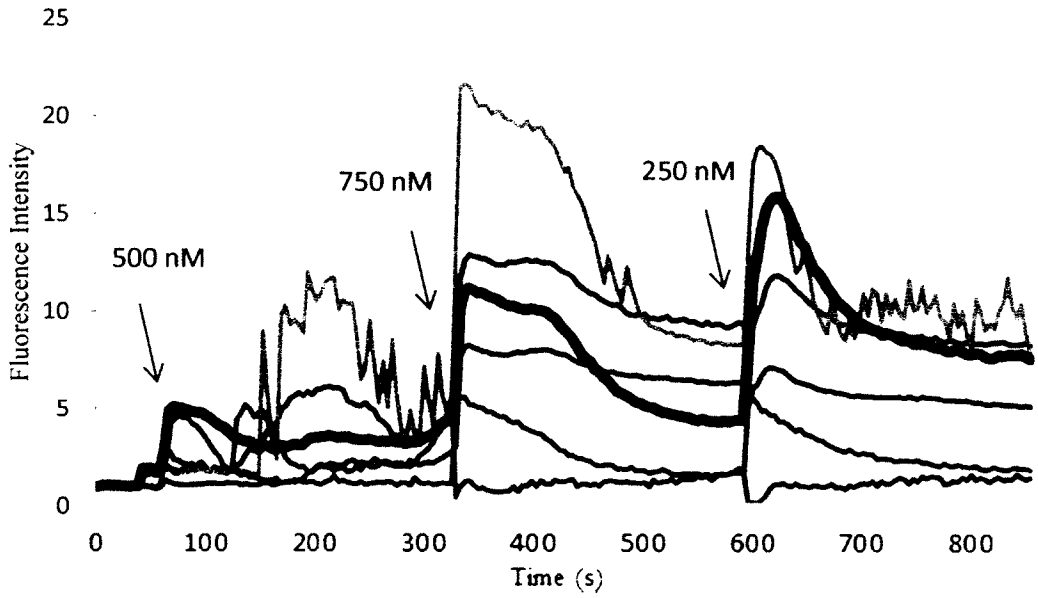


Figure 4.5 Line tracings of primary cortical cells depleted of glia with the additions of 500, 750 and 250 nM glutamate concentrations. *Colored line*= individual ROI, *Black line*= average of n= 72.

The paradigms beginning with the highest glutamate stimulus both have low fluorescence intensity scales, but start to expose trends within varying glutamate concentration sequences. The paradigm in which the sequence is 700, 250 and 500 nM glutamate is represented in the line tracings in Figure 4.6. The neurons respond transiently to the initial stimulus of 750 nM, thus the lower 250 nM concentration in the second treatment responds transiently with a slight biphasic response in intracellular calcium, this could be from intracellular stores of calcium being released [64], see Appendix C for example of wave. The neurons then respond to the third stimulus with a transient response. The response in calcium signaling we are starting to see with the data suggests neurons will respond to varying glutamate concentrations only when the oscillation has returned to its starting treatment baseline value.

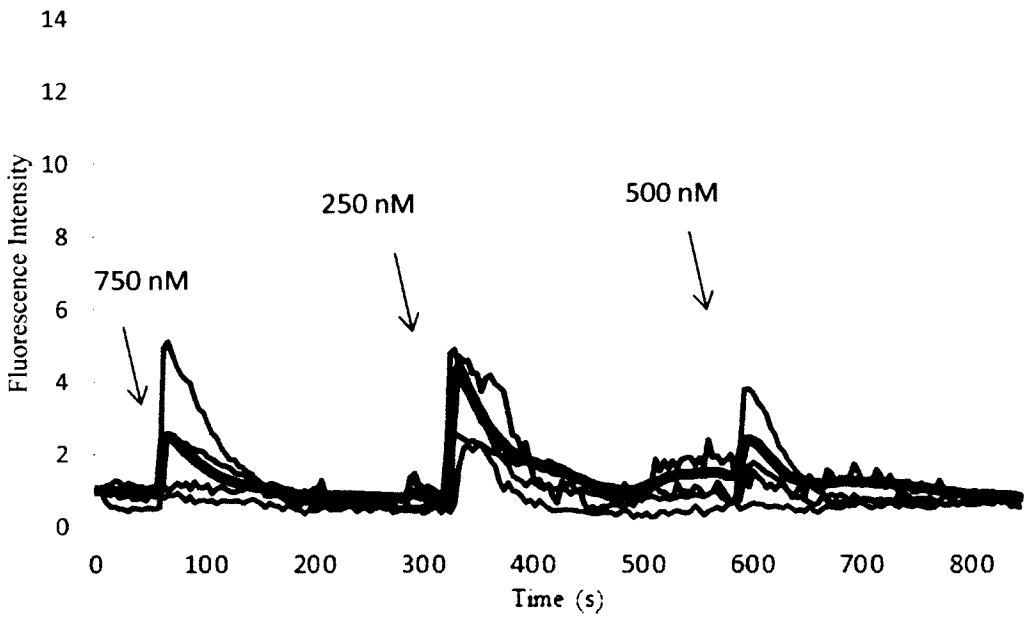


Figure 4.6 Line tracings of primary cortical cells depleted of glia with the additions of 750, 250 and 500 nM glutamate concentrations. *Colored line*= individual ROI, *Black line*= average of n= 94.

This observation is further elucidated in the following paradigm, 750, 500 and 250 nM. As seen in Figure 4.5, the neurons had the ability to transiently respond to the 750 nM concentration within the treatment time; this is not the case for the paradigm shown in Figure 4.7. The line tracings suggest an event where the second treatment is ignored until the first treatment has had sufficient time to recover. We can hypothesize a scenario in which the neurons ignore the signal in part, because the concentration is lower than the first stimuli. Also, the neurons depicted in the line tracings in Figures 4.1 and 4.3, display sequential treatment calcium oscillations where the first treatment is a lower concentration than the second treatment, but the first calcium response does not return to the beginning treatment baseline value, which suggests the second treatment responds with a calcium oscillation because the second stimulus is higher than the first.

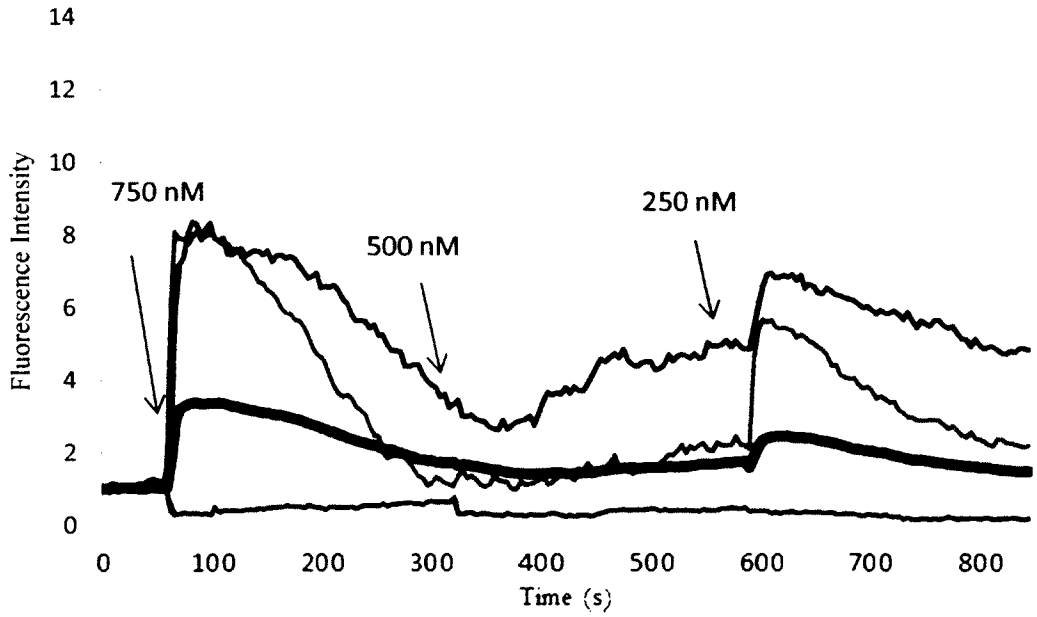


Figure 4.7 Line tracings of primary cortical cells depleted of glia with the additions of 750, 500 and 250 nM glutamate concentrations. *Colored line*= individual ROI, *Black line*= average of n= 79.

### 4.1.2 Calcium Processing in Cultures High in Glia

Glutamate homeostasis is a process carried out by the glial cells. In past experiments of pure astrocyte cultures, data not shown, the glia were unresponsive with calcium influx until glutamate was added in millimolar concentrations exogenously. The same paradigms will be utilized to illuminate the effects glia cells have on calcium processing in the brain.

The normal paradigm in shown in Figure 4.8; each treatment of glutamate has a very sharp-transient, calcium oscillation response. When the line tracings are compared to the normal step-wise increasing additions of glutamate in the cultures depleted of glia, the high in glia cultures have very small area under the curve values.

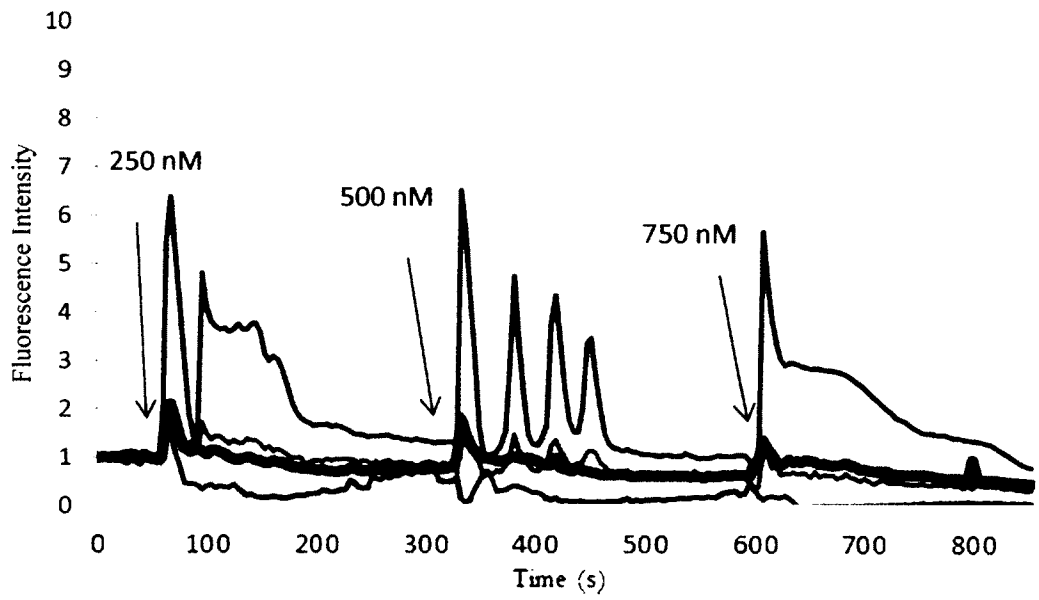


Figure 4.8 Line tracings of primary cortical cells high in glia with the additions of 250, 500 and 750 nM glutamate concentrations. *Colored line*= individual ROI, *Black line*= average of n= 116.

Randomization of the Stimulus. The first randomized paradigm will have the lowest glutamate stimulus proceeded by the highest, 250, 750 and 500 nM, the line tracings are represented in Figure 4.9. Again, the calcium processing response produces very sharp spikes with very little area under the curve. There are also less NumS due to decreased exogenous glutamate to stimulate the neurons in culture.

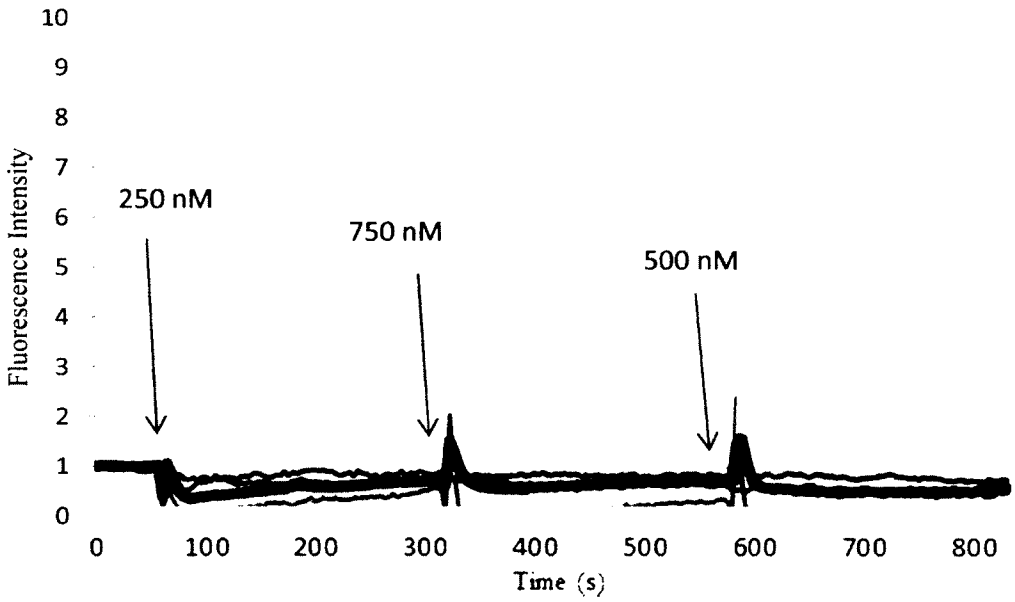


Figure 4.9 Line tracings of primary cortical cells high in glia with the additions of 250, 750 and 500 nM glutamate concentrations. *Colored line*= individual ROI, *Black line*= average of n= 161.

The following randomization paradigm was outsourced for higher level statistics, and the line tracings are shown in Figure 4.10. The tracing shows very low amplitude calcium spikes with transient responses back to experimental baseline. These visual observations correlate with the quantified data in Figure 4.11. The NumS graph displays a low spike value for how many times a cell oscillates throughout the treatments, and AUC depicts a slight decreasing response to glutamate treatment. These results are expected due to the numbers of glia within the cultures reducing the amount of glutamate responsible for producing these type calcium spikes.

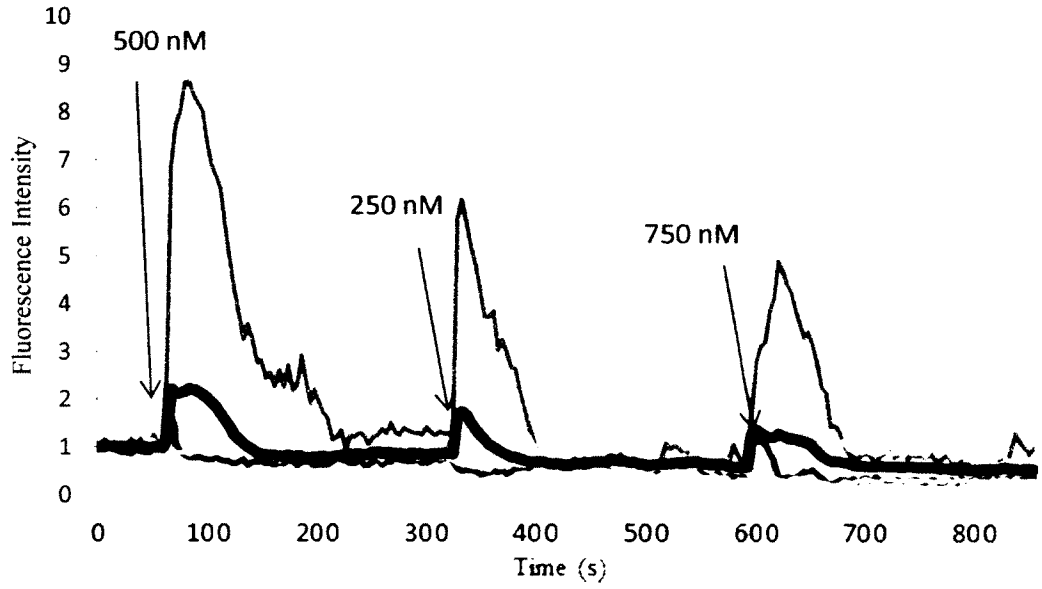


Figure 4.10 Line tracings of primary cortical cells high in glia with the additions of 500, 250 and 750 nM glutamate concentrations. *Colored line*= individual ROI, *Black line*= average of n= 76.

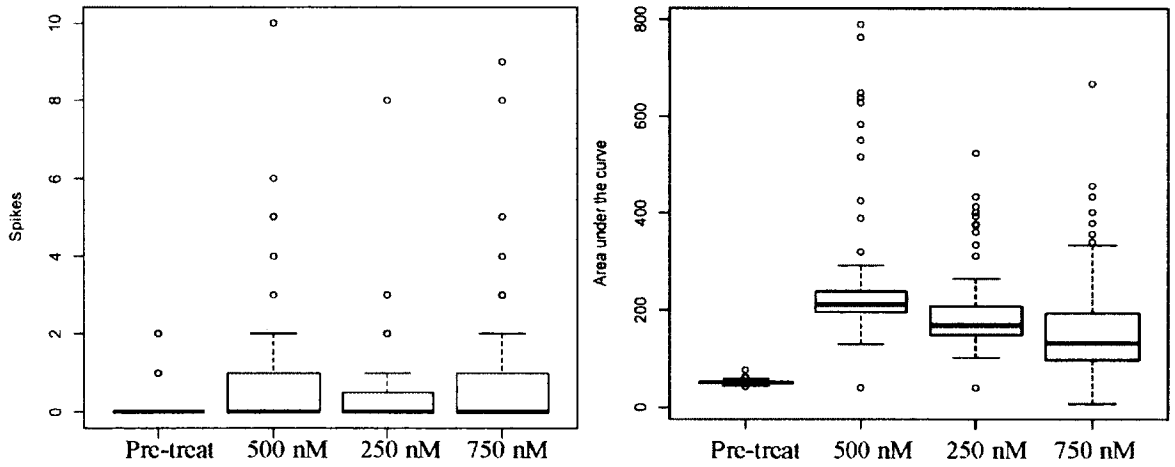


Figure 4.11 Higher statistics for *left)* number of spikes (NumS) and *right)* area under the curve (AUC.) *Circles*- represent outliers.

The next paradigm has the second treatments as the highest glutamate stimulus followed by the lowest glutamate stimuli in the third treatment, 500, 750 and 250 nM

glutamate. Figure 4.12 elucidates how naive neurons to exogenous glutamate concentrations respond with varying calcium transient curves. These line tracings represent the neurons' ability to respond to a large decreasing concentration of glutamate, almost equal to the neurons resting potential, with glia present in the culture.

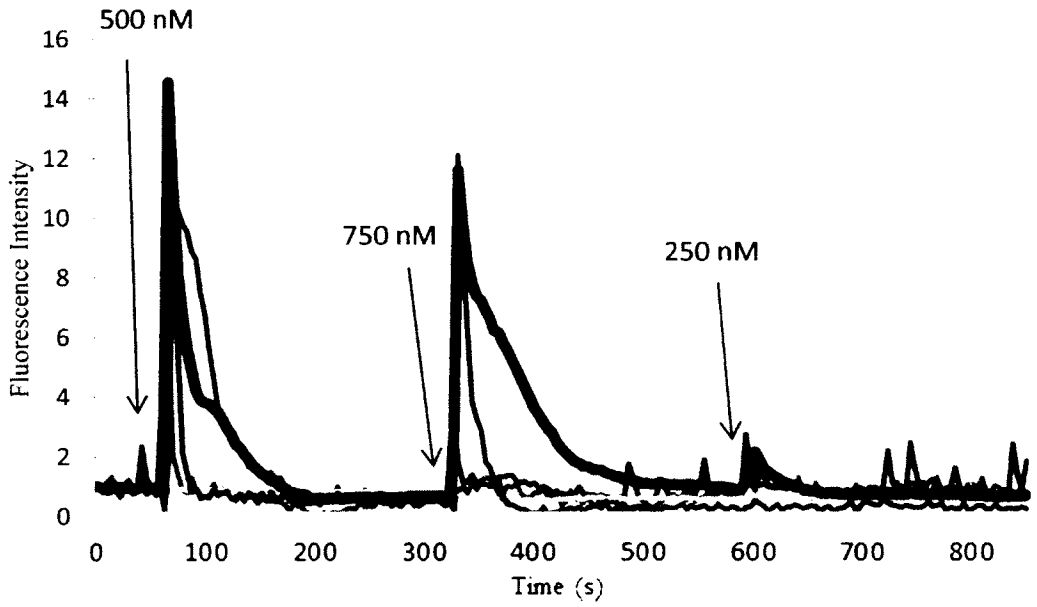


Figure 4.12 Line tracings of primary cortical cells high in glia with the additions of 500, 750 and 250 nM glutamate concentrations. *Colored line*= individual ROI, *Black line*= average of n= 86.

The paradigms in which the greatest glutamate stimuli is in the first treatment are 750, 250 and 500 nM and 750, 500 and 250 nM glutamate. In Figure 4.13, the line tracings fluorescence intensity is low; however, we see the continuing trend of glial cell uptake of exogenous glutamate and neuronal response decreased. The line tracing in Figure 4.14 represents the same trend as the following paradigms; glutamate stimuli do not cause excitotoxic responses at submaximal glutamate concentrations when glial cells

are present in cultures. Also, the glutamate stimuli are quickly taken up by the glial cells as can be seen with the fast transient responses to baseline, suggesting spillover of the glutamate stimulus is not occurring due to the lack of excitotoxic response.

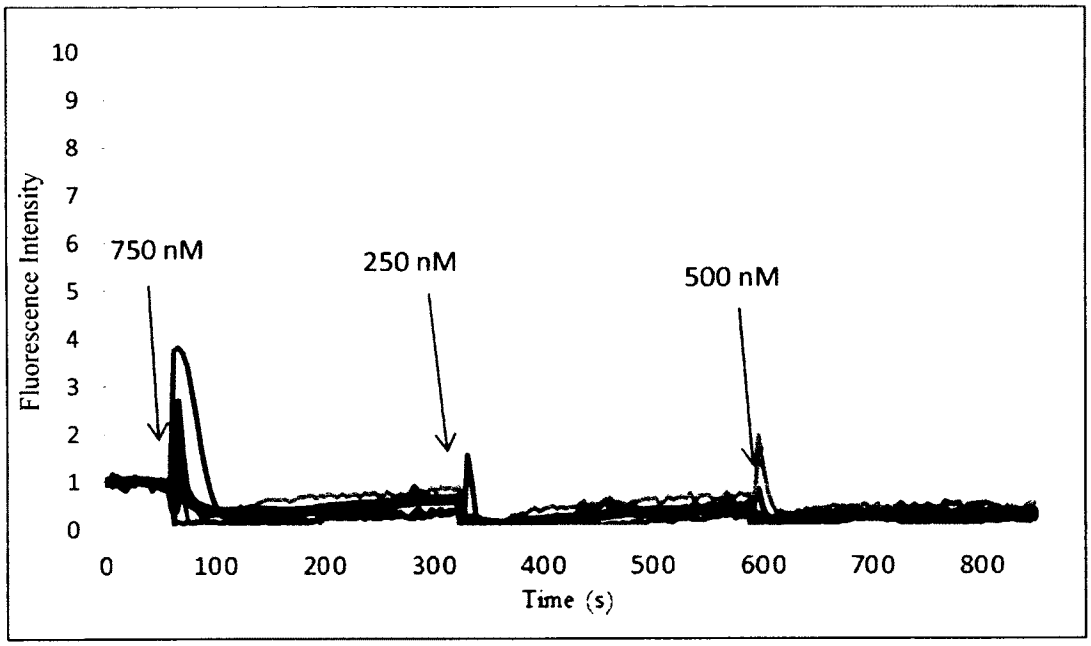


Figure 4.13 Line tracings of primary cortical cells high in glia with the additions of 750, 250 and 500 nM glutamate concentrations. *Colored line*= individual ROI, *Black line*= average of n= 142.

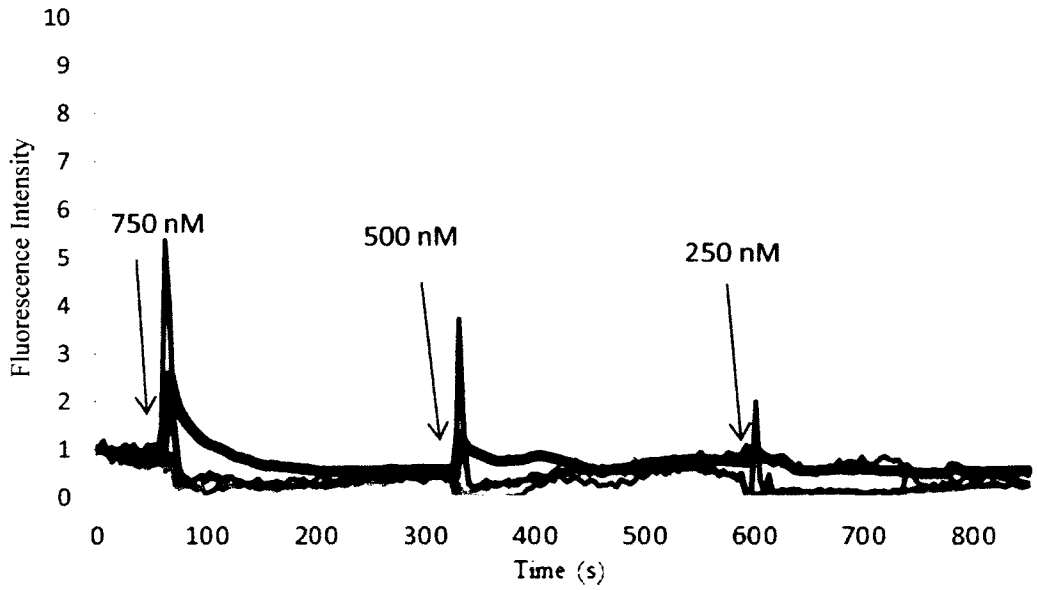


Figure 4.14 Primary cortical cells high in glia with the additions of 750, 500 and 250 nM glutamate concentrations. *Colored line*= individual ROI, *Black line*= average of n= 148.

## 4.2 Comparison of Calcium Processing in Engineered Cultures

### 4.2.1 Normal Paradigm Comparison

The normal paradigm better exposes the glial cell influence on calcium processing when submaximal stimuli are added to the system. This comparison suggests an environment must be engineered to reduce glia in order to facilitate experiments on how neurons process submaximal stimuli. The line tracings are represented in Figure 4.15. The outsourced data is also represented in Figure 4.16 in comparisons to clearly illuminate the effect glial cells have on calcium processing. The scales are different because the effects cannot be appreciated if they were set to the same range. The data clearly suggests a 40-fold decrease in area under the curve when glial cells are present in cultures. Also, the number of spikes per cell by treatment has visibly decreased in glial

rich cultures. The data also suggests a slight decreasing trend in AUC with cultures high in glia to increasing glutamate by treatment, as compared to cultures depleted in glia, which AUC increases by increasing glutamate treatments.

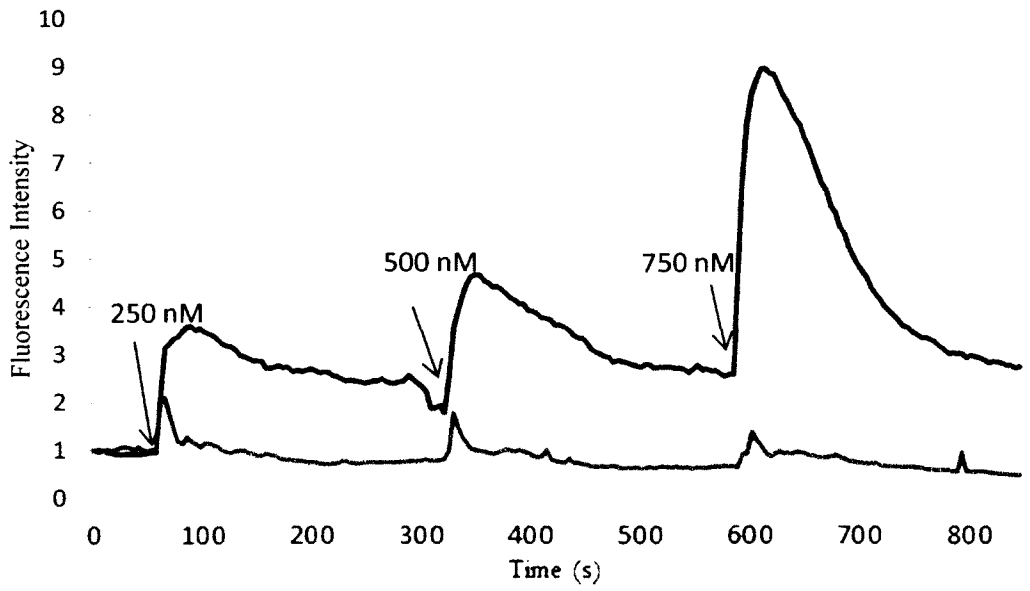


Figure 4.15 Line tracing comparison of engineered environments. *Blue line*= cultures depleted of glia n= 127 *Red line*= cultures high in glia n= 116 with additions of 250, 500 and 750 nM glutamate concentrations.

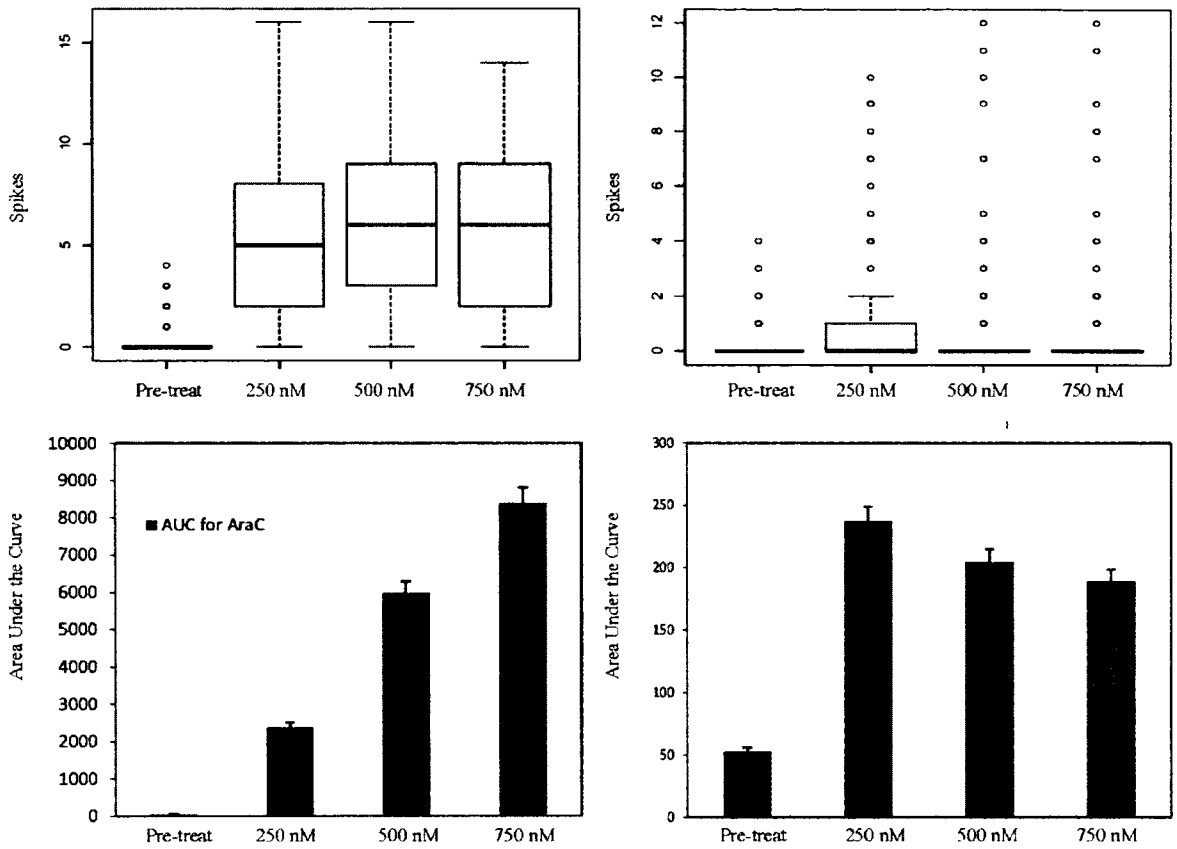


Figure 4.16 *Left top)* NumS in cultures depleted of glia. *Right top)* NumS in cultures high in glia. *Left bottom)* AUC in cultures depleted of glia. *Right bottom)* AUC in cultures high in glia with the additions of 250, 500 and 750 nM glutamate concentrations. *Circles-* represent outliers.

### 4.2.2 Randomization Comparisons of Paradigms

4.2.2.1 Randomization Paradigm 500, 250 and 750 nM Glutamate. This paradigm comparison also has outsourced analysis for AUC and NumS. The line tracing comparison can be seen in Figure 4.17. The comparison elucidates the glial effect on calcium processing of the neurons. This is further observed in a three-fold AUC scale decrease in Figure 4.18 in the higher statistical analysis. Again, a decreasing trend for calcium signaling is observed in cultures high in glia by glutamate treatment independent

of glutamate concentration in area under the curve. The same trend can be observed in depleted glial cultures when the data is compared with the line tracings, treatment 3 has an excitotoxic plateau. The plateau suggests cell death rather than the cell's ability to process calcium. The NumS also suggests glial cells are buffering the neurons response to glutamate with decreased calcium influx behavior.

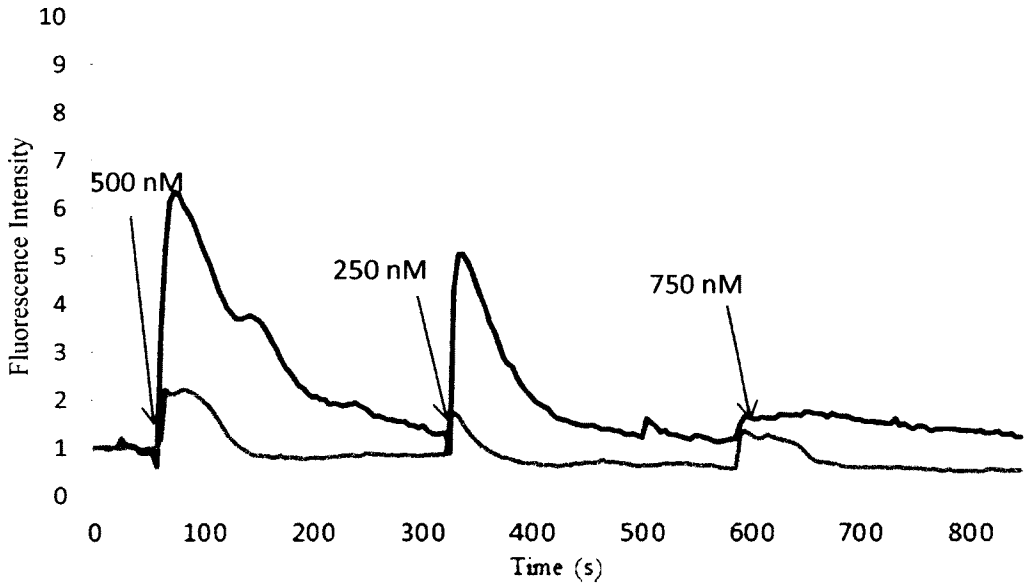


Figure 4.17 Line tracing comparison of engineered environments. *Blue line*= cultures depleted of glia n= 82 *Red line*= cultures high in glia n= 76 with additions of 500, 250 and 750 nM glutamate concentrations.

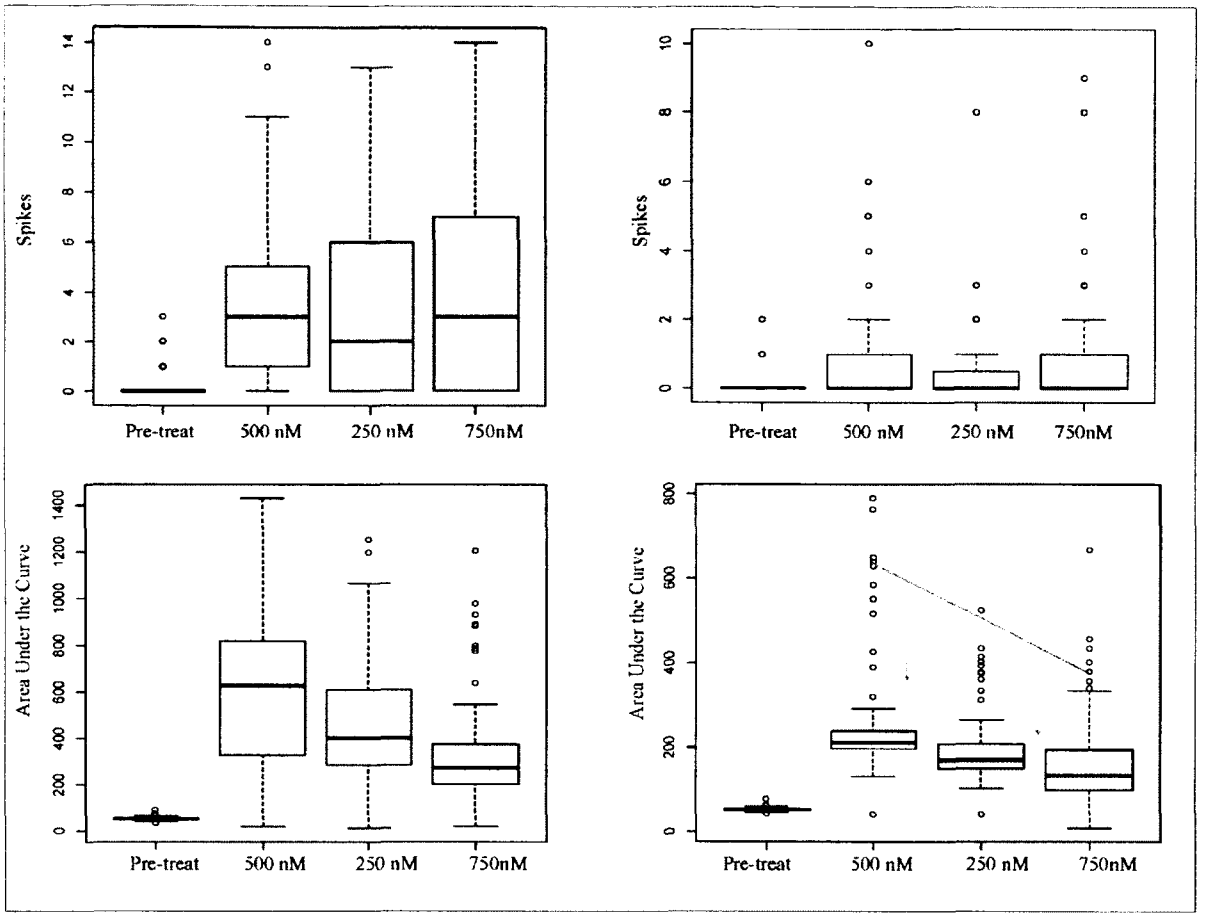


Figure 4.18 *Left top)* NumS in cultures depleted of glia. *Right top)* NumS in cultures high in glia. *Left bottom)* AUC in cultures depleted of glia. *Right bottom)* AUC in cultures high in glia with the additions of 500, 250 and 750 nM glutamate concentrations. *Red line* = trend line for AUC in cultures depleted of glia. This represents the decrease in AUC on the same scale. *Circles-* represent outliers.

4.2.2.2 Randomization Paradigm 250, 750 and 500 nM Glutamate. The following line tracing in Figure 4.19, represents the decreasing AUC trend between the two engineered environments. This data was not outsourced, but would need to be analyzed with higher statistics to determine if the trend is still valid in decreasing AUC per glutamate treatment is independent of glutamate concentration.

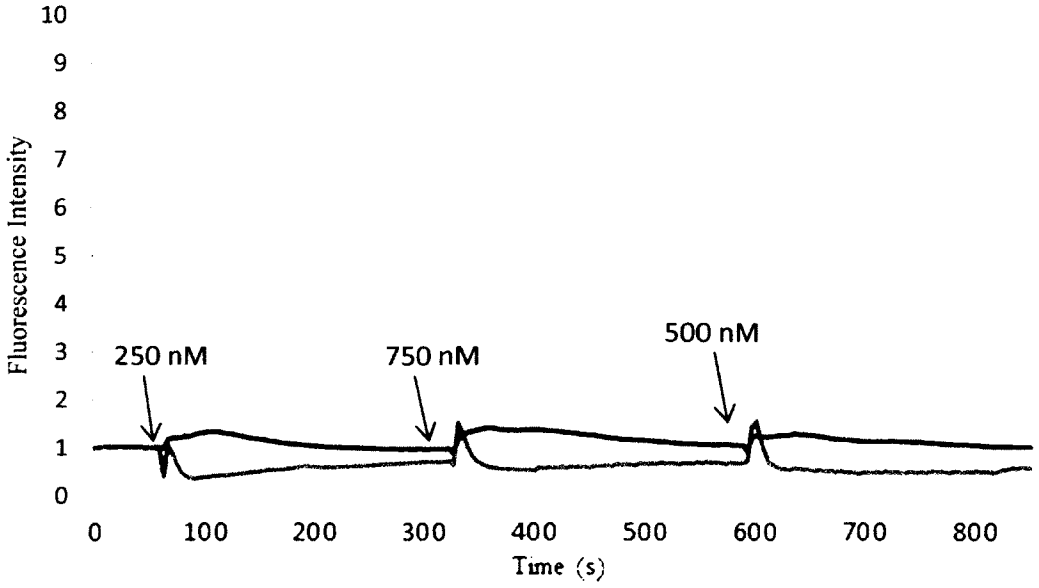


Figure 4.19 Line tracing comparison of engineered environments. *Blue line*= cultures depleted of glia n= 67 *Red line*= cultures high in glia n= 161 with additions of 250, 750 and 500 nM glutamate concentrations.

4.2.2.3 Randomization Paradigm 500, 750 and 250 nM Glutamate.

Figure 4.20 suggests two separate trends: 1) The cultures high in glia affect neuronal processing of calcium and 2) cultures depleted in glia must recognize a glutamate stimulus if the concentration is higher than the prior stimulus. The second trend can be observed by treatments one and two, notice how the first treatment oscillation starts to plateau, but recognizes the second stimulus. The neurons then recover back to starting treatment 2 baseline and recognize the lowest glutamate concentration in treatment 3. This observation is noted in other paradigms.

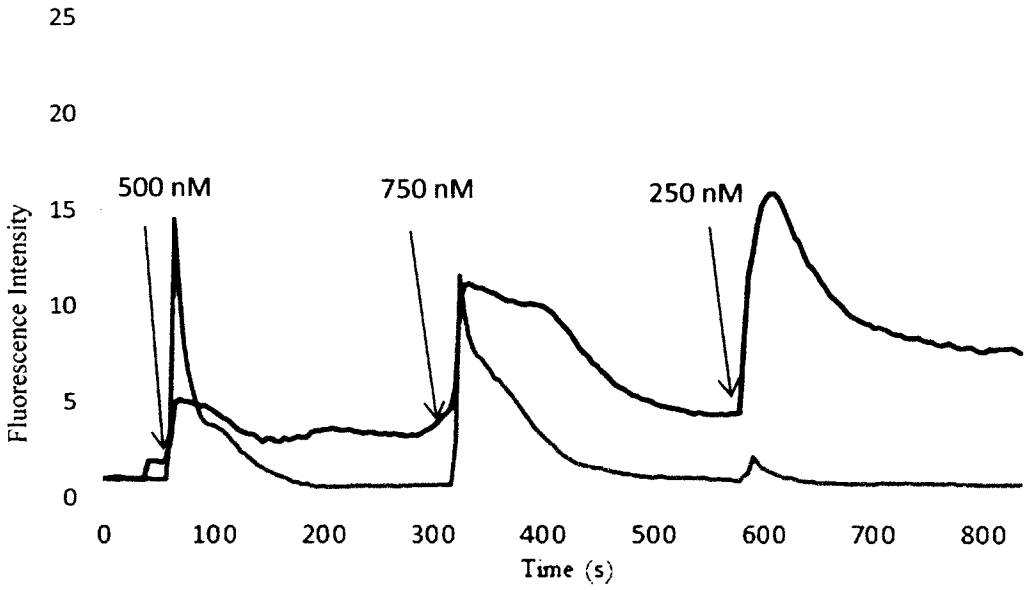


Figure 4.20 Line tracing comparison of engineered environments. *Blue line*= cultures depleted of glia n= 72 *Red line*= cultures high in glia n= 86 with additions of 500, 750, 250 nM glutamate concentrations.

4.2.2.4 Randomization Paradigm 750, 250 and 500 nM Glutamate. The line tracings in Figure 4.21 show the same trend as Figure 4.20 in cultures depleted of glia. Instead of a plateau, a biphasic calcium response is occurring; there have been suggestions in which a biphasic calcium response occurs in part to activation of the ryanodine receptor on the mitochondria [25]. The higher concentration in treatment 3 induces a calcium response. Also, the AUC is visibly reduced for the cultures depleted of glia.

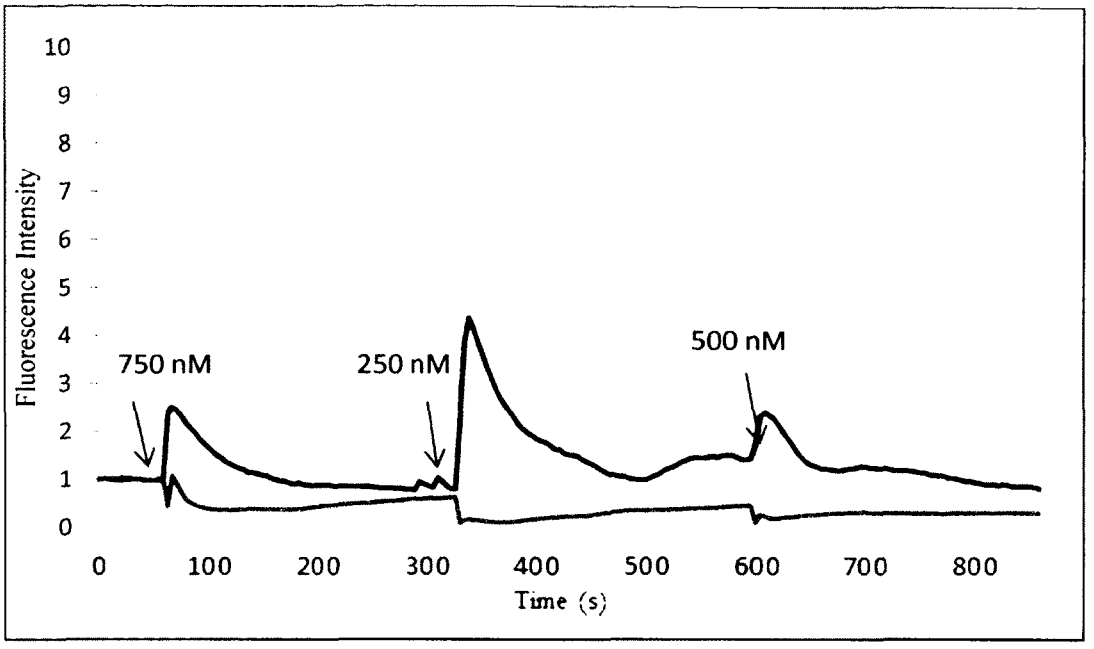


Figure 4.21 Line tracing comparison of engineered environments. *Blue line*= cultures depleted of glia n= 94 *Red line*= cultures high in glia n= 142 with additions of 750, 250 and 500 nM glutamate concentrations.

4.2.2.5 Randomization Paradigm 750, 500 and 250 nM Glutamate. This paradigm elucidates the trend of higher concentrations forcing calcium responses. In Figure 4.22, the treatments are descending in concentration, and displayed in the line tracings between treatments one and two, the cultures depleted in glia ignore the lower concentration in treatment 2. The cells then respond to treatment 3 after an appropriate amount of time has passed. Also, the line tracings display the trend from all previous paradigms, in which area under the curve decreases when glial cells are present in the culture.

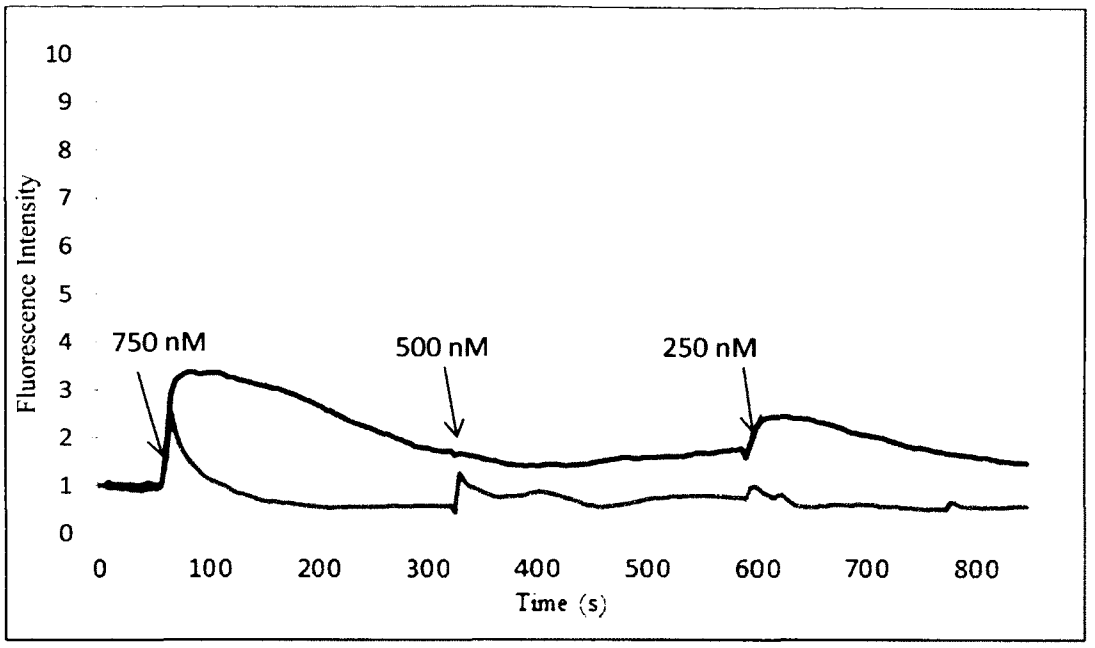


Figure 4.22 Line tracing comparison of engineered environments. *Blue line*= cultures depleted of glia n= 79 *Red line*= cultures high in glia n= 148 with additions of 750, 500 and 250 nM glutamate concentrations.

### 4.2.3 Comparison of Paradigms within the Same Environment

Figure 4.23 represents glia depleted culture line tracings to reveal the changing calcium dynamics between the selected paradigms. This visual helps to compare how paradigms from the same environment change by treatment concentration, and how AUC is affected by the treatment concentration. Figure 4.24 represents the same paradigms as Figure 4.23 but high in glia; a clear observation can be seen in the effects glial cells have on calcium dynamics. The tracings are all very similar in regards to amplitude, response shape and return to baseline. These tracings clearly denote that glial cells dampen neuronal calcium processing in response to glutamate receptor stimulation.

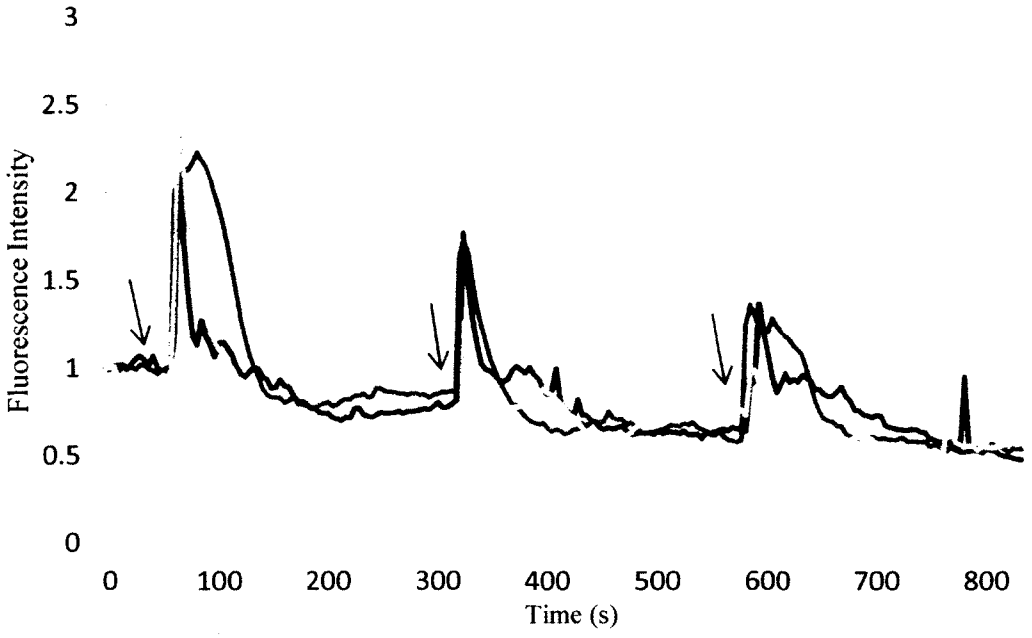


Figure 4.23 Line tracings of selected paradigms of engineered cultures depleted of glia. *Blue line*- 250, 500 and 750 nM GLU *Red line*- 500, 250 and 750 nM GLU *Green line*- 750, 500 and 250 nM GLU

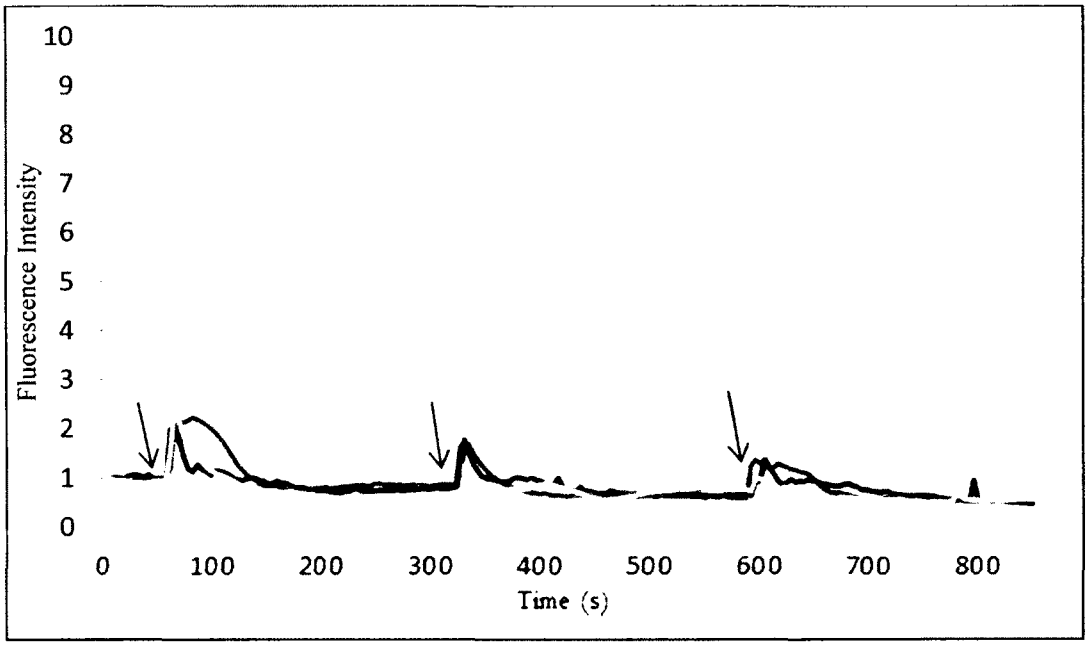


Figure 4.24 Line tracings of selected paradigms of engineered cultures high in glia. *Blue line*- 250, 500 and 750 nM GLU *Red line*- 500, 250 and 750 nM GLU *Green line*- 750, 500 and 250 nM GLU.

# CHAPTER 5

## ENGINEERING A CANCEROUS ENVIRONMENT

To understand the processing of information one must engineer an environment to control cell type and condition in which would be natural *in vivo*: such as metastatic and residual cancerous environments. *In vivo*, a normal function within astrocytes is system Xc-. This system releases one glutamate molecule in exchange for one cystine molecule [46]. This system is exploited in cancerous cells to actually promote tumor invasion.

### 5.1 System Xc- in Glioblastoma

#### 5.1.1 Tumor Invasion Engineered Environment

Under physiological conditions the engineered tumor invasion environment would most likely not occur, but as a controlled experiment to see if system Xc- created an excitotoxic environment for neurons in the absence of glia, it produce a positive effect. Figure 5.1 displays the line tracings for tumor invasion/metastatic environment to submaximal increasing additions of glutamate stimuli, the normal paradigm. The line tracings suggest the neurons in this system could not respond to glutamate stimuli at the beginning of the treatment period, however, produced a delayed response toward the end of each treatment condition.

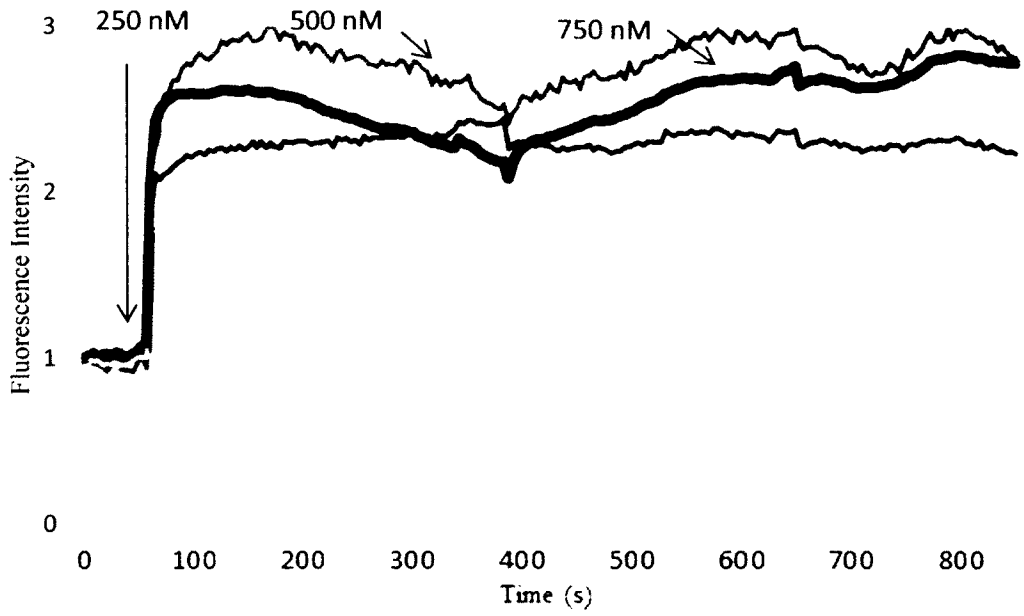


Figure 5.1 Engineered tumor invasion environment 2 DIV in cultures depleted of glia 8 DIV in response to 250, 500 and 750 nM GLU. *Colored lines*- individual ROIs *Black line*- average of n=25.

Figure 5.2 represents the engineered environment for tumor invasion in cultures one would typically see under physiological conditions. The line tracings show a marked decrease in AUC as compared to cultures depleted of glia. The tracings also represent low levels of toxicity. However, not truly represented in the average tracings is the NumS. There were typically very large-scale, sharp calcium spikes at the beginning of each treatment condition. There was also a decline in AUC as glutamate concentration increased.

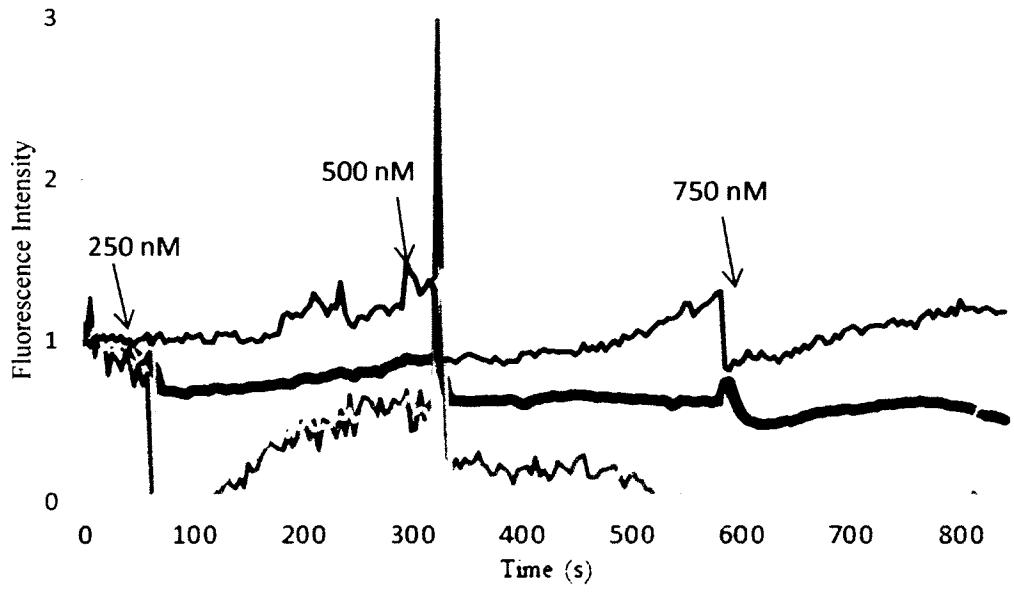


Figure 5.2 Engineered tumor invasion environment 2 DIV in cultures high in glia 8 DIV in response to 250, 500 and 750 nM GLU. *Colored lines-* individual ROIs *Black line-* average of n= 617.

### 5.1.2 Residual Cancer Engineered Environment

The next data set produces a new trend in which the neurons are hyper-excitable. System Xc- must be producing excitotoxic levels of glutamate to produce the type of calcium oscillations produced in the next few microenvironments. Figure 5.3 does not represent this spikey behavior, because the engineered environment lacks glial cells. This outcome was expected, the calcium oscillations are typical for the normal paradigm glutamate stimulations.

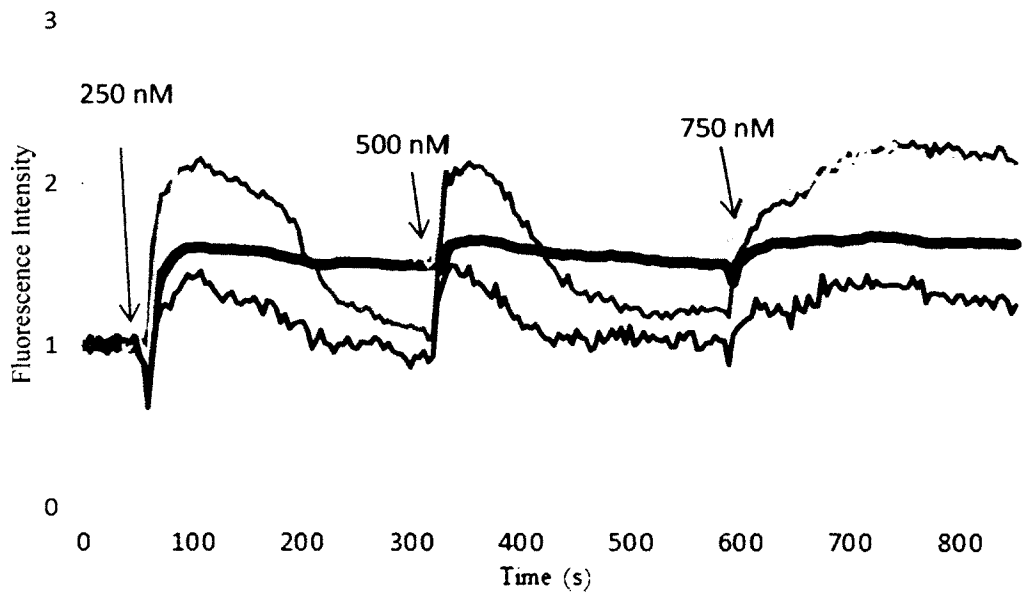


Figure 5.3 Engineered residual cancer environment with cancer cells 2 DIV co-cultured with primary cortical cultures depleted of glia 8 DIV in response to 250, 500 and 750 nM GLU. *Colored lines-* individual ROIs *Black line-* average of n= 132.

Figure 5.4 does however represent the oscillatory behavior. These line tracings are from cultures 8 DIV exposed to cancerous glia for two of the last days in culture. The addition of submaximal glutamate has neurons spiking at very fast rates, but only for approximately the first minute on each condition type. The neurons then cease this epileptic behavior with a typical return to baseline. This NumS behavior was not displayed in the normal engineered cultures; therefore, the data suggests this glutamate induced calcium processing behavior is linked to the excitotoxic environment produced by system Xc-.

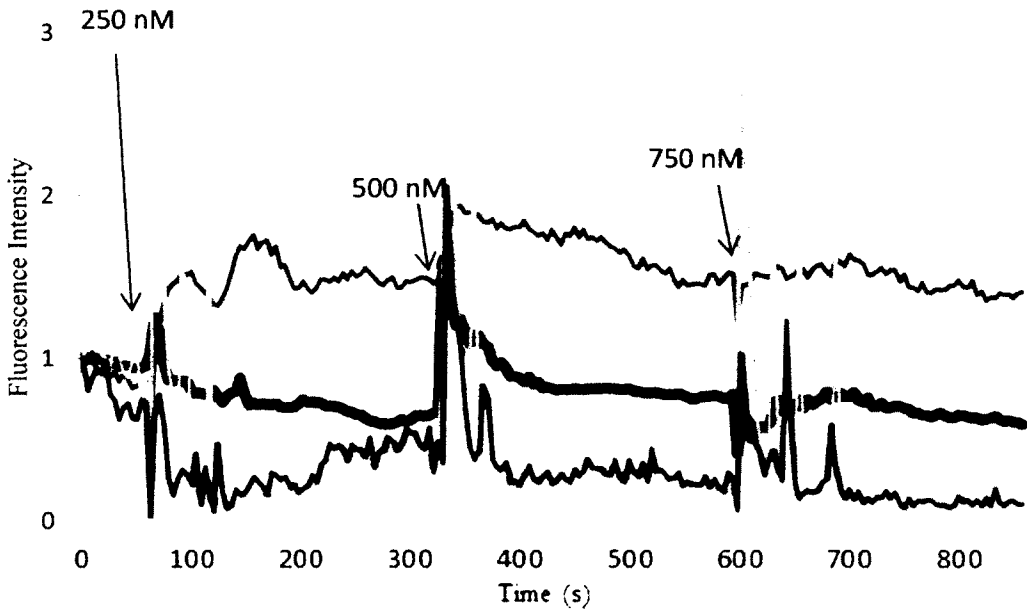


Figure 5.4 Engineered residual cancer environment with cancer cells 2 DIV co-cultured with primary cortical cultures high in glia 8 DIV in response to 250, 500 and 750 nM GLU. *Colored lines*- individual ROIs *Black line*- average of n= 135.

This behavior is further displayed in Figure 5.5. Instead of only the first minute, the oscillatory behavior was produced during the entire treatment time for each condition. This data set remained in culture only 1 day longer, exposed to proliferating cancer cells 1 DIV longer, than the previous data set. These results further suggest system Xc- has produced an excitotoxic environment, and causes oscillatory behavior as seen in Figure 3.7 from the inhibitory antagonist Bicuculline, which mimics epilepsy or in this case seizures which are known to be a side effect of cancer.

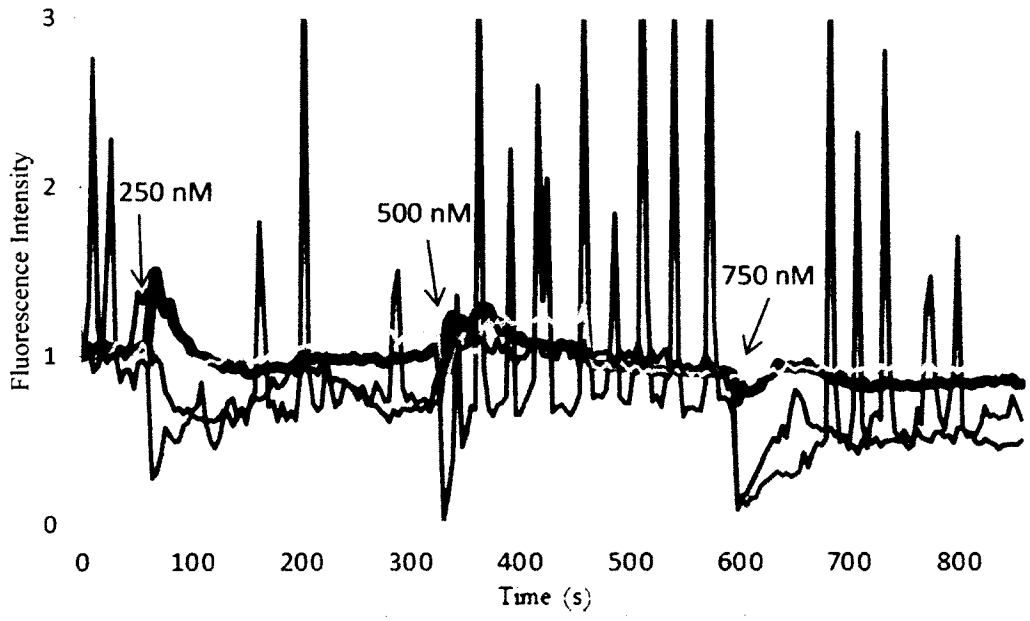


Figure 5.5 Engineered residual cancer environment with cancer cells 3 DIV co-cultured with primary cortical cultures high in glia 9 DIV in response to 250, 500 and 750 nM GLU. *Colored lines*- individual ROIs *Black line*- average of n= 226.

Figure 5.6 compares both DIV of the residual engineered environments for high glia cultures, as well as, an average of the combined cultures. The trend of the lines are almost identical, however, the calcium spiking behavior was much greater in 9 DIV cultures, and the AUC reflects this behavior with slightly higher AUC.

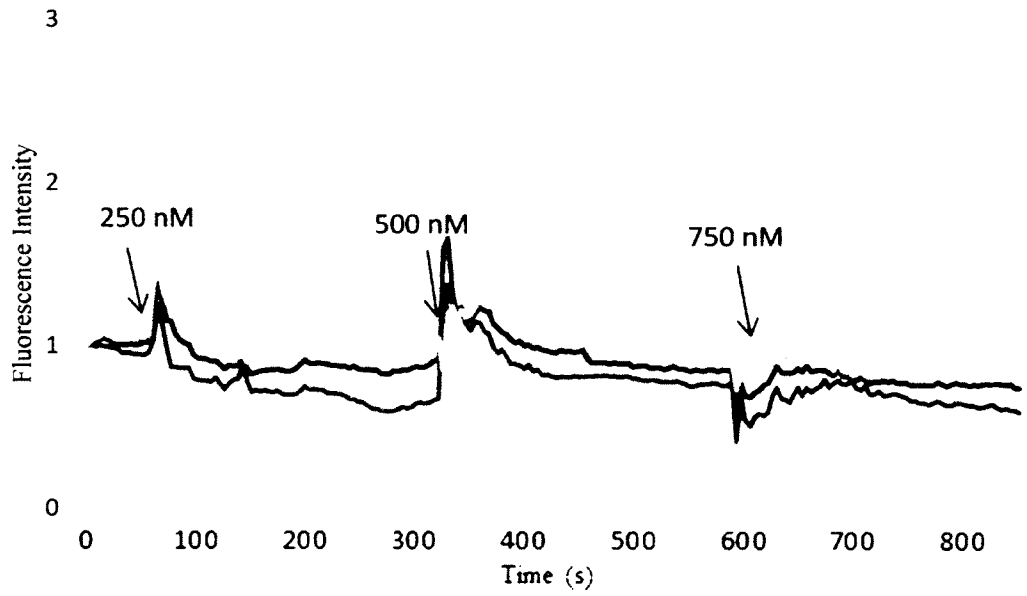


Figure 5.6 Comparison of engineered residual cancer environment with primary cortical cultures high in glia in response to 250, 500 and 750 nM GLU. *Blue line-* average of all residual DIV *Red line-* average of all residual 8 DIV *Green line-* average of all residual 9 DIV.

### 5.1.3 Comparison of Cancerous and Non-Cancerous Engineered Environments

Figure 5.7 compares the line tracings of normal engineered environments to tumor invasion environments with the normal paradigm glutamate additions. The average tracing for tumor invasion shows a decreased area under the curve; however, the calcium levels raise towards the end of the treatment conditions. The normal non-cancerous environment does not display this behavior.

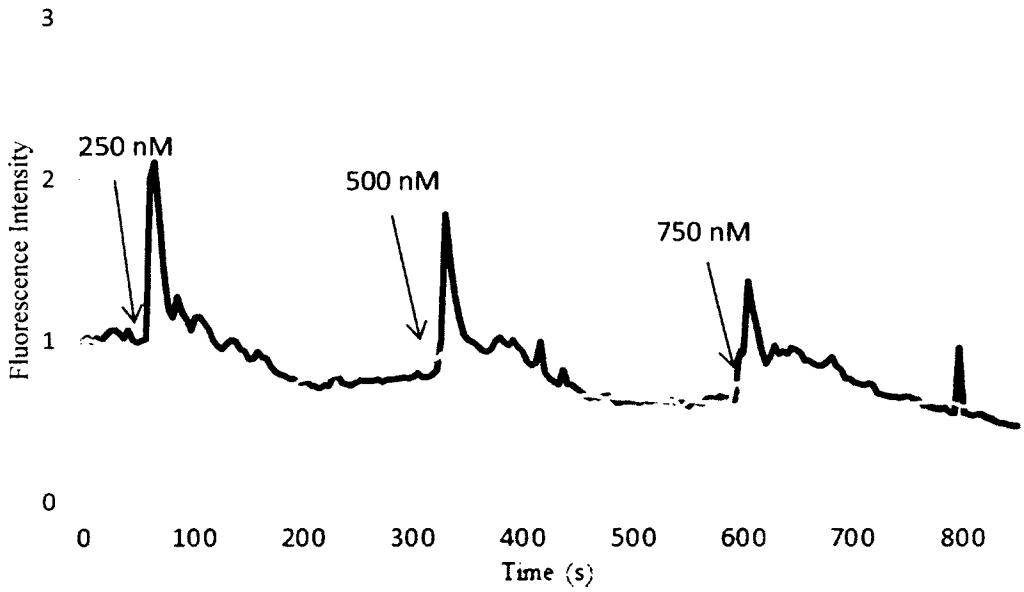


Figure 5.7 Comparison of non-cancerous and cancerous environments. *Green line*- average of tumor invasion environment high in glia. *Black line*- average of cultures high in glia in response to 250, 500 and 750 nM GLU.

Figure 5.8 compares the normal environment with the residual engineered environment, displaying very little differences in the averaged values. However, these data sets would be prime candidates for the higher statistical analysis to determine the number of spikes per treatment. Figure 5.9 compares both engineered cancerous environments to the normal environment.

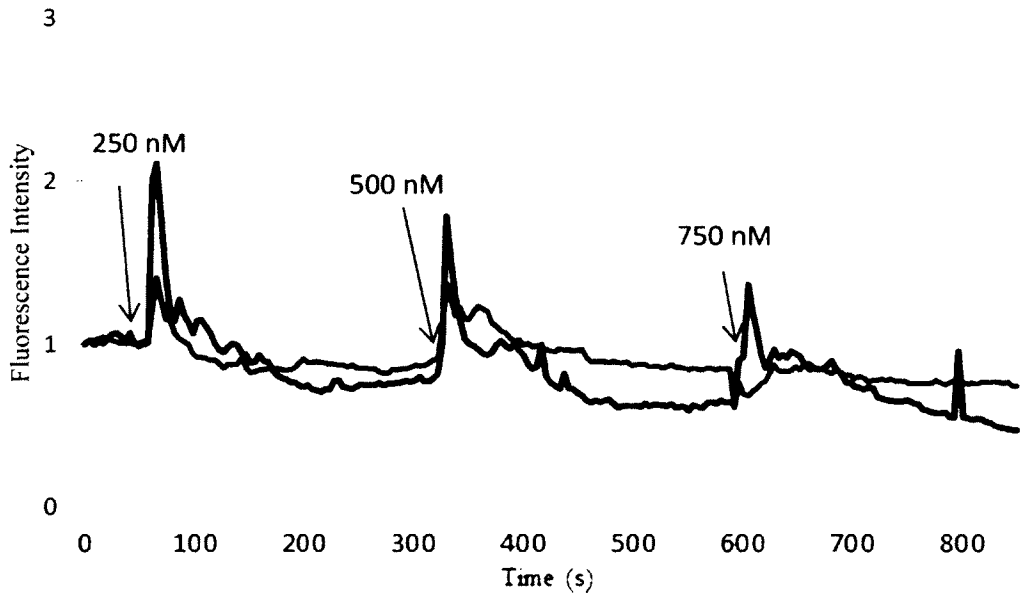


Figure 5.8 Comparison of non-cancerous and cancerous environments. *Blue line-* average of residual cancerous environment high in glia *Black line-* average of cultures high in glia in response to 250, 500 and 750 nM GLU.

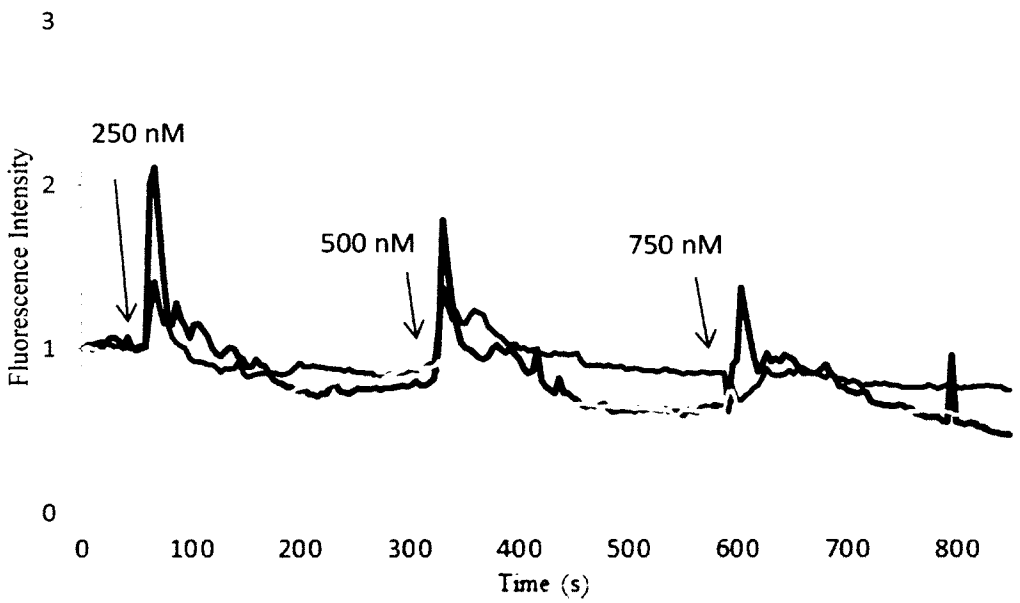


Figure 5.9 Comparison of non-cancerous and cancerous environments. *Blue line-* average of residual cancerous environment high in glia. *Green line-* average of tumor invasion environment high in glia. *Black line-* average of cultures high in glia in response to 250, 500 and 750 nM GLU.

# CHAPTER 6

## DISCUSSION AND CONCLUSIONS

Submaximal glutamate stimuli revealed the importance of both glia and stimulation sequence. An emerging viewpoint in which glia are contributors to calcium processing in the brain has been elucidated by engineering normal cultures and subjecting the cultures to submaximal glutamate stimuli.

Randomization of the stimulus not only suggested the validity of hypothesis 1, which was the ordering of glutamate stimulus is a predictor of subsequent responses, it also provided more trends. These trends include: 1) cultures depleted of glia, the data suggests neurons are unable to modulate calcium loads if the cells have a non-transient calcium response to glutamate, unless 2) the concentration of glutamate is greater than the load the neurons are trying to process, 3) the concentration and order of GLU stimulus determines neuronal response and 4) AUC is representative of both normal signaling and excitotoxicity. Psychology studies were performed in the mid 1950's on randomizing visual stimuli [65]. Verplank also studied the visual system at near-threshold values [66], which is similar to our experiment. Fernburger, studied [67] the differential analysis of weight and how one determines if a weight is heavy or light. In these experiments the subjects determined the stimuli to be heavier, if prior to the determination they held a lighter weight and vice versa for when they held a heavier weight. Verplank tested randomized visual signals and determined the stimuli were

independent of the preceding stimulus [67]. The randomized stimuli concept has not been applied to neuronal cells of which we know, but so far suggests being a great indicator in determining calcium processing in neurons when glutamate is added in nM concentrations. Figure 6.1 is a summary of comparison figures of engineered environments.

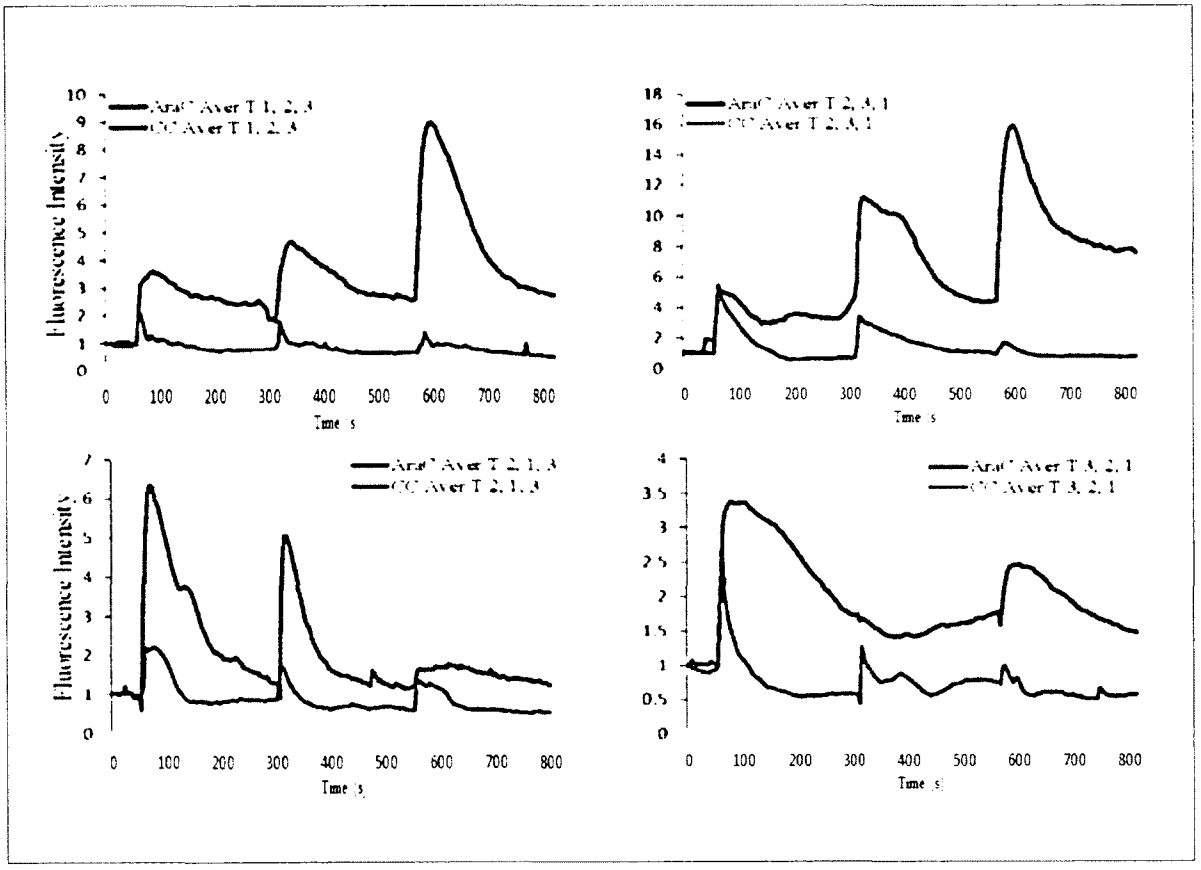


Figure 6.1 *Left top)* Comparison line tracing of depleted of glia cultures with the additions of 250, 500 and 750 nM glutamate concentrations. *Right top)* Comparison line tracing of high in glia cultures with the additions of 500, 250 and 750 nM glutamate concentrations. *Left bottom)* Comparison AUC of depleted of glia cultures with the additions of 250, 500 and 750 nM glutamate concentrations. *Right bottom)* Comparison AUC of high in glia cultures with the additions of 500, 250 and 750 nM glutamate concentrations.

The right side panel is the most revealing of the data sets in this summary. The top right figure, displays how the neurons are forced to process calcium even without treatment one's return of calcium to baseline. The neurons are forced to respond to treatment 2 because the glutamate concentration is higher than the concentration added in the first treatment. Compare the forced data to the bottom right panel, when the concentration in treatment 2 is ignored by the neurons most likely due to the stimuli being weaker than treatment 1. Therefore, concentration order does matter when glia are depleted from cultures. However, cultures high in glia display a decreasing fluorescence trend regardless of order or concentration of GLU.

The data provided substantial information that area under the curve (AUC) is a better predictor of neuronal response to glutamate stimulation than number of spikes (NumS), unless working with cancerous environments. The presence of glia provide a balance for recovery to baseline regardless of concentration order or stimulus, thus validating hypothesis 2, Figure 6.2. Glial cells will affect neuronal calcium dynamics by decreasing the amount of glutamate to which neurons will be exposed, thus altering the influx of calcium into the cytosol. This hypothesis was based on the negative feedback system inherent to the glial cells, the more glia in the system the less glutamate available to stimulate the neurons [15]. Glutamate is the input within the system, glia act as the negative feedback controller. Neuronal calcium response to glutamate within the system is the desired output, as seen in summary Figure 6.2. In this figure, the comparison of the two orders, environments and types of graphs clearly suggests the effect glia have on neuronal calcium processing.

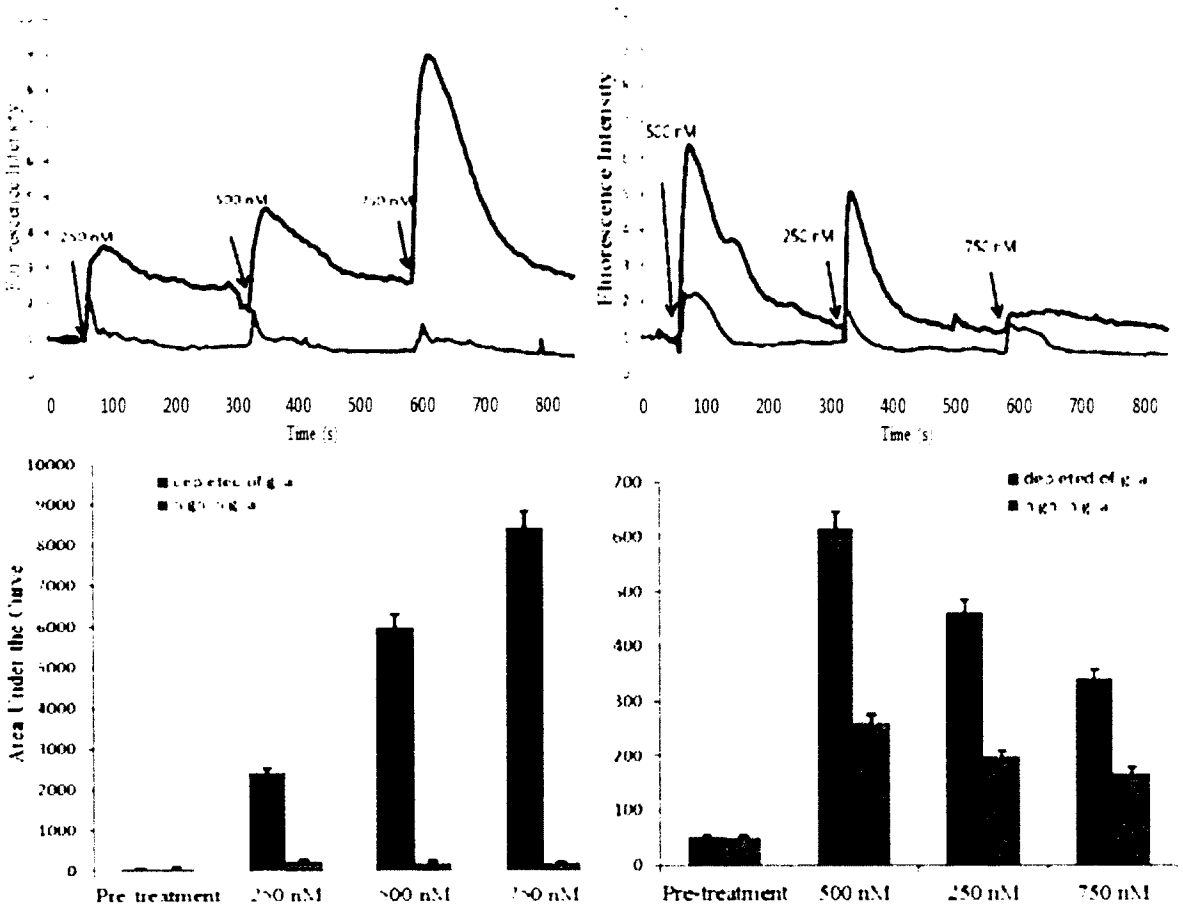


Figure 6.2 *Left top)* Comparison line tracing of depleted of glia cultures with the additions of 250, 500 and 750 nM glutamate concentrations. *Right top)* Comparison line tracing of high in glia cultures with the additions of 500, 250 and 750 nM glutamate concentrations. *Left bottom)* Comparison AUC of depleted of glia cultures with the additions of 250, 500 and 750 nM glutamate concentrations. *Right bottom)* Comparison AUC of high in glia cultures with the additions of 500, 250 and 750 nM glutamate concentrations.

Predation exists in biology (i.e. rabbit versus fox) and can be modeled by a two-compartment model. The models of predatory versus prey relationships have started to emerge in the field of neurophysiology [68, 69]. The negative feedback system responsible for glutamate uptake can be further elucidated with a three-compartment model of Neurons, Glia and Glutamate. This model is under investigation and a simulator

called "Grass, Wolves, Sheep," can be utilized with the current work to predict outcomes of *dynamically changing calcium,* Figure 6.3.

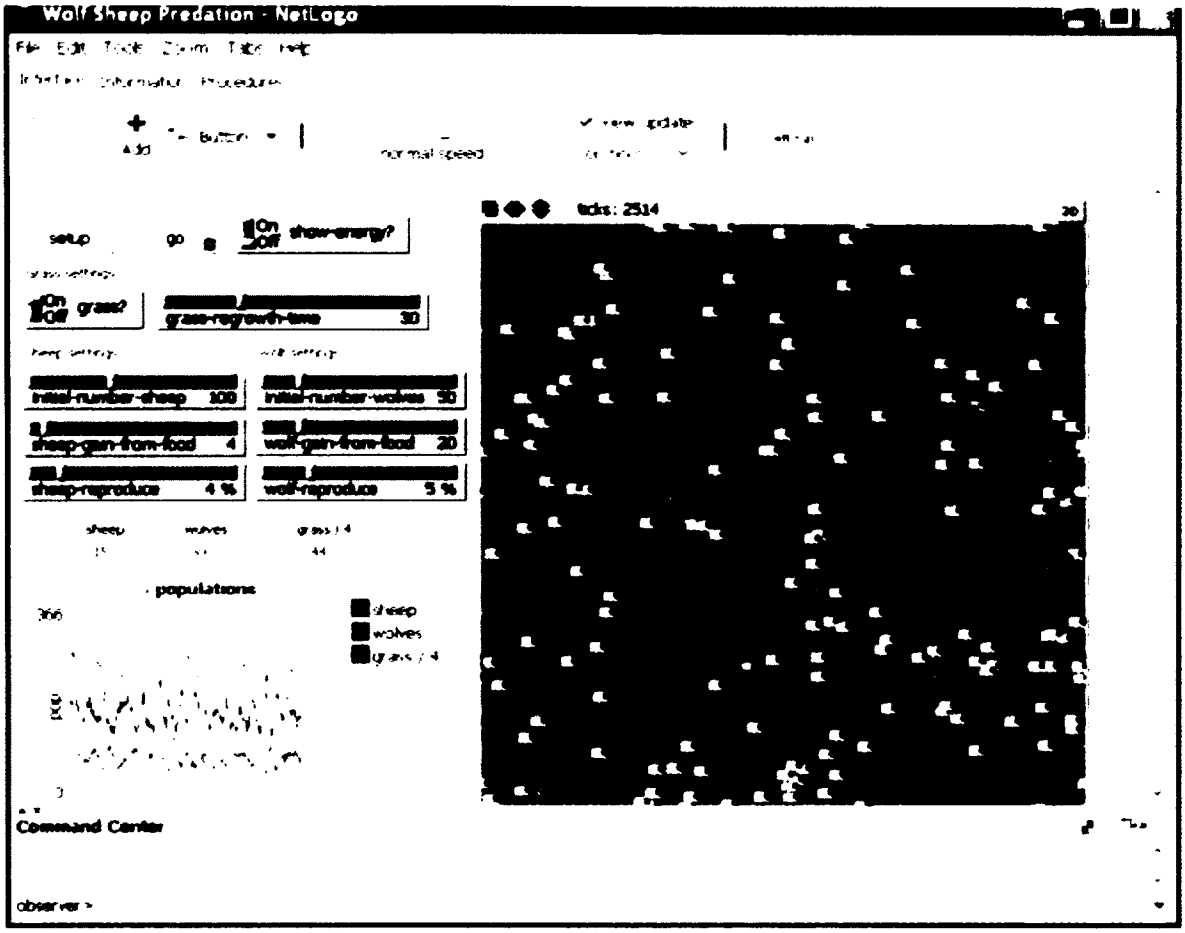


Figure 6.3 Predator/Prey three compartment model of Grass, Wolves, Sheep. This model is under investigation as a simulator of "Neurons, Glia and Glutamate," which can be utilized with the current work to predict outcomes of dynamically changing calcium [70].

Hypothesis 3, the engineered cancerous environments cause excitotoxic responses to normal paradigm glutamate additions compared to normal engineered environments high in glia and the engineered cancerous environments partially disproved this hypothesis, which under physiological conditions, engineered environments high in

glioma, would produce excitotoxic responses. The cells did not provide excitotoxic AUC calcium responses, but it did suggest system Xc- in releasing extracellular glutamate in the residual engineered environments, hyper-exciting the NMDA receptor suggesting an excitotoxic environment. This data is better visualized in NumS, Figures 5.4 and 5.5, which is poorly represented in the averaged line tracings in Figure 5.9, and would greatly benefit from higher order statistics. The engineered tumor invasion environments decreased in AUC per treatment of GLU stimulus.

System Xc- in glioma, is representative of both a negative and positive feedback system. When system Xc- functions as an autocrine signaling factor it is a negative feedback system, but when glutamate is released, the glutamate in the extracellular fluid becomes a positive feedback system to surrounding normal cells. The tissue engineered environments are economical and efficient when compared to *in vivo* testing or acquiring primary cancerous samples and have suggested most importantly the effects a microenvironment can have on calcium processing of submaximal glutamate stimulus. The presence of glia provide a balance for recovery to baseline regardless of concentration order or stimulus, as seen in Figure 6.4. Unexpectedly, the cells did not provide excitotoxic AUC calcium responses, but it did suggest system Xc- is releasing extracellular glutamate in the residual engineered environments, leading to a hyper-excited environment, as shown in our results as excess spiking activity. System Xc- in glioma residual cells, under physiological conditions, produces an excitotoxic environment which increases NumS but not AUC.

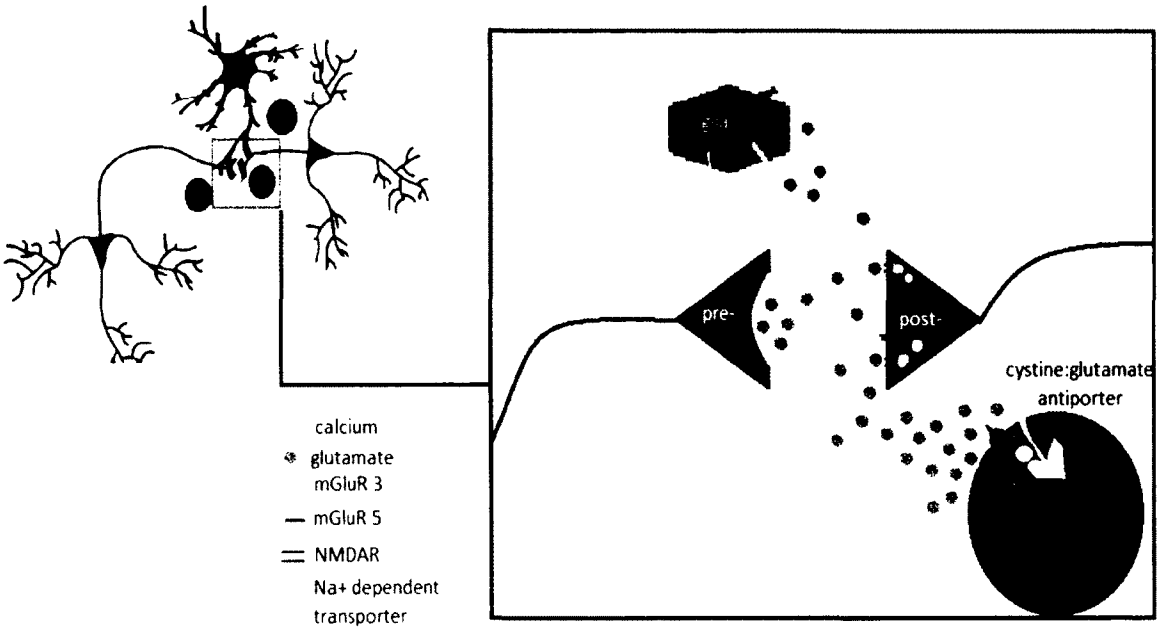


Figure 6.4 Schematic summary of glutamate binding to the NMDAR on the post-synaptic neuron which causes calcium influx.

It is anticipated, this combined experimental/analytical approach will also have utility in understanding additional brain diseases such as glioma and neurodegeneration linked to deregulated homeostatic calcium [49].

# CHAPTER 7

## FURTHERING ANALYSIS OF CALCIUM INFORMATION PROCESSING

To further the investigation of how neuronal calcium information processing is modulated by submaximal glutamate we must also investigate single neuronal responses over time for the different paradigms shown in these studies. Studying individual calcium dynamics could elucidate important aspects of spatiotemporal, synchronized, asynchrony and/or concentration dependent responses when correlated to the averaged calcium dynamics which were investigated throughout the body of this work.

Also, my cell culture work led to two device creations with Kelly Crittenden, Ph.D. and the Uprint® fast prototype machine, that we would like to use in the engineered domains. The first device allows separation of multiple cell cultures in the same substrate. The separation allows for each cell types respective media to be used until the experiment is ready to be implemented, in which case the device can be removed and the cells can be washed or loaded with fluorescence dye, device in Figure 7.1. This device would be used to image cancer cells on one side of the imaging field and normal cells on the other, and determine the effects of cancer cells in proximity to normal cells, but not interlaced within the culture. The other cell culture device stabilizes spheroids or 3-dimensional constructs in liquid for cell culture imaging. The following device was created as an independent study, and we would like to use it in imaging 3-dimensional

spheroids in normal cultures pre-attachment. This device would study acute tumor induction into normal cell environments and how the tumor dynamically responds to the new environment with fluorescence $Ca^{2+}$ imaging. This device can be seen in Figure 7.2.

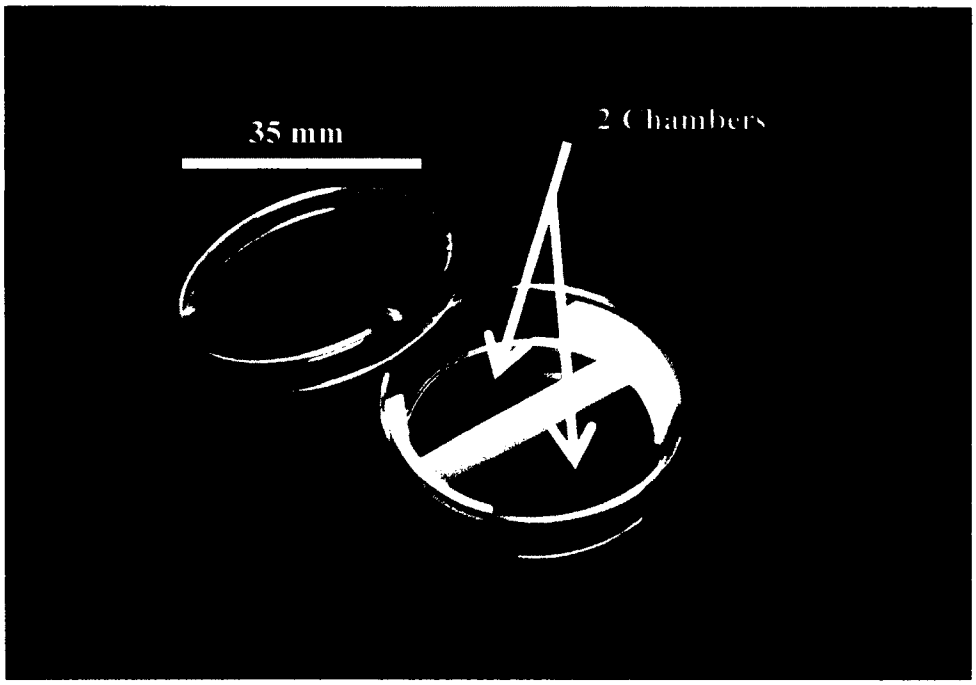


Figure 7.1 Insert cell-culture separation device designed by Kinsey Cotton Kelly and created by Kelly Crittenden, Ph.D.

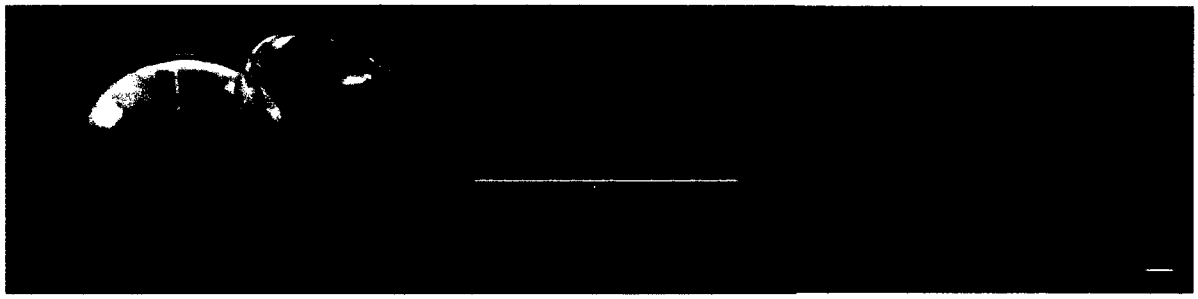

Figure 7.2 *Left)* Spheroid imaging device. *Middle)* Imaging device under observation at 100X magnification. *Scale bar= 900 microns Right)* Merged image of before and post addition of three stimlulus additions of 20X dilution volumes respective of dish volume with minimal movement of 1 μm particle aggregates. *Scale bar= 100* μm.

Elmore [27] notes active and inactive proteins have been identified in the pathways involving apoptosis, but the activation or molecular mechanisms of action of these pathways are still not understood. If we can understand the actions and activation processes, we will be that much further in developing better solutions for disease. Therefore, studying how the presence of brain tumor cells affect intracellular calcium dynamics within the previously studied engineered environments, with an emphasis on the number of spikes can better elucidate how diseased tissue evades apoptosis and alters normal synaptic plasticity.

Another concern involving calcium information processing is whether tissue engineering scaffolds incorporating cortical brain cells alter normal neuronal calcium dynamics due to environmental modulation affecting cell attachment, motility and neurite outgrowth. This paradigm can be evaluated in 2-dimensional scaffolds in which one can control cell growth and attachment. Controlling cell growth is becoming a possibility with protein and polypeptide coated micropatterned surfaces. Numerous studies have been performed to develop techniques of nanoengineered surfaces. At Louisiana Tech University, we are trying to develop a patterning technique that involves synergy between proteins and polymers that are micropatterned by a BioForce NanoeNabler™ molecular printer. The micropatterning research we are performing is related to Mohammad, DeCoster and McShane research. The previous research developed a patterning technique using photolithography and Layer-by-Layer assembly (LbL) of proteins and polypeptides [71, 72]. Their work concluded that neuronal cells displayed an affinity to $sPLA_2$ over the polypeptide (poly-L-lysine) which is known to have adherent properties for neuronal

cells. Figure 7.3 displays the neuronal cells in which have adhered to the micropatterned surface with an affinity to $sPLA_2$ despite surface topography.

Figure 7.3 Micropatterned and nanoengineered surface with neuronal attachment to sPLA2 [73].

Once the above paradigm has been adapted for the NanoeNabler, primary cortical cells can be plated on the nanoengineered surfaces and testing of their biochemical signaling will occur with submaximal additions of glutamate exogenously added to elicit calcium responses. This data can then be correlated to the data previously acquired in the engineered environments to infer whether tissue engineering scaffolds alter normal cortical calcium information processing.

# APPENDIX A

## IACUC, CELL CULTURE, AND MEDIA

## A.1 Institutional Animal Care and Use Committee

Louisiana Tech University

5 September 2011

Dr. Mark DeCoster

Biomedical Engineering

Louisiana Tech University

Campus Box # 58

Dear Dr. DeCoster:

The Louisiana Tech University's Institutional Animal Care and Use Committee (IACUC) examined your protocol entitled: ***The Study of Neuronal Synchrony using Coupled Oscillator Model for Brain Function Restoration*** and has granted approval for an additional two years. This is a modification of the approved protocol entitled: ***Stochastic Resonance of Theta Rhythms in Hippocampal Networks?***

The proposed procedures continue to have scientific merit and were found to provide reasonable and adequate safeguards for the comfort of the animals, the safety of the researchers and the participating students.

Please remember that you are required to keep adequate and accurate records of all procedures, results, and the number of animals used in this protocol for three years after termination of the project. The records must be available for review by the IACUC or state and federal animal use agencies. Each year in October you will be required to complete a summary of animals used for the United States Agricultural Agency (USDA). Note that failure to follow this protocol as approved may result in the termination of research.

If you have any questions please call me at (318) 257- 5206 or via email at jgspaulding@latech.edu.

Sincerely,

James G. Spaulding, Chair

Louisiana Tech University IACUC

A.2 Rat Primary Cervical Disarticulation
IACUC Approved

Remember to pre-treat plates with PLL.

There are two supply lists that need to be gathered and put in place before you begin. If more than seven pups will be sacrificed, split the amount into groups of seven. After each group, a fresh 50 mL tube with 10 mL media will be used to collect tissue. After a collection tube has all seven tissue samples, it will need to be sent to Lab #240 for tissue preparation to help reduce bacteria.

Supplies Needed for Dissection:

1 -Lg dish

4- Diapers

2 -Empty yellow tip containers

1 -Plastic bag

1 -Cervical scissors

1 -Micro-scissors

1 -Curved tip scissors

1 -Small tip forceps

1 -Lg forceps

1 -Small spatula

1-Full wash bottle with 70% Isopropyl alcohol

1 -50 mL centrifuge tubes with 40mLs basal medium eagle (BME)

1 -50 mL centrifuge tube with 10mLs of BME and 0.05% PS (one for every n= 7)

1-Box gloves

1-50 mL centrifuge holder

1-beaker ice

Set-up for dissection:

1. Remove lids from empty yellow pipette tip containers. Fill yellow bottoms half-way with isopropyl alcohol and soak instruments in one container setting both containers at end of dissection table.
2. Place "pinkies" in one lid of yellow container and set on end of dissection table.
3. Place three diapers on dissection table. Two in front of you horizontally and the third above the right diaper in front of you.
4. Place bottom of one large dish in the center of diaper directly in front of you.
5. Place the other large dish bottom to the left of the furthest most diaper. This dish will be for body and waste discard.
6. Place plastic bag next to dish discard.
7. Place 50 mL centrifuge holder on dissection table next to alcohol containing tip box without utensils.

8. Place wash bottle next to box with utensils.
9. Keep basal media, transfer pipettes, gloves, and other supplies on wooden table.
10. Place over head lighting and stereo scope in position above centered dish.

Dissection procedure:

1. Put a pair of gloves on.
2. Place 8-10 mL basal media in centered dish.
3. Place 10 mLs basal media in 50 mL centrifuge tube in holder and recap.
4. Remove one pup from box by pinching skin above spine near lower back and set pinkie on left most diaper.
5. Spray pup with alcohol and pick pup up once more by pinching method.
6. Quickly set cervical scissors behind ear being cautious of paws. Once pup straightens neck make one very quick and decisive cut. Dip scissors in alcohol container without utensils and place scissors on clean diaper.
7. Blot head at point of disarticulation on diaper and discard body in bag.
8. Pinch skin underneath head by neck. Take micro-scissors and place underneath skin at top middle of head at disarticulation point. Cut skin by pulling up and away from surface. Dip scissors to clean.
9. This should expose the skull (transparent appearance). While using the micro-scissors cut skull with same motion as skin. Dip scissors in alcohol to clean and place on diaper with cervical scissors.
10. The skull should separate. With the large forceps, curl back both sides of skull to expose brain. Dip forceps in alcohol to clean.

11. Locate olfactory bulbs and place small spatula between bulbs and the brain. Scoop brain out and into basal media. Dip spatula in alcohol to clean.
12. Take spatula and remove cerebellum at demarcation line and place cerebellum in discard dish. Dip spatula in alcohol to clean and place on diaper.
13. Pierce brain with large forceps (to keep in place) and begin removing meninges and blood vessels with the small tip forceps. Discard waste to discard dish. Remember to turn brain to remove meninges and blood vessels from both sides.
14. Once the blood vessels and meninges are removed, uncap 50 mL tube containing basal media and place all brain tissue into the media. Recap.
15. Remove contents of discard dish and place in the plastic bag.
16. Repeat process until all pups are sacrificed.
17. Once all pups are sacrificed and all waste is in plastic bag, seal bag and store in freezer in room next door.
18. Clean all utensils with alcohol and place in clean diaper.

Supplies needed for tissue culture:

Pretreated plates with Poly-L-lysine

1-Bucket of ice

1- Lg beaker of ice

1- Bottle of Neuronal Culture Media (NCM)

3- 15 mL tubes (three for every seven pups)

1-Trypsin with EDTA (one for every seven pups)

The lab's equipment and disposables cart

Tissue culture procedure:

1. Remove brain tissue from 50 mL pipette by aspirating with 10 mL pipette and pipette aid.
2. Blow out tissue in 15 mL tube.
3. Add 8mL complete media to brain tissue and titrate with a 5 mL pipette. Titrate about 15 times.
4. Let brain tissue settle by place 15mL tube in large beaker of ice for 5 mins.
5. The supernatant will contain the neuronal cells. Remove supernatant and place in 15 mL tube and put on ice.
6. Perform this procedure two more times.
7. Centrifuge and follow cell culturing protocol as usual to count and plate cells.

## A.3 Neuronal Culture Media

Supplies:

Fetal Bovine Serum (FBS) – 25 mL

Horse Serum (HS) – 25 mL

Glucose solution in Sterile D.I. water – (120 mg/mL) 1.25 mL

Glutamine in sterile D.I. water solution – (20 mg/mL) 1.25 mL

Penicillin-Streptomycin solution (Sigma) – 1.25 mL

Ham's F12-K media (ATCC only supplier) – 98 mL

Basal Media Eagle's (BME) – 98.25 mL

Sterile Filtration Unit

Procedure:

1. In the laminar flow hood (sterile environment), transfer the BME into filtration unit.
2. Add (thawed) FBS, and HS to filtration unit

3. Add Glucose solution
4. Add Glutamine solution
5. Add PS
6. Add F12-K
7. Put lid on filtration unit, start vacuum and connect hose.
8. Draw all liquid through (filter will visibly dry due to vacuum).
9. Disconnect/turn off vacuum.
10. Carefully remove upper twist-on portion of filtration unit.
11. Remove sterile cap from separate bag, and place on media flask.
12. Label, date, and initial flask.

## A.4 Locke's Solution

Supplies:

2250.0 mg NaCl

104.4 mg KCl

75.6 mg NaHCO3

84.5 mg CaCl2·2H2O

61.0 mg MgCl2·6H2O*

252.3 mg Glucose

1.25 mL 1 M Hepes

248.75 mL Sterile Purified Water

Sterile filtration unit

* MgCl2·6H2O left out for RDD exposure. Left out last time Lockes was made.

Procedure:

1. Dissolve the components in some of the purified water.

2. Add 100 mL of purified water to vacuum filtration unit.

3. Add water with dissolved components.

4. Add 1.25 mL of 1M stock Hepes.

5. Add remaining amount of purified water.

6. Place cap on unit. Carefully turn on vacuum.

7. Allow all the liquid to pass through the filter. Turn off vacuum before bubbles form.

8. Twist top of vacuum unit off carefully. Screw sterile cap onto container of media.

## A.5 CRL-2303 Media

Supplies:

221.3 mL Delbecco's Modified Eagle's Medium (DMEM)

1.25 mL Penn/Strep (PS)

25 mL Fetal Bovine Serum (FBS)

2.5 mL Amino Acid Solution (ATCC in refrigerator)

Sterile filtration unit

Procedure:

1. Add 110.65 mL DMEM to filtration unit.

2. Add 1.25 mL PS to filtration unit.

3. Add 25 mL FBS to filtration unit.

4. Add 2.5 mL Amino Acid Solution to filtration unit.

5. Add 110.65 mL DMEM to filtration unit.

6. Connect sterile filtration tubing to filtration unit and vacuum nozzle.

7. While holding unit slowly turn on vacuum to a medium drip.
8. Remove vacuum seal before media has been completely filtered.

## A.6 Astrocyte New Media

Supplies:

12.5 mL Horse Serum (5.0%)

12.5 mL Fetal Bovine Serum (5.0%)

1.25 mL Penicillin/Streptomycin (0.5%)

223.75 mL Ham's F-12K media with L-Glutamine

Sterile filtration unit

Procedure:

1. Add 100 mL of Ham's F-12K media to sterile vacuum filtration unit.
2. Add Horse Serum, Fetal Bovine Serum, and P/S to vacuum filtration unit.
3. Add 123.75 mL of Ham's F-12K media to unit.
4. Place cap on unit. Carefully turn on vacuum.
5. Allow all the liquid to pass through the filter. Turn off vacuum before bubbles form.
6. Twist top of vacuum unit off carefully. Screw sterile cap onto container of media.
7. Label media as Astrocyte New Media with date and lab name. Store in refrigerator.

## A.7 Fluo 3/AM Protocol

Make sure the light is off on the hood

Supplies for 2 mL solution:

2 μL Pluronic Acid

4 μL Fluo 3/AM

2 mL Locke's Solution (pre-warmed in incubator at least for 15 min.)

Procedure:

1. All components need to be warmed to room temperature
2. Add 2 mL Locke's Solution to the tube.
3. Add 2 μL Pluronic Acid and mix. (Shake and vortex, should produce small bubbles and look soapy).
4. Add 4 μL Fluo 3/AM (2mg/ml in DMSO) and cap. Mix by inversion.
5. Remove media from one well of a 24 multi-well plate and discard. Add 500 μLs of Loading Solution to the well. Repeat for three additional wells. Place into the incubator to load.
6. Allow 45 mins for Fluo3/AM to load into the cell.
7. Remove the loading solution and discard. Recover the cells in 475 μLs of Locke's Solution for 30 mins.
8. Ready for imaging.

# APPENDIX B

## IMAGE AND DATA ANALYSIS

## B.1 Image Analysis Examples

Figure B.1 depicts regions of interests (ROIs) created around cells in an image analysis software (Image J). These ROIs are representative of all image analysis performed throughout this work. The ROIs are then measured for fluorescence over time and the data is exported to an excel sheet for further analysis.

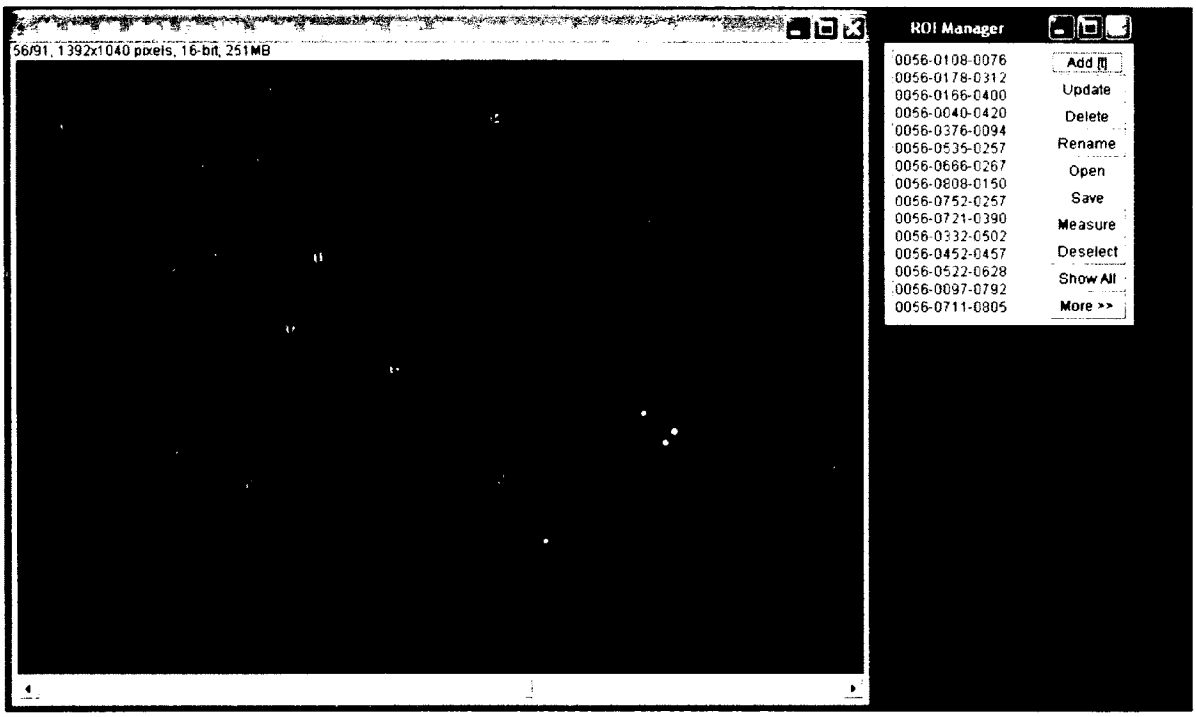


Figure B.1 An example of image analysis when creating regions of interest (ROIs) around individual cells to measure fluorescence intensity over time. Each circle represents an individual ROI.

The excel spreadsheet, Figure B.2, is then assembled in the following steps. Columns are inserted between every object, and the headings are changed from Object [01] to ROI 1 and the blank column to N-ROI 1, these headings and columns can be seen in Figure B.3.

| | A | B | C | D | E | F | G | H | I | J | K | L | M | N | O | P |
|---|---|---|---|---|---|---|---|---|---|---|---|---|---|---|---|---|
| 1 | Time[seconds] | Object[01] | Object[02] | Object[03] | Object[04] | Object[05] | Object[06] | Object[07] | Object[08] | Object[09] | Object[10] | Object[11] | Object[12] | Object[13] | Object[14] | Object |
| 2 | 0.62 | 6184 | 5877 | 13356 | 5345 | 6179 | 14869 | 2678 | 55207 | 4226 | 987 | 3493 | 1912 | 2418 | 523 | 5 |
| 3 | 4.63 | 6096 | 5837 | 12574 | 5293 | 6809 | 14103 | 2663 | 55638 | 4225 | 1018 | 3398 | 1805 | 2289 | 377 | 5 |
| 4 | 8.64 | 6283 | 6116 | 12694 | 5381 | 7335 | 14069 | 2686 | 55415 | 4232 | 981 | 3354 | 1618 | 2399 | 469 | 5 |
| 5 | 12.64 | 6358 | 6078 | 12277 | 5446 | 7860 | 13668 | 2839 | 54593 | 4313 | 902 | 3306 | 1638 | 2118 | 320 | 5 |
| 6 | 16.66 | 6249 | 5835 | 12481 | 5271 | 7815 | 14092 | 2741 | 54568 | 4400 | 979 | 3029 | 1508 | 2085 | 387 | 5 |
| 7 | 20.66 | 5811 | 5790 | 12196 | 5095 | 7775 | 13456 | 2718 | 55459 | 4505 | 852 | 3096 | 1449 | 2160 | 399 | 4 |
| 8 | 24.67 | 6218 | 5694 | 12431 | 5325 | 7966 | 13456 | 2783 | 56191 | 4834 | 978 | 3296 | 1611 | 2132 | 398 | 4 |
| 9 | 28.68 | 6302 | 5749 | 12316 | 5218 | 8190 | 13725 | 2723 | 55209 | 4622 | 1017 | 3081 | 1579 | 2104 | 423 | 5 |
| 10 | 32.69 | 6083 | 5571 | 12188 | 5372 | 8572 | 13678 | 2720 | 54836 | 4730 | 899 | 2942 | 1747 | 2049 | 434 | 4 |
| 11 | 36.69 | 6005 | 5772 | 12157 | 5427 | 8580 | 14009 | 2657 | 55079 | 4424 | 832 | 3024 | 1556 | 2100 | 471 | 4 |
| 12 | 40.71 | 6051 | 5759 | 12562 | 5313 | 8517 | 15484 | 2622 | 54394 | 4543 | 850 | 3151 | 1593 | 2178 | 337 | 4 |
| 13 | 44.71 | 6005 | 5907 | 12479 | 5517 | 8909 | 15145 | 2650 | 54911 | 4606 | 835 | 3064 | 1688 | 2147 | 449 | 5 |
| 14 | 48.72 | 6389 | 6143 | 12430 | 5582 | 9168 | 14917 | 2697 | 56171 | 4259 | 1041 | 3123 | 1596 | 2135 | 389 | 4 |
| 15 | 52.72 | 6244 | 5866 | 12777 | 5618 | 9336 | 14691 | 2780 | 55782 | 4380 | 963 | 3147 | 1679 | 2174 | 392 | 4 |
| 16 | 56.74 | 6661 | 5908 | 12781 | 6045 | 9119 | 14786 | 2907 | 56534 | 4513 | 1076 | 3182 | 1886 | 2280 | 414 | 5 |
| 17 | 60.74 | 5563 | 5393 | 11864 | 5193 | 7725 | 12512 | 2302 | 52655 | 3503 | 1026 | 2706 | 1450 | 1581 | 257 | 4 |
| 18 | 64.75 | 5304 | 5102 | 11698 | 5179 | 7828 | 13037 | 2541 | 52445 | 3430 | 1130 | 2774 | 1407 | 1779 | 354 | 4 |
| 19 | 68.76 | 5503 | 5079 | 11596 | 5169 | 7634 | 13070 | 2344 | 51737 | 3422 | 1034 | 2620 | 1532 | 1826 | 313 | 4 |
| 20 | 72.77 | 5430 | 5268 | 11586 | 5091 | 7962 | 12773 | 2451 | 52079 | 3561 | 1188 | 2560 | 1530 | 1849 | 253 | 4 |
| 21 | 76.77 | 5692 | 5166 | 11469 | 5425 | 8013 | 13026 | 2465 | 51900 | 3377 | 1220 | 2709 | 1528 | 1730 | 251 | 4 |
| 22 | 80.79 | 5776 | 5294 | 11911 | 5574 | 7528 | 12784 | 2412 | 52798 | 3587 | 1141 | 2833 | 1682 | 1675 | 315 | 4 |
| 23 | 84.79 | 5614 | 5077 | 11475 | 5256 | 7186 | 13345 | 2308 | 52100 | 3597 | 1116 | 2633 | 1650 | 1806 | 373 | 4 |

Figure B.2 An example of the spreadsheet exported from image analysis.

| | A | B | C | D | E | F | G | H | I | J | K | L | M | N | O | P |
|---|---|---|---|---|---|---|---|---|---|---|---|---|---|---|---|---|
| 1 | Time[seconds] | ROI 1 | N-ROI 1 | ROI 2 | N-ROI 2 | ROI 3 | N-ROI 3 | ROI 4 | N-ROI 4 | ROI 5 | N-ROI 5 | ROI 6 | N-ROI 6 | ROI 7 | N-ROI 7 | ROI 8 |
| 2 | 0.62 | 6184 | | 5877 | | 13356 | | 5345 | | 6179 | | 14869 | | 2678 | | 55 |
| 3 | 4.63 | 6096 | | 5837 | | 12574 | | 5293 | | 6809 | | 14103 | | 2663 | | 55 |
| 4 | 8.64 | 6283 | | 6116 | | 12694 | | 5381 | | 7335 | | 14069 | | 2686 | | 55 |
| 5 | 12.64 | 6358 | | 6078 | | 12277 | | 5446 | | 7860 | | 13668 | | 2839 | | 54 |
| 6 | 16.66 | 6249 | | 5835 | | 12481 | | 5271 | | 7815 | | 14092 | | 2741 | | 54 |
| 7 | 20.66 | 5811 | | 5790 | | 12196 | | 5095 | | 7775 | | 13456 | | 2718 | | 55 |
| 8 | 24.67 | 6218 | | 5694 | | 12431 | | 5325 | | 7966 | | 13456 | | 2783 | | 56 |
| 9 | 28.68 | 6302 | | 5749 | | 12316 | | 5218 | | 8190 | | 13725 | | 2723 | | 55 |
| 10 | 32.69 | 6083 | | 5571 | | 12188 | | 5372 | | 8572 | | 13678 | | 2720 | | 54 |
| 11 | 36.69 | 6005 | | 5772 | | 12157 | | 5427 | | 8580 | | 14009 | | 2657 | | 55 |
| 12 | 40.71 | 6051 | | 5759 | | 12562 | | 5313 | | 8517 | | 15484 | | 2622 | | 54 |
| 13 | 44.71 | 6005 | | 5907 | | 12479 | | 5517 | | 8909 | | 15145 | | 2650 | | 54 |
| 14 | 48.72 | 6389 | | 6143 | | 12430 | | 5582 | | 9168 | | 14917 | | 2697 | | 56 |
| 15 | 52.72 | 6244 | | 5866 | | 12777 | | 5618 | | 9336 | | 14691 | | 2780 | | 55 |
| 16 | 56.74 | 6661 | | 5908 | | 12781 | | 6045 | | 9119 | | 14786 | | 2907 | | 56 |
| 17 | 60.74 | 5563 | | 5393 | | 11864 | | 5193 | | 7725 | | 12512 | | 2302 | | 52 |
| 18 | 64.75 | 5304 | | 5102 | | 11698 | | 5179 | | 7828 | | 13037 | | 2541 | | 52 |
| 19 | 68.76 | 5503 | | 5079 | | 11596 | | 5169 | | 7634 | | 13070 | | 2344 | | 51 |
| 20 | 72.77 | 5430 | | 5268 | | 11586 | | 5091 | | 7962 | | 12773 | | 2451 | | 52 |
| 21 | 76.77 | 5692 | | 5166 | | 11469 | | 5425 | | 8013 | | 13026 | | 2465 | | 51 |
| 22 | 80.79 | 5776 | | 5294 | | 11911 | | 5574 | | 7528 | | 12784 | | 2412 | | 52 |
| 23 | 84.79 | 5614 | | 5077 | | 11475 | | 5256 | | 7186 | | 13345 | | 2308 | | 52 |

Figure B.3 An example of Excel spreadsheet insertion of columns and heading changes.

Next, an equation is created in the empty column next to the first value in the ROI column. The equation equals the first value cell in each ROI column (i.e. A2) divided by the first value itself, normalizing the first value to one. The N-ROI column equation is then dragged down to the end of the column creating and entire column divided by the first value of the ROI column, this can be seen in Figure B.4.

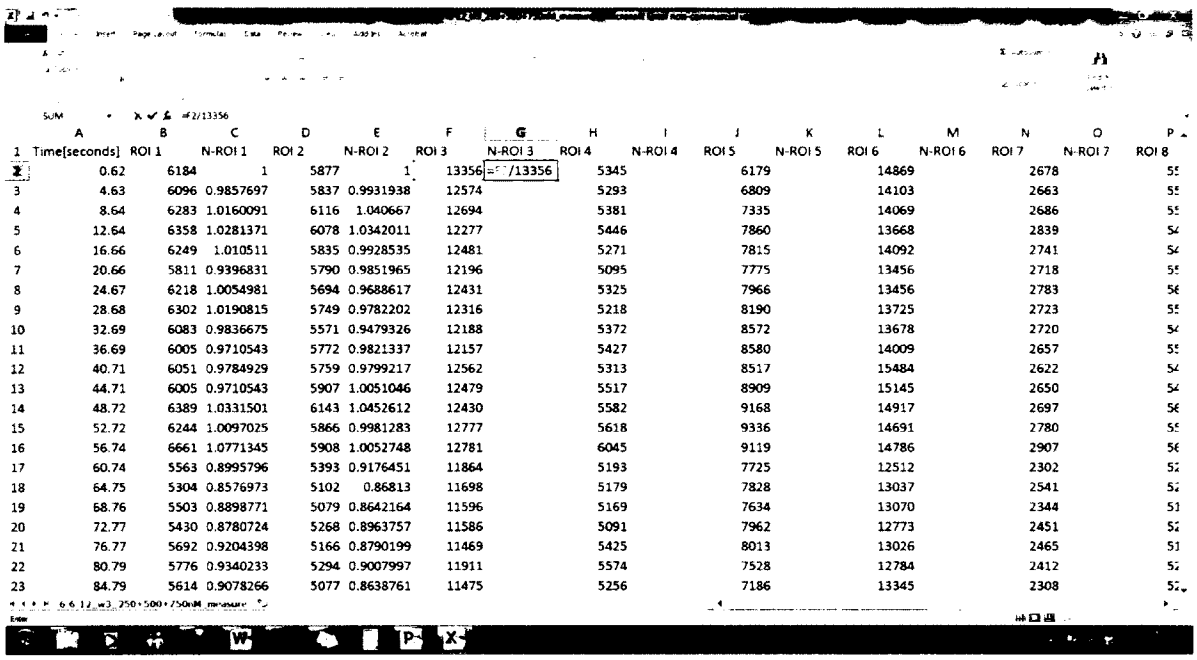

| | A | B | C | D | E | F | G | H | I | J | K | L | M | N | O | P |
|---|---|---|---|---|---|---|---|---|---|---|---|---|---|---|---|---|
| 1 | Time[seconds] | ROI 1 | N-ROI 1 | ROI 2 | N-ROI 2 | ROI 3 | N-ROI 3 | ROI 4 | N-ROI 4 | ROI 5 | N-ROI 5 | ROI 6 | N-ROI 6 | ROI 7 | N-ROI 7 | ROI 8 |
| 2 | 0.62 | 6184 | 1 | 5877 | 1 | 13356 | =[illegible]/13356 | 5345 | | 6179 | | 14869 | | 2678 | | 55 |
| 3 | 4.63 | 6096 | 0.9857697 | 5837 | 0.9931938 | 12574 | | 5293 | | 6809 | | 14103 | | 2663 | | 55 |
| 4 | 8.64 | 6283 | 1.0160091 | 6116 | 1.040667 | 12694 | | 5381 | | 7335 | | 14069 | | 2686 | | 55 |
| 5 | 12.64 | 6358 | 1.0281371 | 6078 | 1.0342011 | 12277 | | 5446 | | 7860 | | 13668 | | 2839 | | 54 |
| 6 | 16.66 | 6249 | 1.010511 | 5835 | 0.9928535 | 12481 | | 5271 | | 7815 | | 14092 | | 2741 | | 54 |
| 7 | 20.66 | 5811 | 0.9396831 | 5790 | 0.9851965 | 12196 | | 5095 | | 7775 | | 13456 | | 2718 | | 55 |
| 8 | 24.67 | 6218 | 1.0054981 | 5694 | 0.9688617 | 12431 | | 5325 | | 7966 | | 13456 | | 2783 | | 56 |
| 9 | 28.68 | 6302 | 1.0190815 | 5749 | 0.9782202 | 12316 | | 5218 | | 8190 | | 13725 | | 2723 | | 55 |
| 10 | 32.69 | 6083 | 0.9836675 | 5571 | 0.9479326 | 12188 | | 5372 | | 8572 | | 13678 | | 2720 | | 54 |
| 11 | 36.69 | 6005 | 0.9710543 | 5772 | 0.9821337 | 12157 | | 5427 | | 8580 | | 14009 | | 2657 | | 55 |
| 12 | 40.71 | 6051 | 0.9784929 | 5759 | 0.9799217 | 12562 | | 5313 | | 8517 | | 15484 | | 2622 | | 54 |
| 13 | 44.71 | 6005 | 0.9710543 | 5907 | 1.0051046 | 12479 | | 5517 | | 8909 | | 15145 | | 2650 | | 54 |
| 14 | 48.72 | 6389 | 1.0331501 | 6143 | 1.0452612 | 12430 | | 5582 | | 9168 | | 14917 | | 2697 | | 56 |
| 15 | 52.72 | 6244 | 1.0097025 | 5866 | 0.9981283 | 12777 | | 5618 | | 9336 | | 14691 | | 2780 | | 55 |
| 16 | 56.74 | 6661 | 1.0771345 | 5908 | 1.0052748 | 12781 | | 6045 | | 9119 | | 14786 | | 2907 | | 56 |
| 17 | 60.74 | 5563 | 0.8995796 | 5393 | 0.9176451 | 11864 | | 5193 | | 7725 | | 12512 | | 2302 | | 52 |
| 18 | 64.75 | 5304 | 0.8576973 | 5102 | 0.86813 | 11698 | | 5179 | | 7828 | | 13037 | | 2541 | | 52 |
| 19 | 68.76 | 5503 | 0.8898771 | 5079 | 0.8642164 | 11596 | | 5169 | | 7634 | | 13070 | | 2344 | | 51 |
| 20 | 72.77 | 5430 | 0.8780724 | 5268 | 0.8963757 | 11586 | | 5091 | | 7962 | | 12773 | | 2451 | | 52 |
| 21 | 76.77 | 5692 | 0.9204398 | 5166 | 0.8790199 | 11469 | | 5425 | | 8013 | | 13026 | | 2465 | | 51 |
| 22 | 80.79 | 5776 | 0.9340233 | 5294 | 0.9007997 | 11911 | | 5574 | | 7528 | | 12784 | | 2412 | | 52 |
| 23 | 84.79 | 5614 | 0.9078266 | 5077 | 0.8638761 | 11475 | | 5256 | | 7186 | | 13345 | | 2308 | | 52 |

Figure B.4 Normalization of data analysis to one.

After the spreadsheet is normalized, only the N-ROI columns are selected to create a line tracing. Hold the control key and highlight all the N-ROI columns, and then select insert line tracing, Figure B.5 on next page. A line tracing graph is then created with frame number on the x-axis and fluorescence intensity on the y-axis, which is unitless since the data is normalized, Figure B.6.

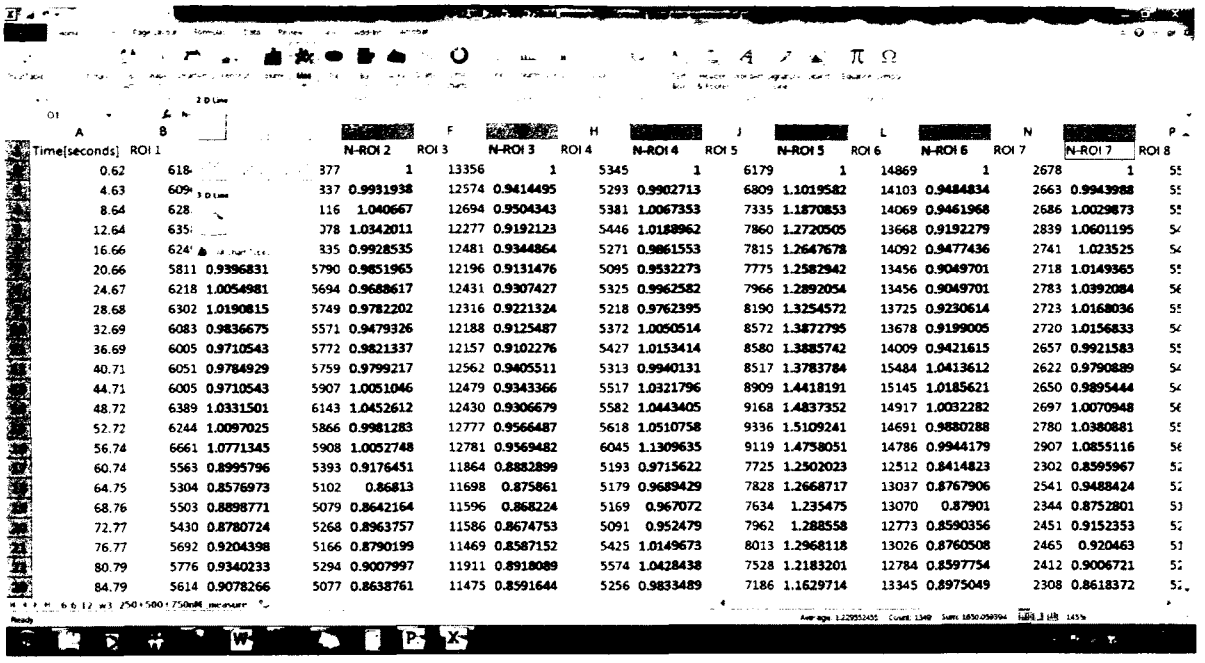

| Time[seconds] | ROI 1 | | N-ROI 2 | ROI 3 | N-ROI 3 | ROI 4 | N-ROI 4 | ROI 5 | N-ROI 5 | ROI 6 | N-ROI 6 | ROI 7 | N-ROI 7 | ROI 8 |
|---|---|---|---|---|---|---|---|---|---|---|---|---|---|---|
| 0.62 | 618 | | 377 | 1 | 13356 | 1 | 5345 | 1 | 6179 | 1 | 14869 | 1 | 2678 | 1 |
| 4.63 | 609 | | 337 | 0.9931938 | 12574 | 0.9414495 | 5293 | 0.9902713 | 6809 | 1.1019582 | 14103 | 0.9484834 | 2663 | 0.9943988 |
| 8.64 | 628 | | 116 | 1.040667 | 12694 | 0.9504343 | 5381 | 1.0067353 | 7335 | 1.1870853 | 14069 | 0.9461968 | 2686 | 1.0029873 |
| 12.64 | 635 | | 378 | 1.0342011 | 12277 | 0.9192123 | 5446 | 1.0188962 | 7860 | 1.2720505 | 13668 | 0.9192279 | 2839 | 1.0601195 |
| 16.66 | 624 | | 335 | 0.9928535 | 12481 | 0.9344864 | 5271 | 0.9861553 | 7815 | 1.2647678 | 14092 | 0.9477436 | 2741 | 1.023525 |
| 20.66 | 5811 | 0.9396831 | 5790 | 0.9851965 | 12196 | 0.9131476 | 5095 | 0.9532273 | 7775 | 1.2582942 | 13456 | 0.9049701 | 2718 | 1.0149365 |
| 24.67 | 6218 | 1.0054981 | 5694 | 0.9688617 | 12431 | 0.9307427 | 5325 | 0.9962582 | 7966 | 1.2892054 | 13456 | 0.9049701 | 2783 | 1.0392084 |
| 28.68 | 6302 | 1.0190815 | 5749 | 0.9782202 | 12316 | 0.9221324 | 5218 | 0.9762395 | 8190 | 1.3254572 | 13725 | 0.9230614 | 2723 | 1.0168036 |
| 32.69 | 6083 | 0.9836675 | 5571 | 0.9479326 | 12188 | 0.9125487 | 5372 | 1.0050514 | 8572 | 1.3872795 | 13678 | 0.9199005 | 2720 | 1.0156833 |
| 36.69 | 6005 | 0.9710543 | 5772 | 0.9821337 | 12157 | 0.9102276 | 5427 | 1.0153414 | 8580 | 1.3885742 | 14009 | 0.9421615 | 2657 | 0.9921583 |
| 40.71 | 6051 | 0.9784929 | 5759 | 0.9799217 | 12562 | 0.9405511 | 5313 | 0.9940131 | 8517 | 1.3783784 | 15484 | 1.0413612 | 2622 | 0.9790889 |
| 44.71 | 6005 | 0.9710543 | 5907 | 1.0051046 | 12479 | 0.9343366 | 5517 | 1.0321796 | 8909 | 1.4418191 | 15145 | 1.0185621 | 2650 | 0.9895444 |
| 48.72 | 6389 | 1.0331501 | 6143 | 1.0452612 | 12430 | 0.9306679 | 5582 | 1.0443405 | 9168 | 1.4837352 | 14917 | 1.0032282 | 2697 | 1.0070948 |
| 52.72 | 6244 | 1.0097025 | 5866 | 0.9981283 | 12777 | 0.9566487 | 5618 | 1.0510758 | 9336 | 1.5109241 | 14691 | 0.9880288 | 2780 | 1.0380881 |
| 56.74 | 6661 | 1.0771345 | 5908 | 1.0052748 | 12781 | 0.9569482 | 6045 | 1.1309635 | 9119 | 1.4758051 | 14786 | 0.9944179 | 2907 | 1.0855116 |
| 60.74 | 5563 | 0.8995796 | 5393 | 0.9176451 | 11864 | 0.8882899 | 5193 | 0.9715622 | 7725 | 1.2502023 | 12512 | 0.8414823 | 2302 | 0.8595967 |
| 64.75 | 5304 | 0.8576973 | 5102 | 0.86813 | 11698 | 0.875861 | 5179 | 0.9689429 | 7828 | 1.2668717 | 13037 | 0.8767906 | 2541 | 0.9488424 |
| 68.76 | 5503 | 0.8898771 | 5079 | 0.8642164 | 11596 | 0.868224 | 5169 | 0.967072 | 7634 | 1.235475 | 13070 | 0.87901 | 2344 | 0.8752801 |
| 72.77 | 5430 | 0.8780724 | 5268 | 0.8963757 | 11586 | 0.8674753 | 5091 | 0.952479 | 7962 | 1.288558 | 12773 | 0.8590356 | 2451 | 0.9152353 |
| 76.77 | 5692 | 0.9204398 | 5166 | 0.8790199 | 11469 | 0.8587152 | 5425 | 1.0149673 | 8013 | 1.2968118 | 13026 | 0.8760508 | 2465 | 0.920463 |
| 80.79 | 5776 | 0.9340233 | 5294 | 0.9007997 | 11911 | 0.8918089 | 5574 | 1.0428438 | 7528 | 1.2183201 | 12784 | 0.8597754 | 2412 | 0.9006721 |
| 84.79 | 5614 | 0.9078266 | 5077 | 0.8638761 | 11475 | 0.8591644 | 5256 | 0.9833489 | 7186 | 1.1629714 | 13345 | 0.8975049 | 2308 | 0.8618372 |

Figure B.5 Example of how to create a line tracing in Excel.

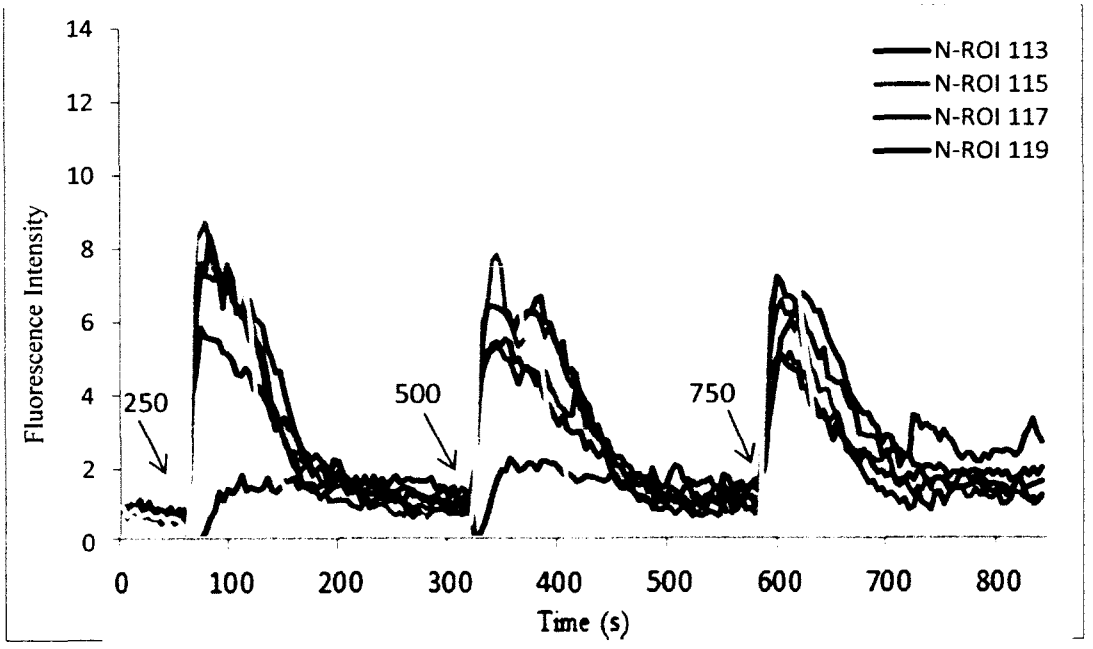


Figure B.6 Example of a line tracing created from normalized data in Excel.

# APPENDIX C

## SUPPLIMENTARY IMAGES AND VIDEOS

## C.1 Images and Videos

Figure C.1 displays calcium fluorescence of astrocytes with potassium chloride and Fluo 8/AM and a 40X oil objective, see DVD for movie.

Figure C.1 The movie displays calcium response to potassium chloride in Astrocytes. The cell in the lower right displays "squiggle lines," these are calcium fluorescing mitochondria. *Scale bar= 20 μm.*

Figure C.2 is a movie which depicts how neurons respond to increasing subthreshold glutamate stimulations depleted of glia. Figure C.3 is a movie which depicts how neurons respond to increasing subthreshold glutamate stimulations high of glia.


Figure C.2 The movie displays calcium response with applied pseudocolor to increasing subthreshold concentrations of glutamate (250, 500 and 750 nM) depleted of glia. The cell in the lower right displays calcium responses with a return to baseline. These are calcium fluorescing mitochondria. *Scale bar= 50 μm.*

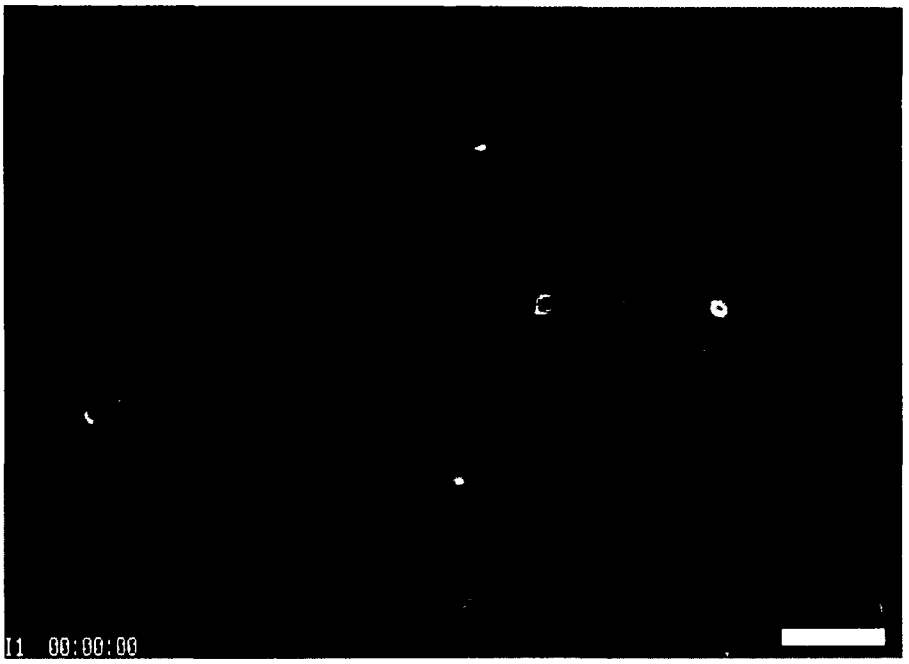


Figure C.3 The movie displays calcium response with applied pseudocolor to increasing subthreshold concentrations of glutamate (250, 500 and 750 nM) depleted of glia. The cell in the lower right displays calcium responses with a return to baseline. These are calcium fluorescing mitochondria. *Scale bar= 50 μm.*

Biphasic response of calcium by the ryanodine receptor from NMDA glutamate stimulus is shown in Figure C.4 [25].

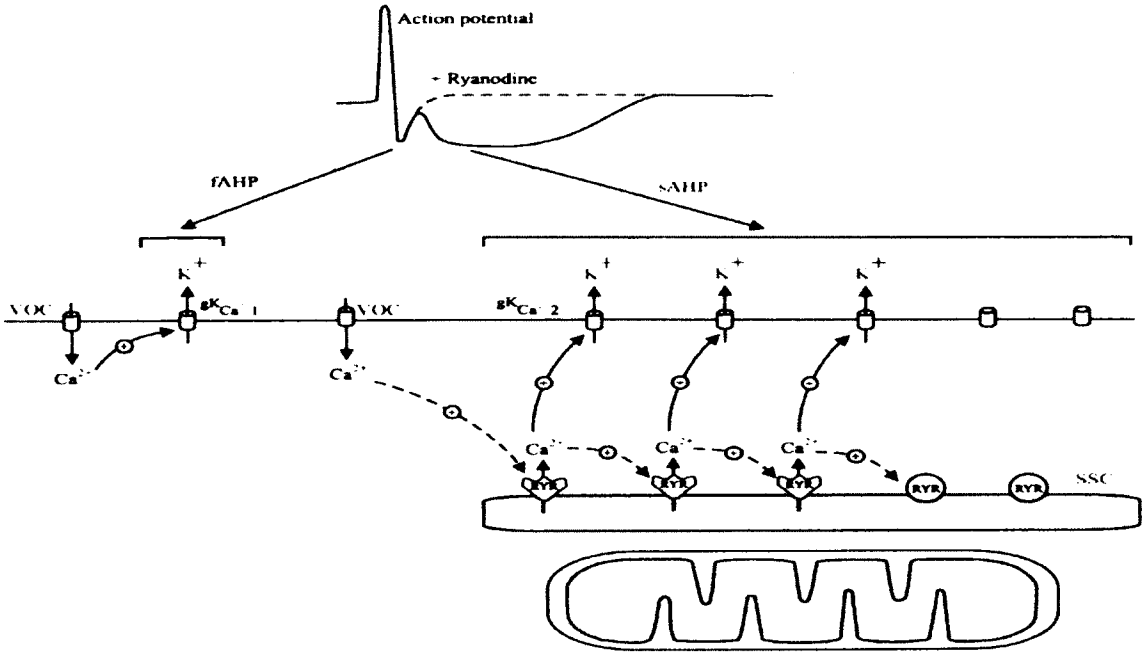


Figure C.4 Biphasic calcium oscillation in neurons [25].

# REFERENCES


[1] Guyton, A.C. and J.E. Hall, Textbook of Medical Pysiology. 11th ed. 2006, Philadelphia, PA: *Elsevier Saunders*.

[2] Byrne, J.H. and J.L. Roberts, From Molecles to Networks: An Introduction to Cellular and Molecular Neurosciences. 2004, USA: *Elsevier Science*.

[3] Niswender, C.M. and P.J. Conn, "Metabotropic glutamate receptors: physiology, pharmacology, and disease." *Annu Rev Pharmacol Toxicol*, 2010. **50**: p. 295-322.

[4] Catterall, W.A., "Voltage-gated calcium channels." *Cold Spring Harb Perspect Biol*, 2011. **3**(8): p. a003947.

[5] Stanika, R.I., et al., "Comparative impact of voltage-gated calcium channels and NMDA receptors on mitochondria-mediated neuronal injury." *J Neurosci*, 2012. **32**(19): p. 6642-6650.

[6] Wanjerkhede, S.M. and R.S. Bapi, "Role of CAMKII in reinforcement learning: a computational model of glutamate and dopamine signaling pathways." *Biol Cybern*, 2011. **104**(6): p. 397-424.

[7] Silva, A.J., "Molecular and cellular cognitive studies of the role of synaptic plasticity in memory." *J Neurobiol*, 2003. **54**(1): p. 224-237.

[8] Upreti, C., et al., "Role of presynaptic metabotropic glutamate receptors in the induction of long-term synaptic plasticity of vesicular release." *Neuropharmacology*, 2012. **22**: p. 22.

[9] Mukherjee, S. and D. Manahan-Vaughan, "Role of metabotropic glutamate receptors in persistent forms of hippocampal plasticity and learning." *Neuropharmacology*, 2013 **66**:p. 65-81.

[10] Ribeiro, F.M., et al., "Group I metabotropic glutamate receptor signalling and its implication in neurological disease." *CNS Neurol Disord Drug Targets*, 2010. **9**(5): p. 574-595.

[11] Singh, P., et al., "Computational investigation of the changing patterns of subtype specific NMDA receptor activation during physiological glutamatergic neurotransmission." *PLoS Comput Biol*, 2011. 7(6): p. e1002106.

[12] Kaufman, A.M., et al., "Opposing roles of synaptic and extrasynaptic NMDA receptor signaling in cocultured striatal and cortical neurons." *J Neurosci*, 2012. **32**(12): p. 3992-4003.

[13] Berridge, M.J., P. Lipp, and M.D. Bootman, "The versatility and universalitiy of calcium signalling." *Nature Reviews Molecular Cell Biology*, 2000. **1**: p. 11-21.

[14] Chalifoux, J.R. and A.G. Carter, "Glutamate spillover promotes the generation of NMDA spikes." *J Neurosci*, 2011. **31**(45): p. 16435-16446.

[15] Alberdi, E., M.V. Sanchez-Gomez, and C. Matute, "Calcium and glial cell death." *Cell Calcium*, 2005. **38**(3-4): p. 417-425.

[16] Goubard, V., E. Fino, and L. Venance, "Contribution of astrocytic glutamate and GABA uptake to corticostriatal information processing." *J Physiol*, 2011. **589**(Pt 9): p. 2301-2319.

[17] Santello, M., C. Cali, and P. Bezzi, "Gliotransmission and the tripartite synapse." *Adv Exp Med Biol*, 2012. **970**: p. 307-31.

[18] Pinton, P., et al., "Calcium and apoptosis: ER-mitochondria $Ca^{2+}$ transfer in the control of apoptosis." *Oncogene*, 2008. **27**(50): p. 6407-6418.

[19] Steinmann, C., et al., "Requirement of inositol 1,4,5-trisphosphate receptors for tumor-mediated lymphocyte apoptosis." *J Biol Chem*, 2008. **283**(20): p. 13506-13509.

[20] Jeroo D. Sinor, S.D., Sriram Venneti, Rachel C. Bliltzblau, Daniel N. Leszkiewicz, Paul A. Rosenberg, Elias Aizenman, "NMDA and glutamate evoke excitotoxicity and distinct cellular locations in rat cortical neurons in vitro." *The Journal of Neuroscience*, 2000. **20**(23): p. 8831-8837.

[21] Majno, G. and I. Joris, "Apoptosis, oncosis, and necrosis. An overview of cell death." *Am J Pathol*, 1995. **146**(1): p. 3-15.

[22] Kerrigan, T.L., et al., "The role of neuronal calcium sensors in balancing synaptic plasticity and synaptic dysfunction." *Front Mol Neurosci*, 2012. **5**: p. 57.

[23] Lazarewicz, J.W., "Calcium transients in brain ischemia: role in neuronal injury." *Acta Neurobiol. Exp.*, 1996. **56**: p. 299-311.

[24] Daikhin, Y. and M. Yudkoff, "Compartmentation of brain glutamate metabolism in neurons and glia." *Journal of Nutrition*, 2000: p. 1026s-1031s.

[25] Berridge, M.J., "Neuronal calcium signaling." *Neuron*, 1998. **21**: p. 13-26.

[26] Latour, I., et al., "Differential mechanisms of Ca2+ responses in glial cells evoked by exogenous and endogeous glutamate in rat hippocampus." *Hippocampus*, 2001. **11**(2): p. 132-145.

[27] Elmore, S., "Apoptosis: a review of programmed cell death." *Toxicol Pathol*, 2007. **35**(4): p. 495-516.

[28] Boehning, D., R.L. Patterson, and S.H. Snyder, "Apoptosis and calcium." *Cell Cycle*, 2004. **3**(3): p. 252-254.

[29] Mattson, M.P. and S.L. Chan, "Neuronal and glial calcium signaling in Alzheimer's disease." *Cell Calcium*, 2003. **34**(4-5): p. 385-397.

[30] Duchen, M.R., "Mitochondria, calcium-dependent neuronal death and neurodegenerative disease." *Pflugers Arch*, 2012. **464**(1): p. 111-121.

[31] Salinska, E., W. Danysz, and J.W. Lazarewicz, "The role of excitotoxicity in neurodegeneration." *Folia Neuropathol*, 2005. **43**(4): p. 322-339.

[32] Pivovarova, N.B. and S.B. Andrews, "Calcium-dependent mitochondrial function and dysfunction in neurons." *FEBS J*, 2010. **277**(18): p. 3622-3636.

[33] Marambaud, P., U. Dreses-Werringloer, and V. Vingtdeux, "Calcium signaling in neurodegeneration." *Mol Neurodegener*, 2009. **4**: p. 20.

[34] Lazarov, O. and R.A. Marr, "Neurogenesis and Alzheimer's disease: at the crossroads." *Exp Neurol*, 2010. **223**(2): p. 267-281.

[35] Association, A.s., 2012 "Alzheimer's disease facts and figures." *Alzheimer's and Dementia: The Journal of the Alzheimer's Association*, 2012. **8**: p. 131-168.

[36] Menard, C. and R. Quirion, "Group 1 metabotropic glutamate receptor function and its regulation of learning and memory in the aging brain." *Front Pharmacol*, 2012. **3**: p. 182.

[37] NIH/, G.I.N.I.o.A., "Inside the brain: an interactive tour." *Alzheimer's Association*, 2012. p. 1-16.

[38] Qin, S., et al., "System Xc- and apolipoprotein E expressed by microglia have opposite effects on the neurotoxicity of amyloid-beta peptide 1-40." *J Neurosci*, 2006. **26**(12): p. 3345-3356.

[39] Mattson, M.P., "Pathways towards and away from Alzheimer's disease." *Nature*, 2004. **430**(7000): p. 631-639.

[40] Surmeier, D.J., J.N. Guzman, and J. Sanchez-Padilla, "Calcium, cellular aging, and selective neuronal vulnerability in Parkinson's disease." *Cell Calcium*, 2010. **47**(2): p. 175-182.

[41] Fan, M.M. and L.A. Raymond, "N-methyl-D-aspartate (NMDA) receptor function and excitotoxicity in Huntington's disease." *Prog Neurobiol*, 2007. **81**(5-6): p. 272-293.

[42] Association, N.S., "Stroke 101 fact sheet." *National Stroke Association,* 2009. p. 1-2.

[43] Cross, J.L., et al., "Modes of neuronal calcium entry and homeostasis following cerebral ischemia." *Stroke Res Treat*, 2010. p. 316862.

[44] Dohare, P., S. Varma, and M. Ray, "Curcuma oil modulates the nitric oxide system response to cerebral ischemia/reperfusion injury." *Nitric Oxide*, 2008. **19**(1): p. 1-11.

[45] Harukuni, I. and A. Bhardwaj, "Mechanisms of brain injury after global cerebral ischemia." *Neurol Clin*, 2006. **24**(1): p. 1-21.

[46] Bridges, R., et al., "Thinking outside the cleft to understand synaptic activity: contribution of the cystine-glutamate antiporter (System xc-) to normal and pathological glutamatergic signaling." *Pharmacol Rev*, 2012. **64**(3): p. 780-802.

[47] Schubert, D. and D. Piasecki, "Oxidative glutamate toxicity can be a component of the excitotoxicity cascade." *J Neurosci*, 2001. **21**(19): p. 7455-62.

[48] Ye, Z. and H. Sontheimer, "Glioma Cells Release Excitotoxic Concentrations of Glutamate." *Cancer Res*, 1999. **59**: p. 4383-4391.

[49] Lyons, S.A., et al., "Autocrine glutamate signaling promotes glioma cell invasion." *Cancer Res*, 2007. **67**(19): p. 9463-9471.

[50] Sontheimer, H., "A role for glutamate in growth and invasion of primary brain tumors." *J Neurochem*, 2008. **105**(2): p. 287-295.

[51] Bordji, K., et al., "Activation of extrasynaptic, but not synaptic, NMDA receptors modifies amyloid precursor protein expression pattern and increases amyloid-ss production." *J Neurosci*, 2010. **30**(47): p. 15927-15942.

[52] Perea, G. and A. Araque, "Properties of synaptically evoked astrocyte calcium signal reveal synaptic information processing by astrocytes." *J Neurosci*, 2005. **25**(9): p. 2192-2203.

[53] Barreto-Chang, O.L. and R.E. Dolmetsch, "Calcium imaging of cortical neurons using Fura-2 AM." *J Vis Exp*, 2009(23).

[54] Zhang, Y.F., et al., "Novel glycine-dependent inactivation of NMDA receptors in cultured hippocampal neurons." *Neuroscie Bull*, 2012. **28**(5): p. 550-560.

[55] Mangiola, A., et al., "Invasive tumor cells and prognosis in a selected population of patients with glioblastoma multiforme." *Cancer*, 2008. **113**(4): p. 841-846.

[56] Kao, J.P., A.T. Harootunian, and R.Y. Tsien, "Photochemically generated cytosolic calcium pulses and their detection by Fluo-3." *The Journal of Biological Chemistry*, 1989. **264**(14): p. 8179-8184.

[57] Idowu, R.A., "A Study o Cellular Dynamics in Culture Using Fluorescence Microscopy- A statistical and mathematical approach, in mathematics and statictics." *Louisiana Tech University*, 2012. p. 198.

[58] Newcomb, R. and A. Palma, "Effects of diverse omega-conopeptides on the in vivo release of glutamic and gamma-aminobutyric acids." *Brain Res*, 1994. **638**(1-2): p. 95-102.

[59] Burger, P.M., et al., "Synaptic vesicles immunoisolated from rat cerebral cortex contain high levels of glutamate." *Neuron*, 1989. **3**(6): p. 715-720.

[60] Zorumski, C.F., S. Mennerick, and J. Que, "Modulation of excitatory synaptic transmission by low concentrations of glutamate in cultured rat hippocampal neurons." *Journal of Physiology*, 1996. **495**(8): p. 465-477.

[61] Sather, W., et al., "Activation and desensitization of n-methyl-d-aspartate receptors in nucleated outside-out patches from mouse neurons." *Journal of Physiology*, 1992. **450**: p. 643-672.

[62] DeCoster, M.A., et al., "Calcium dynamics in neurons treated with toxic and non-toxic concentrations of glutamate." *Neuroreport*, 1992. **3**(9): p. 773-776.

[63] Krebs, M.O., et al., "Does bicuculline antagonize NMDA receptors? Further evidence in the rat striatum." *Brain Res*, 1994. **634**(2): p. 345-348.

[64] Berridge, M.J., "Neuronal calcium signaling." *Neuron*, 1998. **21**: p. 13-26.

[65] Verplanck, W.S. and D.S. Blough, "Randomized stimuli and the non-independence of successive responses at the visual threshold." *J Gen Psychol*, 1958. **59**(2): p. 263-272.

[66] Verplanck, W.S., J.W. Cotton, and G.H. Collier, "Previous training as a determinant of response dependency at the threshold." *J Exp Psychol*, 1953. **46**(1): p. 10-14.

[67] Fernberger, S.W., "Interdependence of judgments within the series for the method of constant stimuli." *Journal of Experimental Psychology*, 1920. **3**: p. 126-150.

[68] Agranovich, A. and Y. Louzoun, "Predator-prey dynamics in a uniform medium lead to directed percolation and wave-train propagation." *Phys Rev E Stat Nonlin Soft Matter Phys*, 2012. **85**(3 Pt 1): p. 031911.

[69] Mehta, M.R., "Neuronal dynamics of predictive coding." *Neuroscientist*, 2001. **7**(6): p. 490-495.

[70] Puentedura, R.R., "A simple wolf-sheep grass simulation." *Hippasus*, 2009. p. 1-3.

[71] Mohammed, J.S., M.A. DeCoster, and M.J. McShane, "Micropatterning of nanoengineered surfaces to study neuronal cell attachment in vitro." *Biomacromolecules*, 2004. **5**: p. 1745-1755.

[72] Javeed Shaikh Mohammed, M.A.D., and Michael J. McShane, "Fabrication of interdigitated micropatterns of self-assembled polymer nanofilms containing cell-adhesive materials." *Langmuir*, 2006. **22**: p. 2738-2746.

[73] Mohammed, J.S., M.A. DeCoster, and M.J. McShane, "Lithography combined with multilayer nanoassembly: versatile approach to fabricate nanocomposite micropatterns for biointerfaces." *IEEE*, 2005: p. 305-308.